

目
次

**U.S. - JAPAN COORDINATED PROGRAM
FOR
MASONRY BUILDING RESEARCH**



PB93-212876

REPORT NO. 1. 1-1

**A COMPARISON OF THE BEHAVIOR
OF CLAY AND CONCRETE MASONRY
IN COMPRESSION**

by

**R. H. ATKINSON
G. R. KINGSLEY**

SEPTEMBER 1985

supported by :

NATIONAL SCIENCE FOUNDATION

GRANT NO. ECE-8412279

Atkinson-Noland & Associates





PB93-212876

A COMPARISON OF THE BEHAVIOR OF CLAY AND CONCRETE MASONRY IN COMPRESSION

conducted by:

ATKINSON-NOLAND & ASSOCIATES, INC.

2619 Spruce Street
Boulder, Colorado 80302
(303) 444-3620

Project Director and
Principal Investigator: Richard H. Atkinson

Project Engineer: Gregory R. Kingsley

September 1985

ia

PREFACE

This report presents the results of Category 1.0, Task 1.1 of the U.S. Coordinated Program for Masonry Building Research. The program constitutes the United States part of the United States - Japan, coordinated masonry research program conducted under the auspices of The Panel on Wind and Seismic Effects of the U.S. - Japan Natural Resources Development Program (UJNR).

This material is based on work supported by the National Science Foundation under Grant No. CEE - 8412279. Program Director : Dr. A. J. Eggenberger.

Any opinions, findings, and conclusions or recommendations expressed in this publication are those of the authors and do not necessarily reflect the views of the National Science Foundation and the United States Government.

Reproduced from
best available copy.

ABSTRACT

Current design codes do not distinguish between clay and concrete masonry for purposes of design, assuming that both materials behave identically under load. The research community has not, however, established that this assumption is justified, and, at great expense, continues to conduct separate research for each material. The primary objective of this project, then, was to investigate the extent to which clay and concrete hollow unit masonry have similar behavioral characteristics.

Ten series of tests, each consisting of five clay and five concrete prisms were conducted to determine the influence of unit size, grouting, mortar strength, grout strength, bond pattern, load direction, and platen restraint on the relative behavior of clay and concrete masonry. It was concluded that, while clay and concrete prisms sometimes exhibited different failure mechanisms and responded differently to some parameter changes, the shapes of the compressive stress strain curves were consistently similar, and the two masonry types could therefore be considered as one material for purposes of design.

TABLE OF CONTENTS

LIST OF FIGURES	iii
LIST OF TABLES	v
1. INTRODUCTION	1
1.1 PROBLEM STATEMENT	1
1.2 OBJECTIVE	2
1.3 SCOPE	2
1.3.1 UNIT WIDTH	3
1.3.2 UNGROUTED PRISMS	3
1.3.3 MORTAR STRENGTH	3
1.3.4 GROUT STRENGTH	3
1.3.5 BOND PATTERN	4
1.3.6 LOAD DIRECTION	4
1.3.7 REDUCED PLATEN CONSTRAINT	4
2. BACKGROUND	5
2.1 INTRODUCTION	5
2.2 HOLLOW OR GROUTED CONCRETE MASONRY RESEARCH	6
2.2.1 HAMID AND DRYSDALE	7
2.2.2 HEGEMIER ET AL	7
2.2.3 PRIESTLY AND ELDER	8
2.2.4 MAURENBRECHER	9
2.3 HOLLOW OR GROUTED CLAY MASONRY RESEARCH	9
2.3.1 MILLER AND RIDINGER	10
2.3.2 BIA	11
2.3.3 BROWN AND WHITLOCK	11
3. MATERIAL PROPERTIES AND TEST PROCEDURES	13
3.1 INTRODUCTION	13
3.2 MASONRY UNITS	13
3.3 MORTAR	15
3.4 GROUT	17
3.5 PRISM CONSTRUCTION	23
3.6 PRISM INSTRUMENTATION	24
3.7 PRISM TRANSPORTATION	26
3.8 TEST MACHINE	27
3.9 INTERFACE FRICTION REDUCTION	28
3.10 PRISM TESTS	28
3.11 MODIFICATION OF STRESS/STRAIN DATA TO ACCOUNT FOR MACHINE STIFFNESS	29
4. RESULTS OF PRISM TESTS	33
4.1 STRESS/STRAIN CURVES	33

4.1.1	ULTIMATE STRENGTH AND STRAIN	33
4.1.2	SECANT MODULUS AND SLOPE OF FALLING BRANCH	52
4.1.3	RESIDUAL STRENGTH	53
4.1.4	TOUGHNESS	53
4.1.5	POISSON'S RATIO	53
4.1.6	COMPONENT MATERIALS	54
4.2	FAILURE MODES	54
4.2.1	GROUTED PRISMS	54
4.2.2	UNGROUTED PRISMS	54
4.2.3	PRISMS LOADED PARALLEL TO THE BEDJOINT	55
4.2.4	PRISMS WITH REDUCED PLATEN CONSTRAINT	55
5.	DISCUSSION OF RESULTS	57
5.1	INTRODUCTION	57
5.2	EFFECT OF UNIT SIZE	57
5.3	EFFECT OF GROUTING	58
5.4	EFFECT OF MORTAR TYPE	60
5.5	EFFECT OF GROUT STRENGTH	60
5.6	EFFECT OF BOND PATTERN	61
5.7	EFFECT OF LOADING DIRECTION	61
5.8	EFFECT OF REDUCED PLATEN CONSTRAINT	62
5.9	FAILURE MODES	65
5.10	AGREEMENT OF RESULTS WITH PREVIOUS WORK	66
5.11	SHAPE OF THE STRESS-STRAIN CURVES	66
5.12	IMPLICATIONS ON DESIGN	72
5.11.1	WORKING STRESS DESIGN	72
5.11.2	ULTIMATE STRENGTH DESIGN	73
6.	CONCLUSIONS	75
6.1	SUMMARY	75
6.2	CONCLUSIONS	75
6.3	RECOMMENDATIONS FOR FUTURE STUDIES	76
	REFERENCES	79
	APPENDIX: INDIVIDUAL TEST RESULTS	85

LIST OF FIGURES

FIGURE NO.	TITLE	PAGE NO.
3.1	Hollow unit dimensions	14
3.2	Distribution of mortar strength	17
3.3	Grout compaction in clay prisms	21
3.4	Grout compaction in concrete prisms	22
3.5	Mortared and grouted areas of prisms	24
3.6	Prism instrumentation	25
3.7	Prism instrumentation for reduced platen restraint series	26
3.8	Prism in place in test machine	27
3.9	Uncorrected stress-strain data	32
3.10	Corrected stress-strain data	33
4.1	Stress-strain data: 6" grouted - clay	35
4.2	Stress-strain data: 6" grouted - concrete	35
4.3	Stress-strain data: 4" grouted - clay	36
4.4	Stress-strain data: 4" grouted - concrete	36
4.5	Stress-strain data: 8" grouted - clay	37
4.6	Stress-strain data: 8" grouted - concrete	37
4.7	Stress-strain data: 6" ungrouted - clay	38
4.8	Stress-strain data: 6" ungrouted - concrete	38
4.9	Stress-strain data: 8" ungrouted - clay	39
4.10	Stress-strain data: 8" ungrouted - concrete	39
4.11	Stress-strain data: running bond - clay	40
4.12	Stress-strain data: running bond - concrete	40
4.13	Stress-strain data: type s mortar - clay	41
4.14	Stress-strain data: type s mortar - concrete	41
4.15	Stress-strain data: high strength grout - clay	42
4.16	Stress-strain data: high strength grout - concrete	42
4.17	Stress-strain data: load // to bedjoint - clay	43
4.18	Stress-strain data: load // to bedjoint - concrete	43
4.19	Stress-strain data: reduced platen restraint-clay	44
4.20	Stress-strain data: reduced platen restraint-concrete	44
4.21	Example of vertical strain gage data	45
4.22	Example of horizontal strain gage data	45
4.23	Example of external LVDT data	46
4.24	Example of strain gage data from reduced platen constraint tests	47
4.25	Clay prism failures	48
4.26	Concrete prism failures	49
4.27	Failure of clay prism with reduced platen constraint	50
4.28	Failure of concrete prism with reduced platen constraint	51
5.1	Prism strength vs. unit size for grouted prisms and ungrouted prisms	58

5.2	Distribution of secant modulus data for clay and concrete prisms	68
5.3	Distribution of peak strain data for clay and concrete prisms	69
5.4	Distribution of area-under-curve at 1.5 X ϵ_p for clay and concrete prisms	70
5.5	Distribution of area-under-curve at 2.0 X ϵ_p for clay and concrete prisms	71

LIST OF TABLES

TABLE NO.	TITLE	PAGE
3.1	UNIT PROPERTIES	15
3.2	SAND GRADATION	16
3.3	GROUT PROPERTIES	20
4.1	PRISM TEST DATA	34



I. INTRODUCTION

1.1 PROBLEM STATEMENT

Masonry construction in seismic zones is usually grouted hollow concrete block or grouted clay unit masonry. Current building codes that include masonry design criteria [39] do not differentiate between clay and concrete masonry for purposes of design, assuming that the different materials behave identically under load. The research community has not, however, established that this assumption is justified, and has typically considered clay and concrete to be separate and unique materials. It is important, then, for the efficient progress of future masonry research and the subsequent development of design standards, to investigate the extent to which the two distinct types of masonry materials have similar engineering behavior characteristics.

While numerous researchers have examined the behavior of clay or concrete masonry [1-44], few have studied both materials simultaneously under similar conditions [26,22,12,42]. So despite the abundance of data available, the inherent variability of masonry materials and the sensitivity of test results to laboratory procedures [7] makes it difficult to assimilate and compare the existing data. Furthermore, there are few studies of clay or concrete masonry so similar in scope that the effect of a single isolated variable can be compared between two studies of different materials.

Few researchers [19,35] have had the opportunity to

obtain stress-strain data beyond ultimate strength for high strength masonry specimens. It is essential to obtain complete post-peak stress-strain curves for both clay and concrete masonry for development of ultimate strength and limit-states design standards.

1.2 OBJECTIVE

The objective of this study was to conduct parallel compression tests of clay and concrete masonry prisms under essentially identical conditions, and to determine if the two materials may justifiably be considered identical for purposes of design. In addition, an effort was made to exercise careful control of laboratory practices as a step towards better standardization of laboratory procedures (The laboratory practices will be documented in separate reports).

1.3 SCOPE

Over one hundred four-unit high clay and concrete masonry prisms were tested in uniaxial compression to strains well beyond the strain at ultimate strength. Both clay and concrete units were limited to nominally 16" long hollow units; cavity wall construction was not within the scope of this investigation. Ten series of tests, each including ten prisms, (five clay and five concrete), were conducted, in which one parameter was changed for each series. Most series had counterparts in other research programs in order to facilitate comparisons. The "baseline" or control series consisted of grouted stack-bond prisms, nominally 6 inches

in width, and constructed with type-N mortar. The remaining nine series are described individually below. It should be emphasized that each of the parameter studies was cursory in nature; no attempt was made to conduct a comprehensive study over a wide range of variable values, since this type of study has been done elsewhere [6,8]. The purpose was to observe the relative effect of each parameter on clay and concrete prisms.

1.3.1 UNIT WIDTH

The effect of varying unit width was investigated by including two additional series, one with nominal 4-inch width units and the other with nominal 8 inch width units. The changing unit size was also reflected in the increasing ratio of grouted-to-gross area.

1.3.2 UNGROUTED PRISMS

Two series of ungrouted prisms were included, one with nominal 6-inch width units and another with nominal 8-inch width units.

1.3.3 MORTAR STRENGTH

One series of prisms was constructed with Type S mortar rather than the standard Type N mortar used for all other prisms.

1.3.4 GROUT STRENGTH

One series contained grout with doubled cement content and reduced water-cement ratio in order to investigate the effect of grout properties on prism behavior.

1.3.5 BOND PATTERN

One series of prisms was constructed in running bond rather than stack-bond.

1.3.6 LOAD DIRECTION

It is well known that masonry does not behave isotropically for many types of stress states. The degree of anisotropy displayed by the prisms was investigated by loading one series in a direction parallel to the bed joints.

1.3.7 REDUCED PLATEN RESTRAINT

It has been proposed that masonry prisms be tested in a manner such that the frictional restraint of the platens on the prism ends be reduced such that the failure mechanism of prisms would approximate that which occurs in full size walls [30]. One series was tested with lubricated Teflon sheets on prism ends in order to investigate the influence of platen restraint on the relative lateral stress distributions and failure modes of clay and concrete prisms.

2. BACKGROUND

2.1 INTRODUCTION

A survey of published research studies of masonry behavior at the material level reveals that the majority of work has been directed toward concrete block masonry. Conventional clay solid-unit masonry has also been studied, but relatively few studies have been directed towards hollow clay unit masonry. The studies on concrete block masonry have included concentric and eccentric axial loadings on both grouted and ungrouted specimens, [4,8,18,19,26,42] and also shear strength, and direct and flexural tensile strength studies on the same materials [9,14,15].

Most information on clay unit masonry has been limited to conventional solid or cored-unit construction [6,12,42]. This type of masonry is not usually reinforced except when it is employed in multiple-wythe construction with a grouted reinforced core between wythes. Available data for hollow unit clay masonry is generally limited to ungrouted masonry [17,22,28,30,36] with very little data available on grouted unit clay masonry [6].

A significant limitation for all of the studies listed above is that no information on post-peak behavior is provided. Many studies provide only strength data while many of those studies that did include deformation measurements are of limited use, as often the researcher would remove the deformation transducers (typically LVDT's) prior to the brittle, explosive failures experienced to avoid damage to

the transducer.

To obtain the complete stress-strain curve for masonry requires a large capacity, very stiff testing machine which have only recently become available in the form of the most recent generation of servo-controlled hydraulic testing machines. The only available results on the complete stress-strain curve for masonry are from studies of New Zealand concrete and clay unit masonry [34,35,38]. These studies have noted the apparent similarity between the post-peak response of masonry and plain concrete.

Most of the studies cited above have concentrated on a single type of masonry with a limited range of variables considered. Only a few investigators have tested a wide range of masonry types, sizes and strengths in the same study [12,22,26]. Thus, information on which to evaluate the commonality of masonry behavior is quite limited.

A limited selection of recent, immediately pertinent studies are briefly outlined in the following two sections. They are presented in separate sections for clay and concrete, and are limited to hollow unit masonry studies.

2.2 HOLLOW OR GROUTED CONCRETE MASONRY RESEARCH

Concrete masonry has enjoyed significantly more attention than hollow clay masonry. Several studies covering stress strain behavior under uniaxial compression and eccentric compression are listed in the following sections.

2.2.1 HAMID AND DRYSDALE [7,8,10,16]

Hamid and Drysdale have investigated the influence of many parameters on concrete block prisms under axial [8,16] and eccentric [10] compressive loading. Results show that the average compressive strength of grouted prisms (based on the gross area) was less than for similar ungrouted prisms (based on the net area). The authors emphasize that superposition of grout strength and ungrouted prism strength is not justified due to the incompatibility of the block and grout deformation characteristics. They suggest that the lateral expansion of the grout induces increased tensile stresses in the block that lead to splitting failure of the block at lower axial compressive strains than for ungrouted prisms. Also of interest is their finding that large increases in mortar or grout strength result in relatively small increases in prism strength. Mortar joint thickness also had little significant effect on prism strength.

While some deformation data was recorded, most results are presented only in terms of compressive strength.

2.2.2 HEGEMIER et.al [19]

Hegemier conducted a study to evaluate the effect of various parameters on the results of grouted concrete prism tests. In particular they investigated the influence of prism height, platen restraint, mortar strength, mortar joint thickness, bond pattern and bearing plate thickness. Like Hamid and Drysdale, they observed that mortar joint thickness and mortar strength had little influence on prism

strength. Bond pattern had a significant effect, as some running bond prisms showed a 16% lower compressive strength than stack bond prisms. Platen restraint was also shown to have a significant effect on prism strength, yielding f'_m values that were from 35 to 62 percent greater than for prisms with reduced end restraint.

While deformations were measured in each test, and tests were carried into the post peak region, the only measure of performance presented is compressive strength.

2.2.3 PRIESTLY AND ELDER [35]

Priestly and Elder conducted a study of grouted concrete prisms in compression which, in addition to compressive strength, measured stress-strain characteristics- such as strain at maximum stress and slope of the post-peak falling branch of the stress strain curve. Parameters investigated included masonry unit thickness, loading rate, presence of flue (vertical) reinforcement and presence of confining plates. Results showed that, with minor adjustments, the Kent-Park stress-strain model for concrete [21] predicted behavior of confined and unconfined prisms adequately.

The presence of confining plates changed the failure mode from vertical splitting to one involving a shear/compression failure, and significantly increased the ductility of the prisms. Block width and vertical reinforcement had little influence on masonry behavior.

The nature of their study was preliminary and no at-

tempt was made to investigate a wide range of material parameters or specimen configurations. Still, this is the most informative work to date covering the complete stress-strain behavior of grouted hollow concrete masonry.

2.2.4 MAURENBRECHER [26,27]

Maurenbrecher has conducted investigations into the effect of test procedures on masonry prisms [27] and also the effect of eccentric loading on prism behavior [26]. These studies include both clay brick prisms and ungrouted concrete block prisms. However, the clay unit used is a small modular brick while the concrete is a hollow masonry unit, so geometric differences might render direct comparison of data unjustified. Parameters considered in ref.[27] were prism height-to-thickness ratio, capping, mortar bedding, workmanship, loading rate, age, and bond pattern. For concrete block masonry, only capping techniques and mortar bedding were investigated. Mortar bedding was shown to have no effect on strength. Running bond brick prisms were 7-13% weaker than stack bond. Deformation data were not reported.

2.3 HOLLOW OR GROUTED CLAY MASONRY RESEARCH

Compared to hollow concrete masonry, hollow clay masonry is a relatively new structural material. According to Miller [28], hollow clay units were first developed on the East Coast in the 1950's, but soon fell out of use. Then in the early 1970's, the hollow clay unit was revived in Colorado, and is now becoming more popular throughout the U.S..

Relatively little research on hollow clay masonry behavior has been done. Two projects of a preliminary nature were done at the University of Colorado in 1979 [28,36]. A fairly large scale project was carried out by the Brick Institute of America [45], but the results from that study were never published. In 1982, a thorough study of hollow clay masonry prisms in compression was done at Clemson by Brown and Whitlock [6]. These are briefly discussed below.

2.3.1 MILLER AND RIDINGER [28,26]

Two studies at the University of Colorado filled the need for preliminary data on hollow clay masonry, providing information on the compressive strength of hollow units, and ungrouted hollow unit prisms. Prism parameters investigated were mortar type, mortar bedding (faceshell or net area), prism height, and prism end restraint. For end-restrained prisms, faceshell capping resulted in a 13-22% decrease in compressive strength from net area capped prisms [28]. A 1607% increase in mortar strength (from 317 psi to 5412 psi) resulted in only a 55% increase in prism strength (from 4749 psi to 7351 psi).

Ridinger continued the study, concentrating on the effect of mortar and unit properties on prism behavior. In his study, deformation measurements were made on units, mortar, and prisms, and the results were used to develop a simple, linear elastic failure criteria for ungrouted prisms.

2.3.2 BIA [45]

In the early 70's, The Brick Institute of America (BIA) undertook a large scale study of hollow clay masonry prisms and walls in compression, flexure, and shear. The first phase of that program, completed in January 1973, was limited to the testing of ungrouted hollow clay unit prisms in compression. Parameters investigated were unit thickness, prisms slenderness, mortar type, and mortar bedding. Compressive strength and Young's modulus were recorded for each prism. In all, 640 prisms were tested.

BIA reported no significant difference in compressive strength between face-shell and net area mortar bedding, when strength is based on the bedded area. Mortar strength had a significant effect on prism strength. Relative to Type S mortar, Type N prisms had a relative strength of 0.81 and type M mortar had a relative strength of 1.14. The unit strength is reported to have little correlation to prism strength.

2.3.3 BROWN AND WHITLOCK [6]

This study is apparently the only previously available source of information on grouted hollow clay masonry prisms. The objective was to determine the factors that affect the compressive strength of grouted hollow clay prisms and to develop a model to predict the performance of such prisms based on material properties. The following conclusions are excerpted directly from the paper. It should be noted that the term "compressive strength" refers to failure load, not

failure stress.

1. Grouting of a hollow brick prism will generally increase its compressive strength, all other things being equal.

2. Compressive strength of grouted hollow brick prisms increases sharply with increased mortar compressive strength.

3. Compressive strength of grouted hollow brick prisms is improved significantly by grouting only if good quality grout is used. Weaker grouts can result in a reduction of compressive strength.

4. Compressive strength of hollow brick prisms decreases approximately linearly with increasing coring percentage. Weaker grouts result in a greater reduction than stronger grouts.

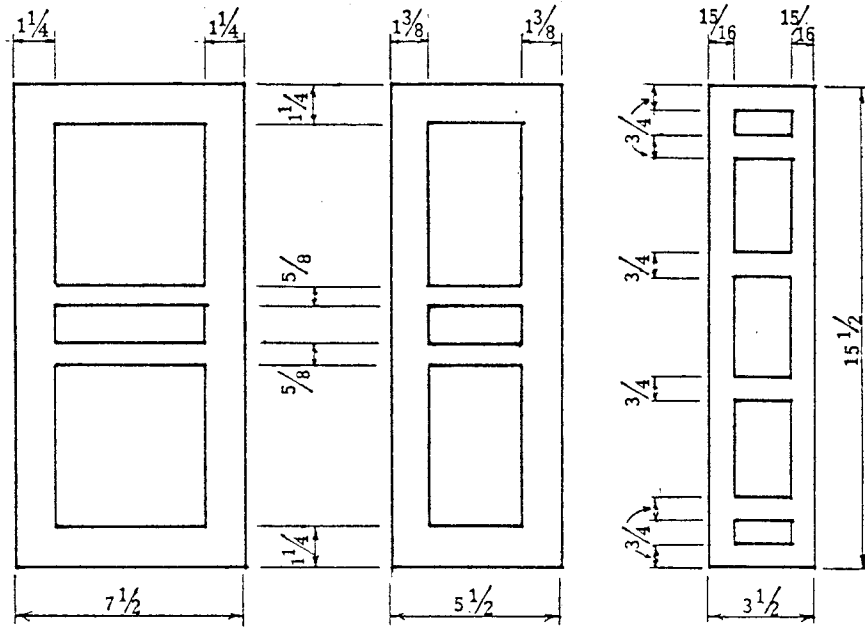
3. MATERIAL PROPERTIES AND TEST PROCEDURES

3.1 INTRODUCTION

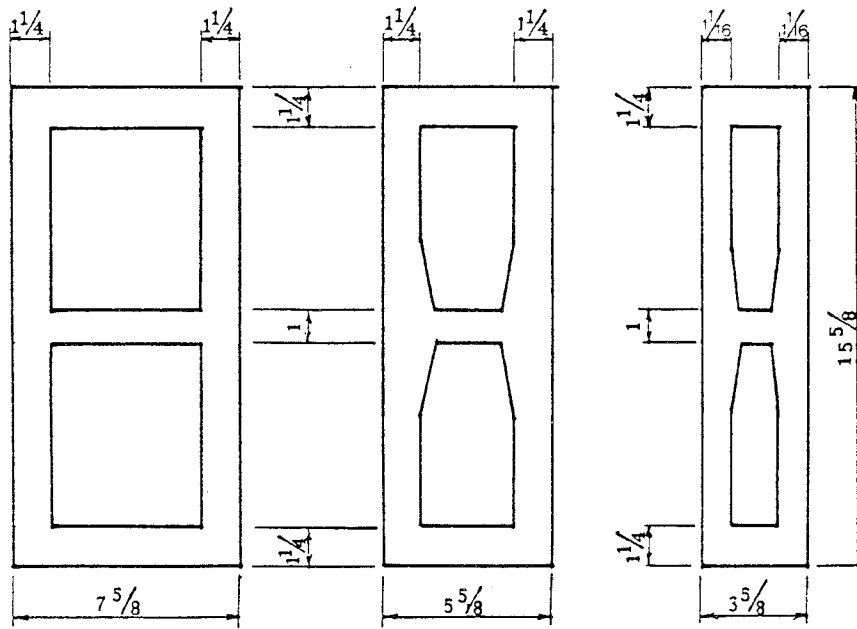
The following sections describe the materials and procedures used throughout construction and testing of all masonry prisms. Laboratory procedures were consistent and easily repeatable. Given identical materials, and careful construction, test results should be easily replicated in other laboratories. Further details concerning construction and testing of masonry specimens are provided in references 30, 46, and 47.

3.2 MASONRY UNITS

The clay and concrete masonry units were chosen such that the unit dimensions would be as similar as possible, thus eliminating unit size as a potential difference between clay and concrete prism tests. Thus, a nominally 4 inch deep concrete unit was used rather than the common 8 inch deep unit. The one significant geometric difference between the units was the central webs: the clay units had multiple webs while the concrete units had only one. The clay units were provided by the Atlas Brick Co. of Utah, and the concrete units were provided by the Concrete Masonry Association of California and Nevada. Figure 3.1 shows the dimensions of the units presented in the producer's literature. Measured dimensions were within $\pm 1/16$ " of these values. Table 3.1 gives values of material properties measured in accordance with the given ASTM Standards.



CLAY UNITS



CONCRETE UNITS

FIGURE 3.1 HOLLOW UNIT DIMENSIONS

TABLE 3.1 UNIT PROPERTIES

UNIT NOMINAL WIDTH	MATERIAL	1	2	3	ABSORPTION % of UNIT WEIGHT	CORE AREA GROSS AREA
		fb psi	ft psi	IRA gm/30in ²		
4"	CLAY	8974	-	15	9	0.28
6"	CLAY	12936	585	26	10	0.32
8"	CLAY	11344	-	25	10	0.44
4"	CONCRETE	3904	-	61	9	0.30
6"	CONCRETE	3583	300	55	10	0.37
8"	CONCRETE	3125	-	59	12	0.45

1 Uniaxial Compressive Strength, measured according to ASTM C140-75
2 Splitting Tensile Strength, measured according to ASTM C1006-84
3 Initial Rate of Absorption, measured according to ASTM C67-78
4 Absorption (24 hour immersion), measured according to ASTM C67-78

3.3 MORTAR

The standard mortar mix, used, with one exception, for all prism series was a Type N portland cement-lime mix with volumetric proportions of 1:1:6 (cement:lime:sand). The exception was for one series built with Type S mortar with volumetric proportions of 1:1/2:4-1/2.

The cement used in this study was a Type I cement made by Martin Marietta. Midway through the project, the cement plant was sold, and the identical product was marketed under the new name "Mountain States".

The lime was Type S, and was manufactured by Genstar.

The sand used was a dried, bagged "all purpose sand" manufactured by the Rio Grande Co. in Denver, Colorado. The

sand gradation, given in Table 3.2, shows that the sand conforms to ASTM C144-76 gradation requirements.

Mortar mixing was done in accordance with ASTM C305-65. One batch of mortar was made for each prism. The small batches were used to prevent mortar from sitting too long on the board.

Standard 2-inch mortar cubes (ASTM C109-73) were made for every batch of mortar. Frey [13] found that mortar mixed to a flow of 115 more closely matched the condition of mortar after unit suction than mortar mixed to the more workable flow of 130. In accordance with this finding, mortar was mixed to a flow of 115 for making cubes, and water was then added to bring the flow up to 130 for the mortar used to build prisms. This was done in precisely the

TABLE 3.2 SAND GRADATION

SIEVE NUMBER	% PASSING	ASTM LIMITS (C144 AND C404)
4	100	100
8	99.5	95 - 100
16	93.5	70 - 100
30	69.5	40 - 75
50	26.5	10 - 35
100	4.0	2 - 15
200	0.3	-

same manner for each batch, resulting in a water/cement ratio, for Type N mortar, of 1.2 for the cubes and 1.45 for laying prisms.

Figure 3.2 shows the statistical distribution of the strength for all Type N mortar cubes made in this project. Over one hundred batches of mortar were made by two people over a six month period. The coefficient of variation of 0.10 was considered to be satisfactory.

3.4 GROUT

The cement and sand used in the grout were the same as those used in the mortar. Coarse aggregate was a pea gravel with a maximum aggregate size of 3/8" in accordance with ASTM C404-76. Grout conformed to ASTM C476-71, and was

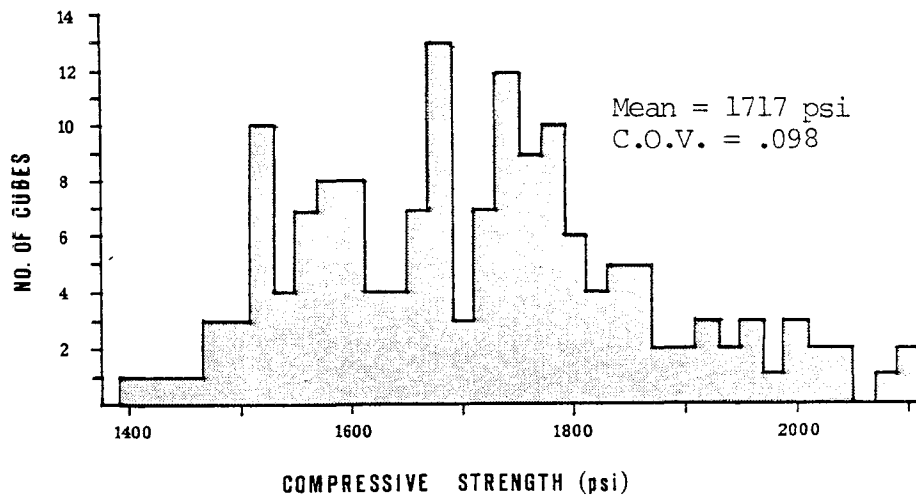


FIGURE 3.2 DISTRIBUTION OF MORTAR STRENGTH

mixed to a volumetric proportion of 1:3:2 (cement:sand:gravel), with a water/cement ratio of 0.75. One batch, for the "strong grout" series, had mix proportions of 1:1.5:1, w/c = 0.44. In addition, all grout contained an admixture: SIKA Grout Aid, Type II. It has been shown [1, 23, 24, 29, 44] that including such an admixture in grout minimizes the number of flaws and shrinkage cracks in the grout. The admixture was considered to be necessary in order to insure consistency and repeatability in prism construction.

Grout was mixed in a twenty gallon capacity Triumph paddle mixer. There is no ASTM standard for laboratory preparation of grout. The procedure for grout mixing was as follows:

- (1) Start with a clean, wet mixing bowl. Add all of required water.
- (2) Start mixer at slow speed, and add sand over a period of one minute.
- (3) Add cement over a period of one minute.
- (4) Add gravel over a period of one minute.
- (5) Stop the mixer and add grout admixture. Mix for one minute.
- (6) Stop the mixer and let it sit for one minute, use this time to scrape any material from the sides of the bowl.
- (7) Mix for another two minutes.

Grout was poured immediately after mixing. Since the admixture used contained expansive agents and super plasticizers that were time sensitive, no delay between mixing and pouring was tolerated. All grout was poured in a single lift to the top of the prism. A stinger-type mechanical

vibrator was then inserted to the bottom of the cavity, and slowly drawn out with a side-to-side motion over 15 seconds. Usually, settlement of the grout occurred, dropping the level of grout down between 1/2 and a whole unit height (i.e. 2 to 4 inches in a nominal 16 inch high prism). The grout was then topped off, and the vibrator was inserted 1 or 2 inches into the grout for about 4 seconds. Finally, the grout was struck off flush with the top of the unit. Grout was struck off again, about 30 minutes after pouring, if visible expansion occurred.

Time did not permit sampling and testing of every batch of grout, but a representative sample of grout was poured in both clay and concrete prisms for evaluation of grout properties. Kingsley [23] found that the UBC standard field test for grout [40] did not represent the compressive strength of grout in hollow clay masonry. Therefore, sample cores (2-1/4" diameter x 4-1/2" long) for testing grout compressive strength were removed directly from the cavities of grouted prisms. Ends were milled smooth and parallel, and cores were tested in uniaxial compression. Table 3.3 gives the results of those tests.

Examination of the grout strengths in Table 3.3 reveals two important points. First, the strength of grout cast in concrete prisms is not the same as for grout from the same batch cast in clay prisms. Thus grout strength is dependent on the masonry units it is cast against. Second, the small strength increase from "normal" to "strong" grout -- 15% for

TABLE 3.3 GROUT PROPERTIES

GROUT	UNIT MATERIAL	MEAN COMPRESSIVE STRENGTH	NUMBER OF SPECIMENS	C.O.V.
NORMAL	CLAY	3205	3	0.02
NORMAL	CONCRETE	4226	4	0.08
STRONG	CLAY	3724	4	0.16
STRONG	CONCRETE	4437	4	0.18

clay and 5% for concrete -- is not in keeping with the 100% increase in cement content and the 41% decrease in water-cement ratio. Experience with concrete and mortar [13] suggests that a greater increase in strength might have been expected. Thus the migration of water from grout to the surrounding masonry units, and the resulting shrinkage and decrease in grout water-cement ratio, have a profound effect on grout properties [24,29,31].

In order to evaluate the thoroughness of compaction and presence of flaws and shrinkage cracks in the grout cores, representative prisms were cut vertically through the grout cores. Figures 3.3-3.4 show photographs of representative specimens. Figure 3.3 shows the shrinkage cracks visible

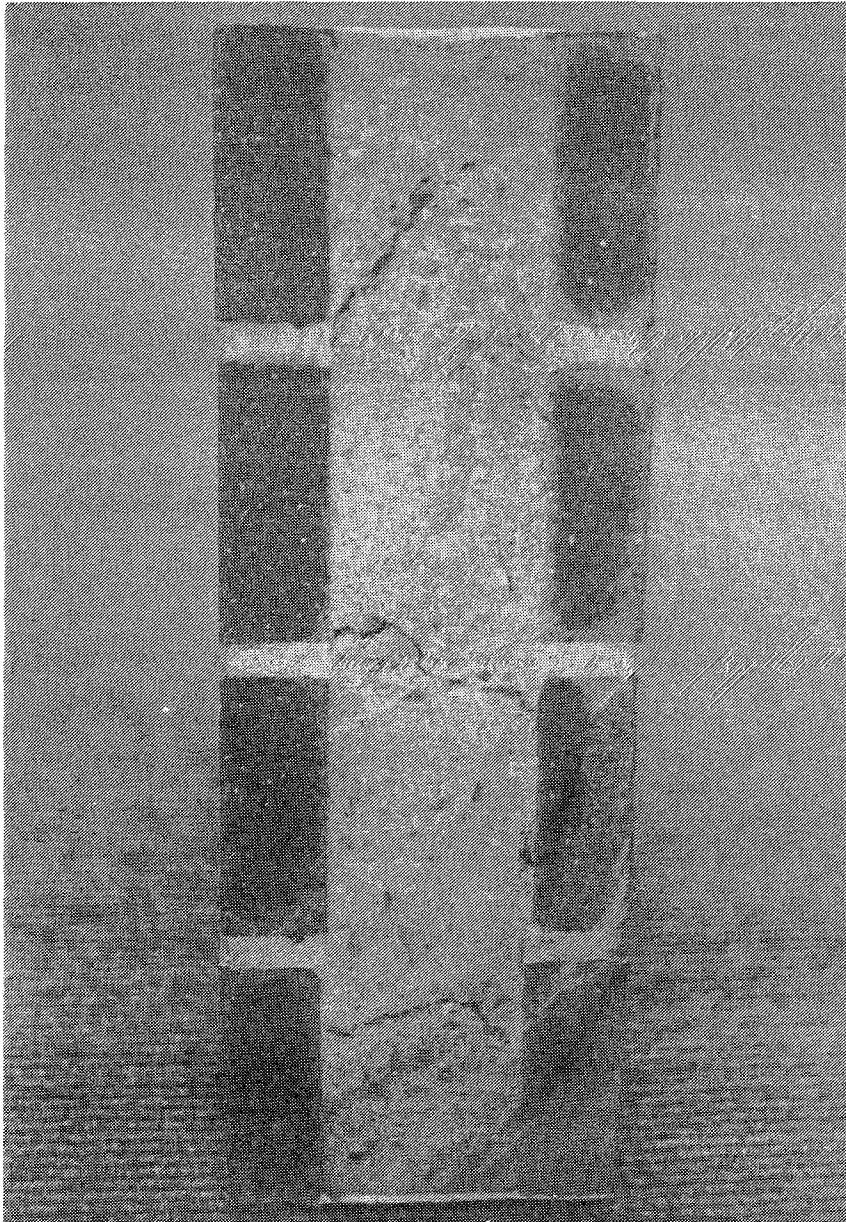


FIGURE 3.3 GROUT COMPACTION IN CLAY PRISMS

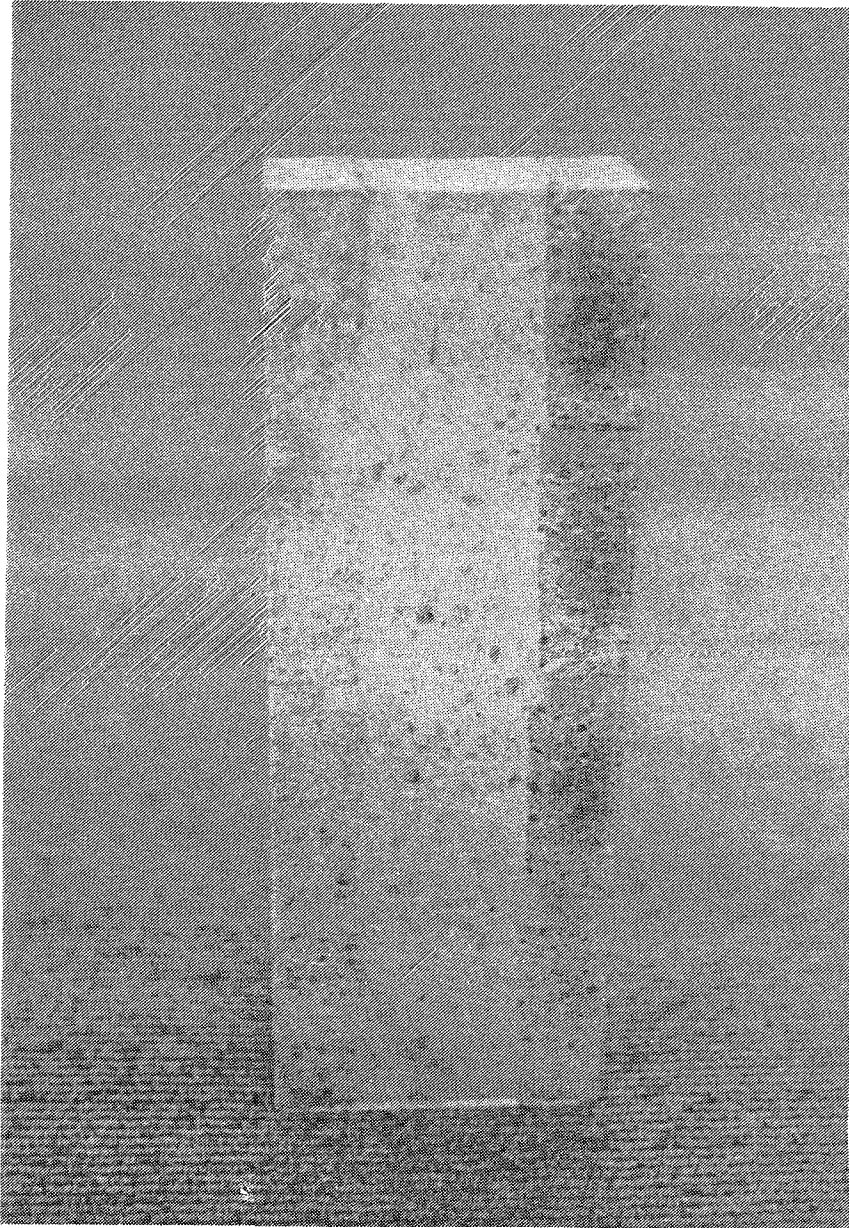


FIGURE 3.4 GROUT COMPACTION IN CONCRETE PRISMS

for the normal grout/clay specimens. The effect of these cracks on compressive strength is reflected in the low values for normal grout in clay, shown in Table 3.3.

It is important to note that the suction of water from grout and mortar was not proportional to the IRA's of the units [24]. While the concrete units had much higher IRA's (see Table 3.1), the grout and mortar in contact with the clay units lost water much more quickly than in the concrete units. This was evident by the quick rate that mortar and grout stiffened when in contact with the clay units. Grout was too stiff to vibrate within 10 minutes after pouring in the clay prisms, but grout from the same batch cast in concrete prisms remained plastic up to 30 minutes after pouring.

3.5 PRISM CONSTRUCTION

Prisms were constructed with the aid of a jig, which was designed to insure consistent mortar joint thickness, plumbness, and end parallelism. All prisms were four units high and all had full mortar bedding. (Fig. 3.5).

Capping, was done on smooth glass plates using a high strength gypsum plaster (US Gypsum Hydrostone). Prisms were air-cured from 40-60 days at an average temperature of 71 degrees Fahrenheit.

A detailed description of the prism building jig and the procedures for construction and capping of prisms are provided in reference [46].

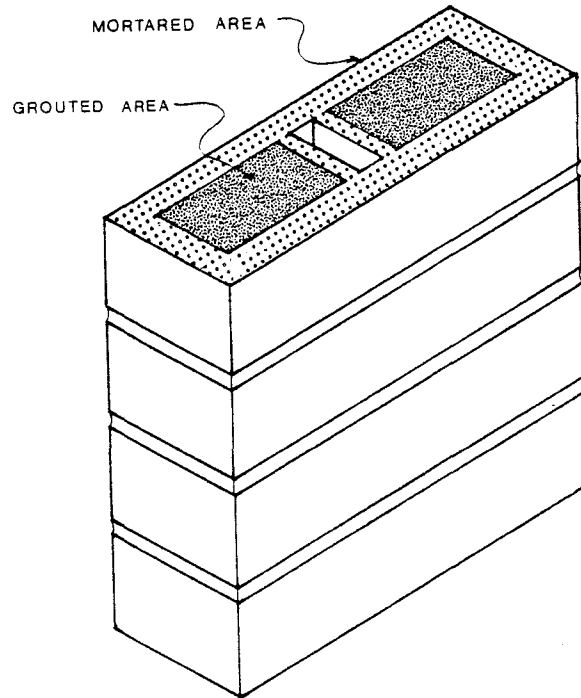


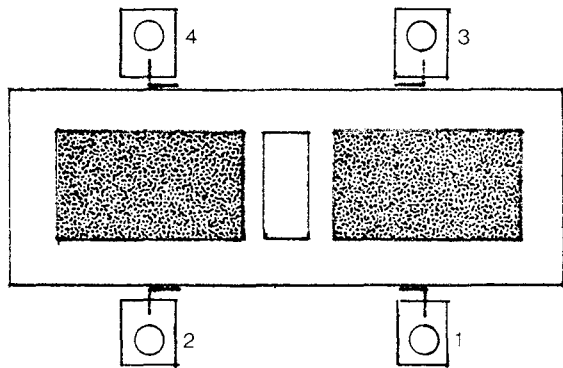
FIGURE 3.5 MORTARED AND GROUTED AREAS OF PRISMS

3.6 PRISM INSTRUMENTATION

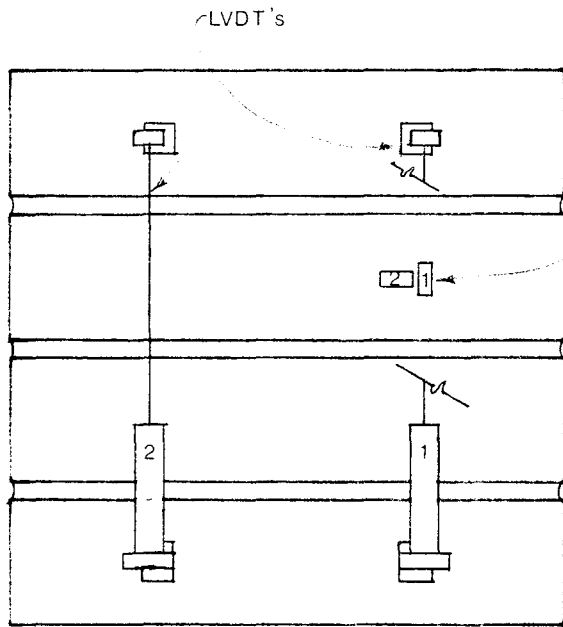
Each prism was instrumented as shown in Fig. 3.6. Four LVDT's (Schaevitz HRDC 200) were mounted, with a 12" gage length between the top and bottom units. The mounting angles were epoxied in place using a spacer bar to insure that a LVDT location was identical for all prisms.

Four strain gages, (Micro-Measurements Type EA-06-250BB-120), two vertical and two horizontal, were mounted on opposite sides of a middle unit as shown in Fig. 3.6. Before mounting the gages, the unit surface was coated with a fast setting polyester resin compound (Celtite 21-05) and ground smooth.

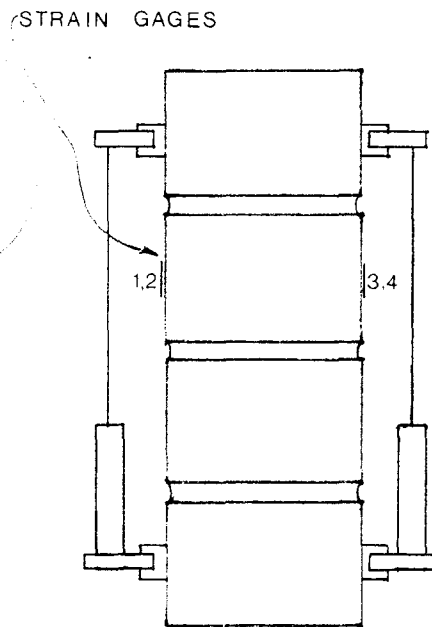
The prisms tested with reduced platen restraint had no



TOP



FRONT



SIDE

FIGURE 3.6 PRISM INSTRUMENTATION

externally mounted LVDT's or vertical strain gages. Instead, a series of horizontal strain gages were fixed to the top two units of the prism as shown in Figure 3.7. Gages 1-5 were on the wide face and gages 6-10 were on the narrow face. The different instrumentation for the reduced platen constraint prisms was designed to determine how the reduced restraint affected the relative lateral strain distribution in clay and concrete masonry.

3.7 PRISM TRANSPORTATION

While the prisms were constructed in Boulder, Colorado, they were tested 35 miles away at the Federal Bureau of Reclamation Laboratory in Denver. In order to avoid specimen damage during transportation, the prisms were clamped, 10 at a time, between two foam padded wooden pallets

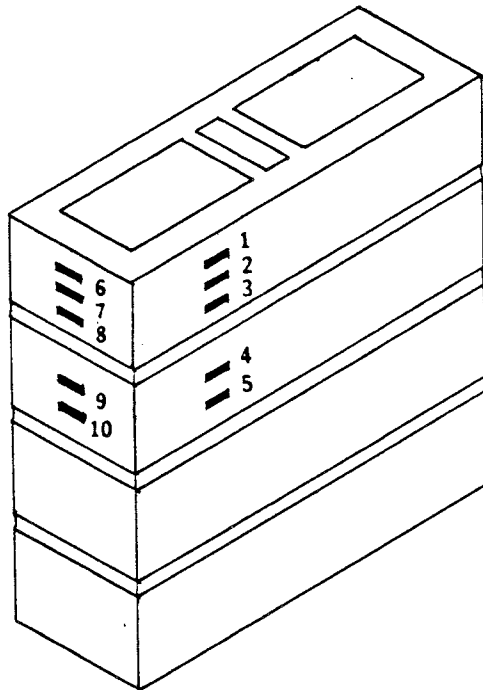


FIGURE 3.7 PRISM INSTRUMENTATION
FOR REDUCED PLATEN RESTRAINT

specially constructed for the job. This insured that the prisms would not slide, rock, or fall over during the trip. The system was effective, as no prisms were damaged during transportation throughout the project. Prisms were transported at least one week before testing so prisms were at room temperature when tested.

3.8 TEST MACHINE

Prisms were tested in a 1,000,000 lb. capacity, servo-controlled hydraulic testing machine (Figure 3.8.). The hydraulic system was controlled by an MTS-443 controlling system.

The platens are 21 inch square milled steel plates. The bottom platen is four inches thick and rests on another

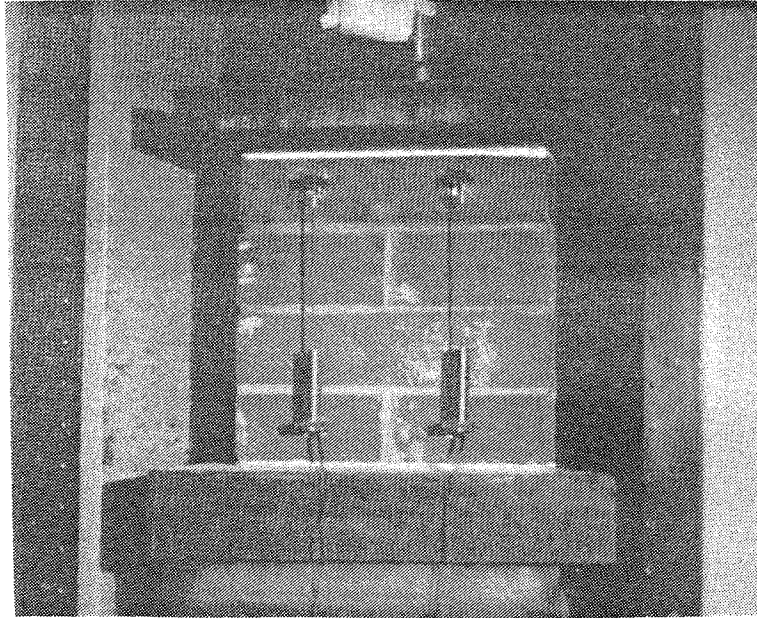


FIGURE 3.8 PRISM IN PLACE IN TEST MACHINE

steel plate 4" x 18" x 18". The top platen is two inches thick and is suspended from a 12" diameter spherical head. Originally, the bottom platen was only two inches thick, and rested on a 4-7/8" diameter load cell. This platen was found to be unacceptably flexible, and the results of five prisms tests conducted with it were discarded. Previous researchers [4,19,37] have also noted problems with platen flexibility affecting test results.

The flexibility inherent in the machine was measured by compressing a strain-gaged aluminum cylinder and comparing deformations measured by the strain gages with those measured by the machine's internal ram LVDT. The machine flexibility so measured was 5.37×10^{-5} in/kip.

3.9 INTERFACE FRICTION REDUCTION

For the one series of prisms to be tested with reduced platen restraint, an interface friction reduction system (I.F.R.) was employed. The I.F.R. consisted of two sheets of 0.005" thick teflon separated by a thin film of Mobil axle grease. This system, placed between a smooth gypsum plaster cap and a milled steel platen on both ends of a prism, has been shown to have a coefficient of friction of 0.014 [2].

3.10 PRISM TESTS

For each test, the prism was carefully centered in the machine, and preloaded to a load of 50 lb. At this point, a zero reading was taken on all LVDT's (four mounted on

specimen and one internal ram LVDT), strain gages and the load cell. A displacement was then applied to the specimen using a standard ramp function at a rate of 25,875 $\mu\text{in}/\text{min}$. (approximate strain rate = .0017 in/in/min). At increments of 1500 μin , load and displacements were recorded by an HP 3497 data acquisition system, and an HP85 microcomputer. The test was continued well beyond ultimate load, and terminated when the load capacity of the prism remained relatively constant with continuing displacement. Data were stored and backed up on disks for plotting and printouts.

3.11 MODIFICATION OF STRESS-STRAIN DATA TO ACCOUNT FOR MACHINE STIFFNESS

Prism deformations were measured by an internal ram LVDT and by four external LVDT's mounted directly to the prism (Figure 3.6). Figure 3.9 is a sample of typical stress-strain data from a prism test, showing both RAM and external LVDT results. Large discrepancies exist between the two curves. These are the result of the machine take-up, reflected in the initial stiffening portion of the RAM curve, and machine flexibility, which is reflected in the softer loading curve and steeper falling branch on the RAM LVDT stress-strain curves [35].

While the external LVDT's give a more accurate loading curve than the RAM LVDT, cracking and spalling of the unit faceshells at failure renders the external LVDT's useless for measuring post-peak deformations. In order to take advantage of the more complete data provided by the RAM

LVDT, a technique similar to that developed by Priestley and Elder [35] was adopted to adjust the stress-strain curve for machine take up and flexibility effects.

The corrected RAM LVDT displacement were calculated using the following formula:

$$\Delta_{pc} = \Delta_p - \Delta_t - F_m P$$

$$\epsilon = \Delta_{pc}/h$$

where:

Δ_{pc} = corrected RAM displacement at a load P (in.)

Δ_p = uncorrected RAM displacement a load P (in.)

Δ_t = machine take-up (in.)

F_m = machine flexibilty = 5.37×10^{-5} in /kip
P = load (kips)

ϵ = strain at a load P (in/in)

h = prism height (in)

The machine take-up, Δ_t , was determined for each curve individually by extending the linear portion of the stress-strain curve down to the horizontal axis and defining Δ_t as the displacement at the intersection.

Priestley and Elder [35] also included the effect of elastic unloading of the top and bottom units during the falling branch of the curve. This effect was not included here, as observed failures often included the end units.

Figure 3.10 shows the curve of Figure 3.9 corrected for machine stiffness. The agreement between the LVDT curve and the RAM curve was good for most cases, but for others the corrected curve remained softer for the loading portion than the external LVDT's showed. For this reason, measurements

of initial stiffness were taken from average external LVDT plots while post peak data was taken from corrected RAM plots.

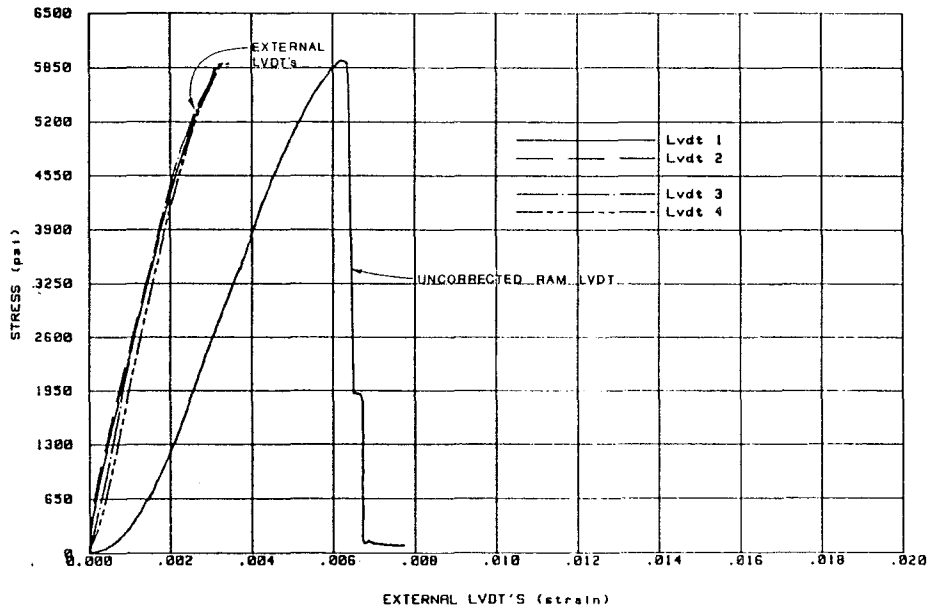
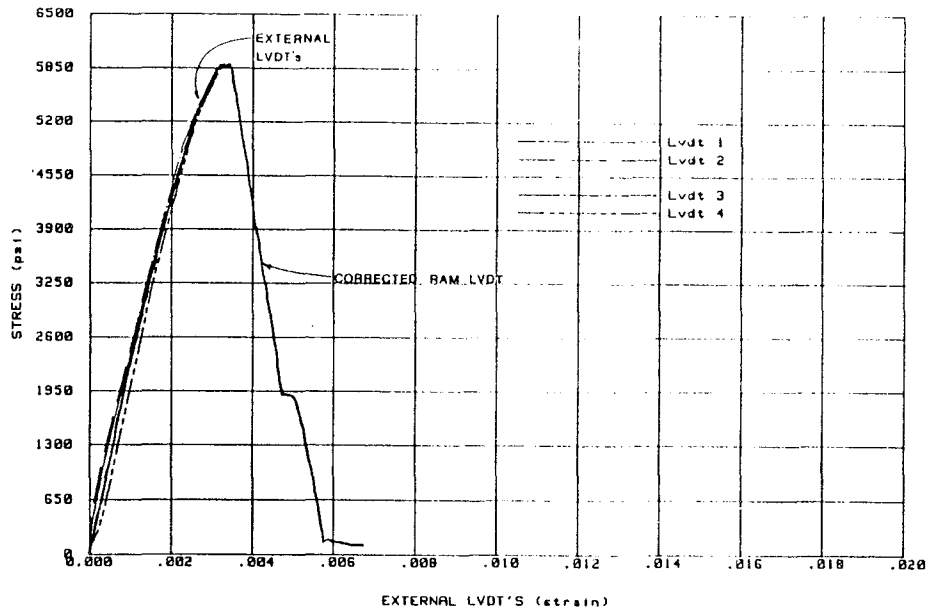


FIGURE 3.9 UNCORRECTED STRESS-STRAIN DATA



3.10 CORRECTED STRESS-STRAIN DATA

4. RESULTS OF PRISM TESTS

4.1 STRESS-STRAIN DATA

The prism test results are summarized in Table 4.1 and Figures 4.1 - 4.24. The RAM-LVDT stress-strain curves from all of the prism tests, adjusted for machine error as described in Section 3.11, are presented in Figures 4.1 - 4.20. Representative data from the externally mounted LVDT's and strain gages are presented in Figures 4.21 - 4.23. (See Figure 3.6 for location of LVDT's and strain gages). Figure 4.24 shows example lateral strain data from the reduced platen constraint tests. A complete listing of LVDT data is given in Appendix A. Lateral strain data from the reduced platen constraint tests are also given in Appendix A. Strain gage data for the remaining prism tests are not available at this time.

Table 4.1 contains a summary of important parameters derived from Figures 4.1 - 4.20. The following sections describe these parameters in more detail.

4.1.1. ULTIMATE STRENGTH AND STRAIN

The reported ultimate strength (f'_m) is the maximum stress attained by a prism, calculated by dividing the maximum load by the net loaded area. For grouted prisms, the net area equals the gross cross-sectional area of the units, and for ungrouted prisms the net area of the unit is used.

The peak strain (ϵ_p) is the strain corresponding to the ultimate strength described above. The strain reported

TABLE 4.1

TEST SERIES	MATERIAL ULTIMATE STRENGTH		STRAIN AT SEGANT ULTIMATE		SLOPE OF FALLING BRANCH		RESIDUAL STRENGTH AT ULT. STRAIN		TOUGHNESS AT 1.5 C _p AT 2.0 C _p		TOUGHNESS AT 1.5 C _p AT 2.0 C _p		POISSON'S RATIO AT 50% f' _m		UNIT STRENGTH		MORTAR CUBE STRENGTH		GROUT STRENGTH	
	f' _m psi	Es ksi	C _p in/in	Es ksi	ksi	f' _r % of f' _m	psi	% of T	psi	% of T	E _{sec} /f' _m	% of T	psi	% of T	psi	psi	psi	psi	psi	psi
6" GROUTED	5765	2317	.0030	2317	-3190	0.07	11.46	156%	166	402	0.442	12900	1671	12900	1671	3200	3200	3200	3200	3200
CONC.	4084	2340	.0024	2340	-2530	0.06	7.64	153	168	573	0.274	3600	1884	3600	1884	4200	4200	4200	4200	4200
4" GROUTED	3946	2365	.0021	2365	-1960	0.08	5.14	166	197	599	-	9000	1602	9000	1602	3200	3200	3200	3200	3200
CONC.	3037	1523	.0025	1523	-2110	0.07	5.04	151	167	502	-	3900	1812	3900	1812	4200	4200	4200	4200	4200
8" GROUTED	4523	2627	.0022	2627	-2660	0.07	9.31	151	168	581	0.360	11300	1709	11300	1709	3200	3200	3200	3200	3200
CONC.	4040	2609	.0023	2609	-2180	0.07	8.92	155	175	646	0.280	3100	1369	3100	1369	4200	4200	4200	4200	4200
6" UNGROUTED	5704	1837	.0032	1837	-3480	0.07	9.24	162	169	322	0.243	12900	1638	12900	1638	-	-	-	-	-
CONC.	2602	1429	.0027	1429	-2960	0.05	4.13	147	169	549	0.266	3600	1709	3600	1709	-	-	-	-	-
8" UNGROUTED	5373	2167	.0028	2167	-2590	0.06	10.27	150	168	403	0.218	11300	1583	11300	1583	-	-	-	-	-
CONC.	2113	1234	.0028	1234	-2390	0.07	3.96	143	155	584	-	3100	1690	3100	1690	-	-	-	-	-
6" RUNNING BOND	4745	2151	.0024	2151	-2550	0.06	9.31	156	176	453	-	12900	1872	12900	1872	3200	3200	3200	3200	3200
CONC.	3622	1918	.0026	1918	-2310	0.06	7.02	154	180	530	0.239	3600	1754	3600	1754	4200	4200	4200	4200	4200
6" TYPE S MORTAR	5595	2352	.0024	2352	-3100	0.05	11.97	150	161	420	-	12900	3419	12900	3419	3200	3200	3200	3200	3200
CONC.	4172	2334	.0025	2334	-2400	0.03	7.60	153	171	560	-	3600	3589	3600	3589	4200	4200	4200	4200	4200
6" STRONG GROUT	5993	2249	.0030	2249	-3000	0.05	12.84	152	162	375	0.283	12900	1689	12900	1689	3700	3700	3700	3700	3700
CONC.	4201	2270	.0025	2270	-2600	0.05	7.89	153	169	540	0.287	3600	1727	3600	1727	4400	4400	4400	4400	4400
6" LOADED PARALLEL TO BEDJOINT	3551	15131	.00331	15131	-2890	0.05	6.82	144	157	426	0.253	12900	2004	12900	2004	3200	3200	3200	3200	3200
CONC.	4177	2239	.0020	2239	-2470	0.06	7.22	157	182	536	0.293	3600	1919	3600	1919	4200	4200	4200	4200	4200
6" REDUCED PLATEN CONSTRAINT	4774	19631	.00301	19631	-3200	0.07	7.93	161	-	411	-	12900	1518	12900	1518	3200	3200	3200	3200	3200
CONC.	3488	19101	.00251	19101	-3380	-	5.10	-	-	548	-	3600	1556	3600	1556	4200	4200	4200	4200	4200

1 These values taken from RAM LVDT data where external LVDT data were inadequate or incomplete.

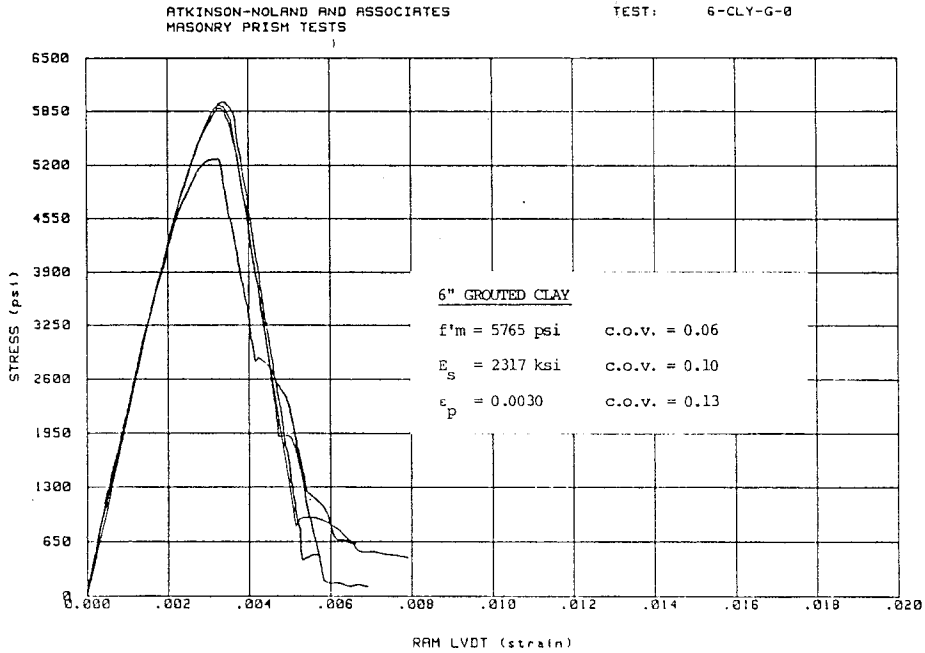


FIGURE 4.1 STRESS-STRAIN DATA: 6" GROUDED -- CLAY

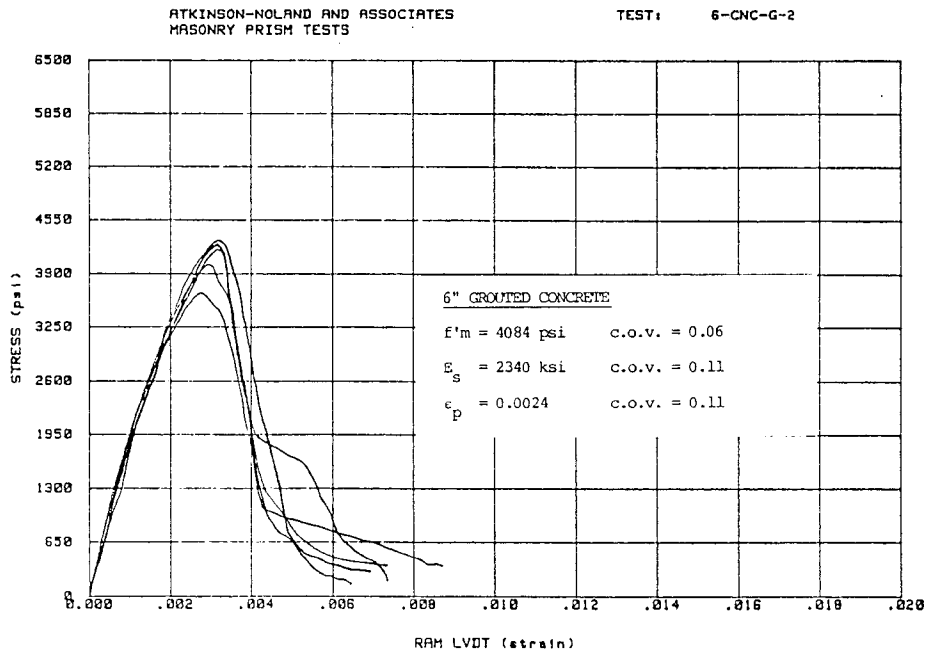


FIGURE 4.2 STRESS-STRAIN DATA: 6" GROUDED -- CONCRETE

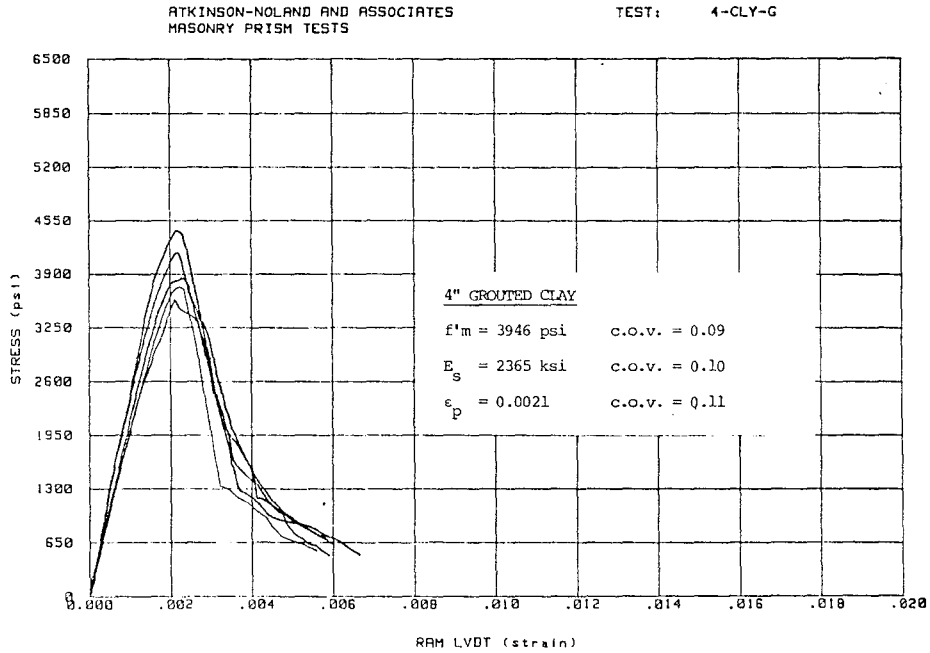


FIGURE 4.3 STRESS-STRAIN DATA: 4" GROUDED -- CLAY

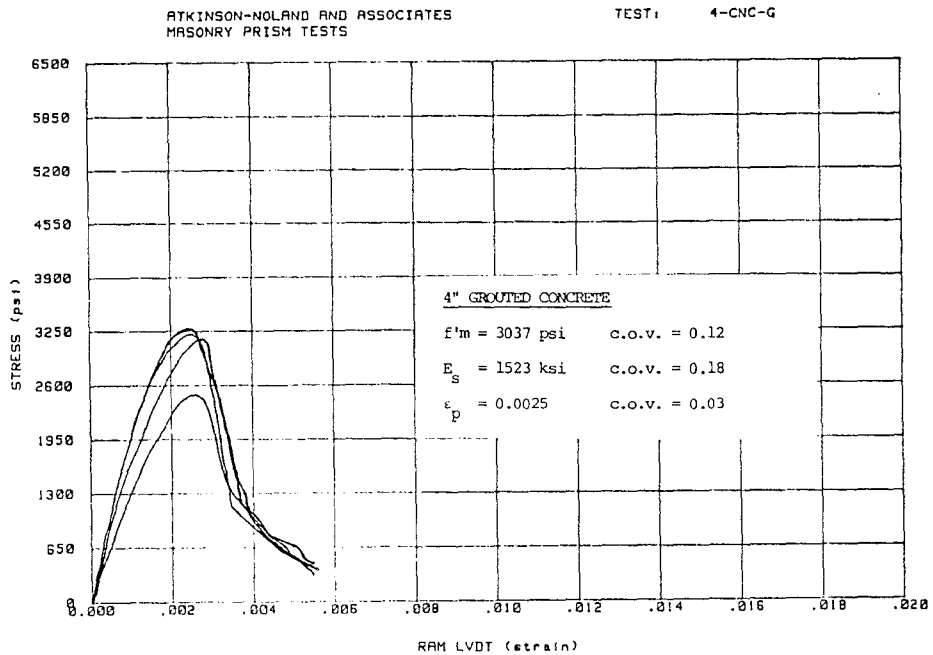


FIGURE 4.4 STRESS-STRAIN DATA: 4" GROUDED -- CONCRETE

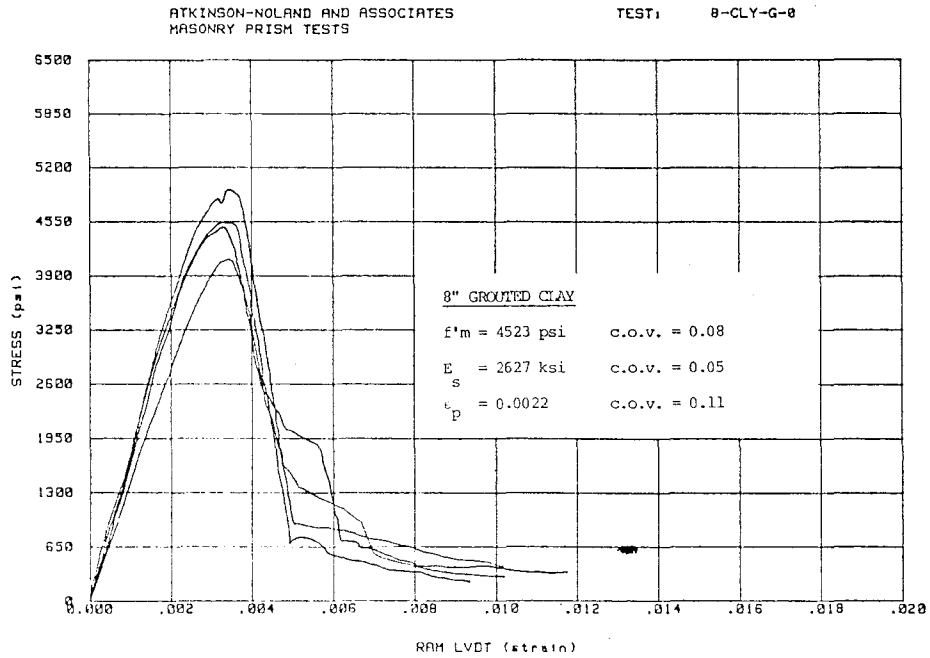


FIGURE 4.5 STRESS-STRAIN DATA: 8" GROUTED - CLAY

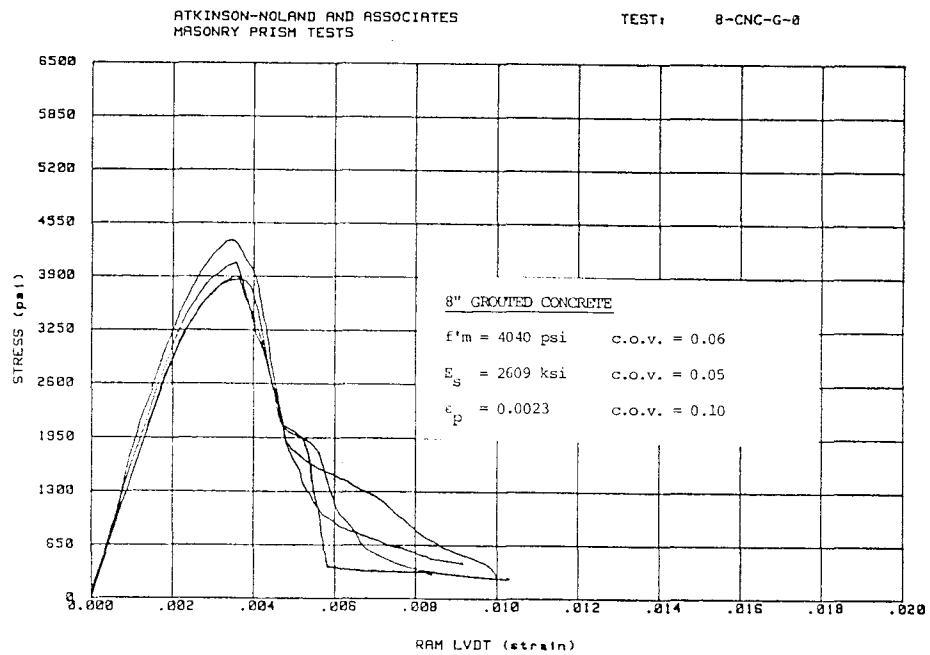


FIGURE 4.6 STRESS-STRAIN DATA: 8" GROUTED - CONCRETE

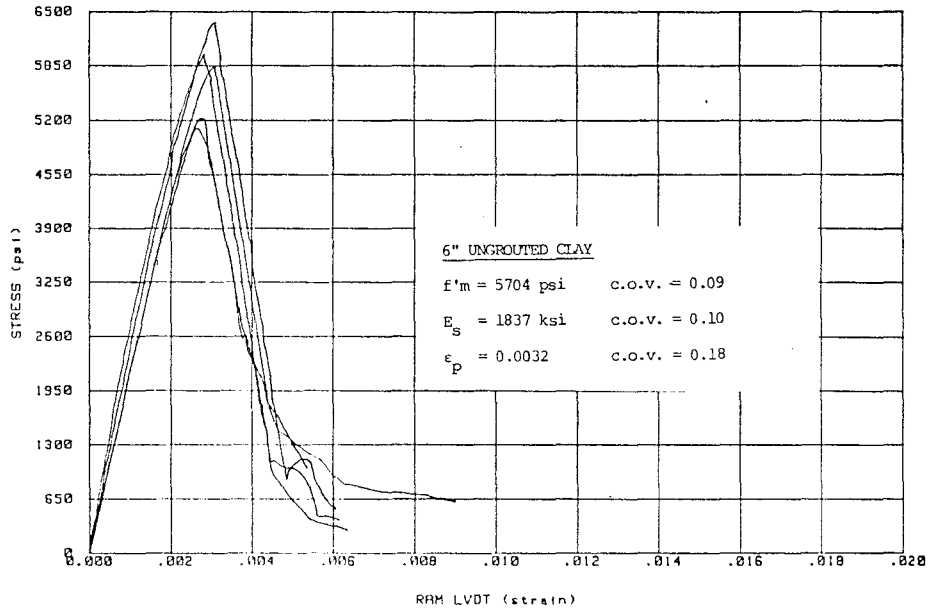


FIGURE 4.7 STRESS-STRAIN DATA: 6" UNGROUTED - CLAY

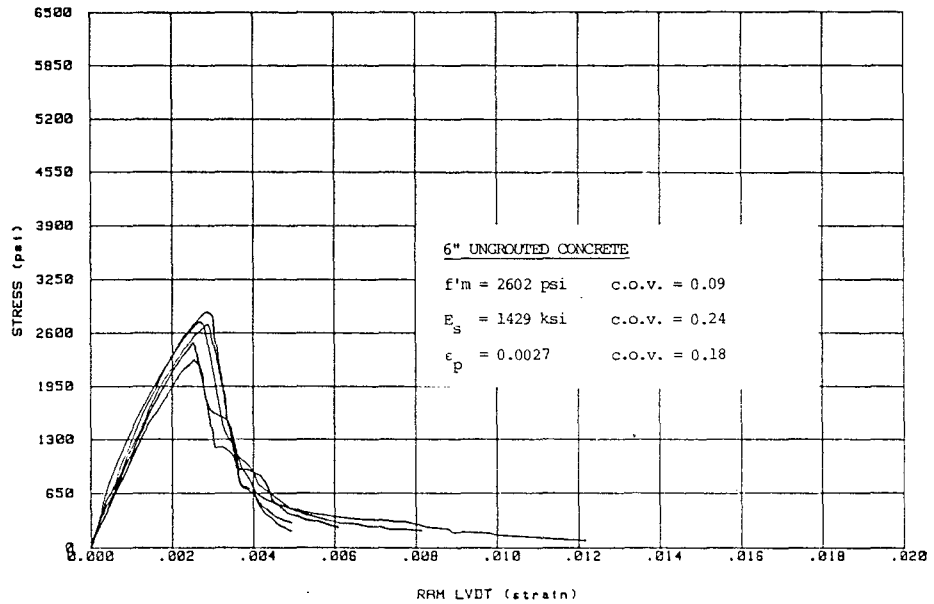


FIGURE 4.8 STRESS-STRAIN DATA: 6" UNGROUTED - CONCRETE

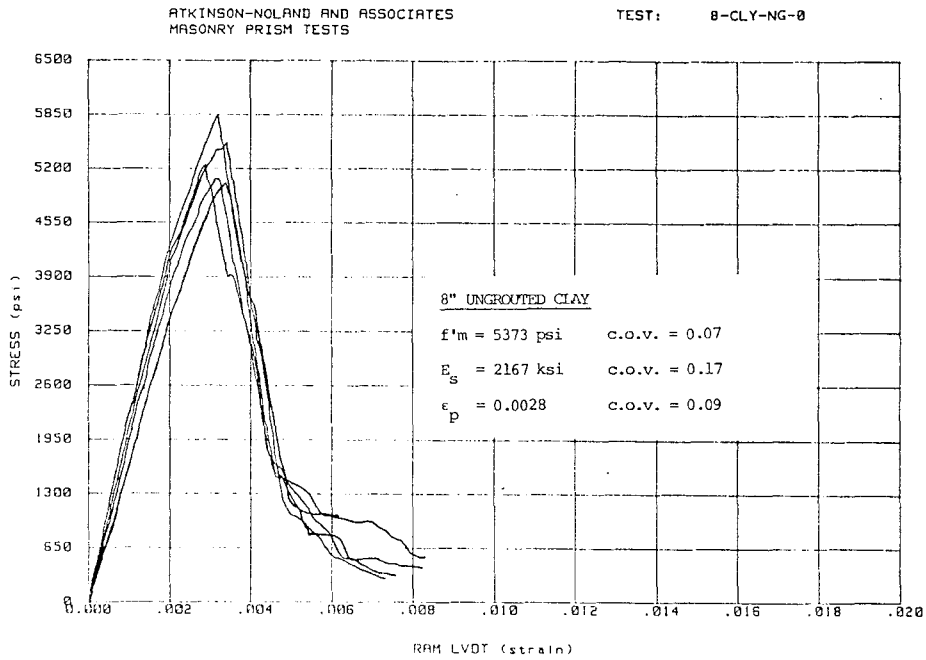


FIGURE 4.9 STRESS-STRAIN DATA: 8" UNGROUTED - CLAY

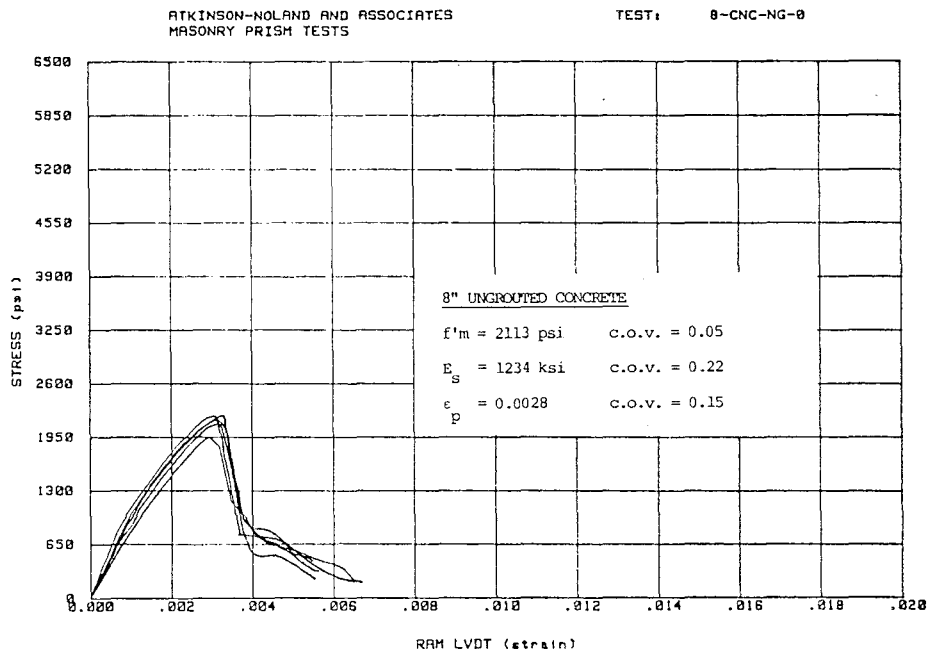


FIGURE 4.10 STRESS-STRAIN DATA: 8" UNGROUTED - CONCRETE

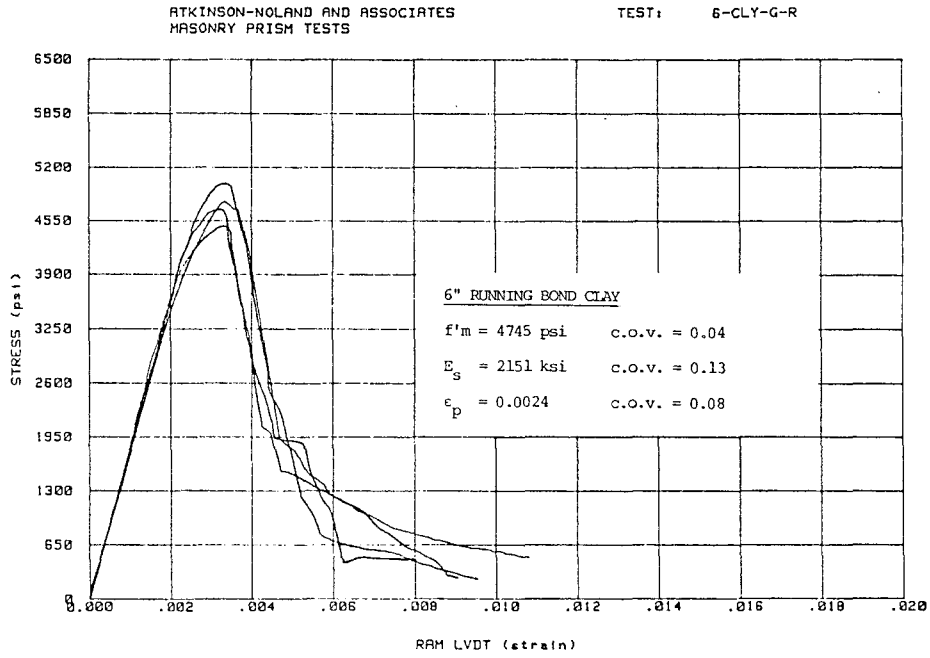


FIGURE 4.11 STRESS-STRAIN DATA: RUNNING BOND - CLAY

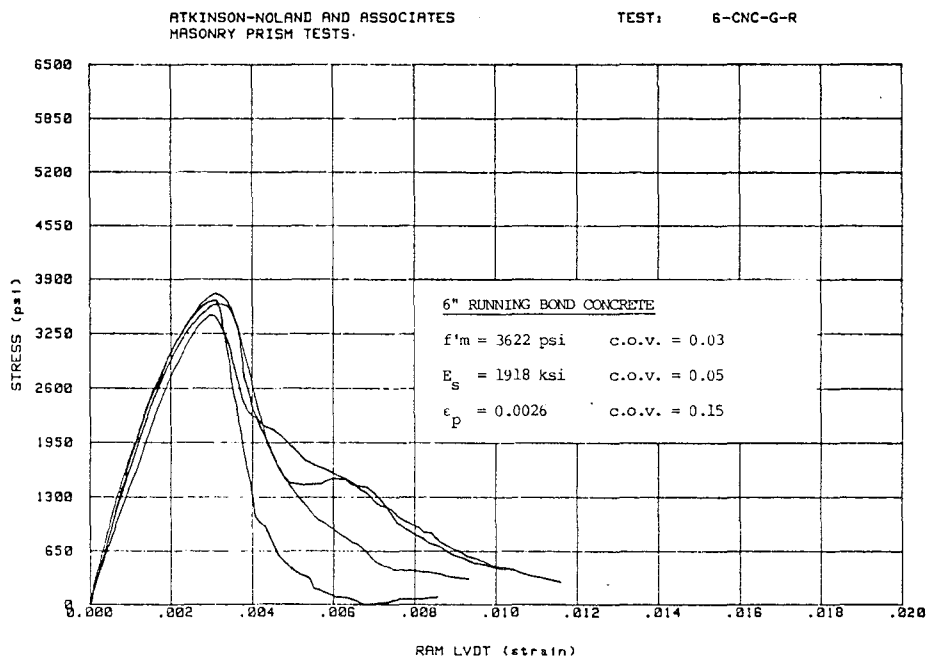


FIGURE 4.12 STRESS-STRAIN DATA: RUNNING BOND - CONCRETE

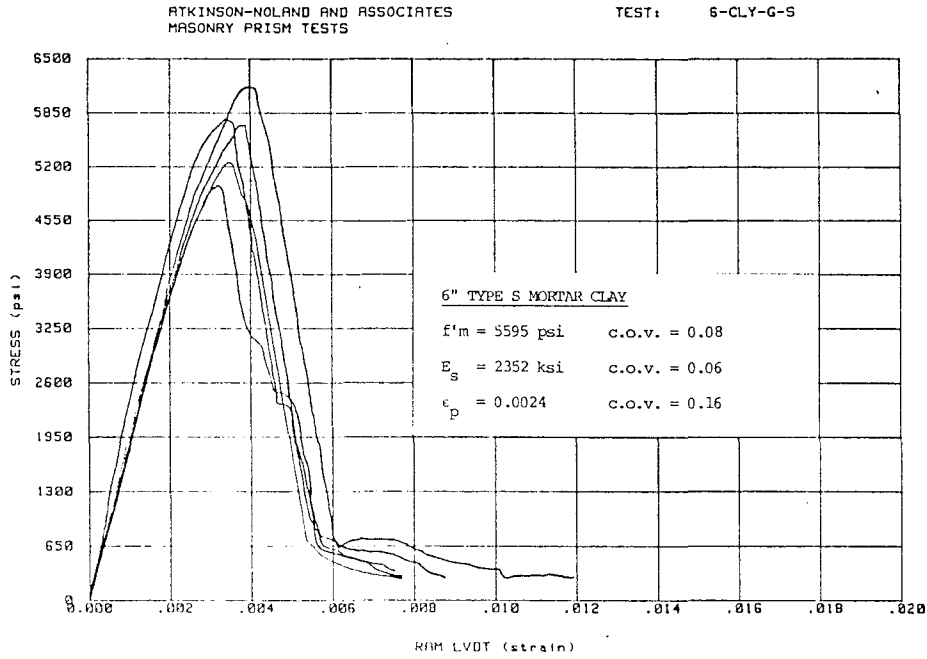


FIGURE 4.13 STRESS-STRAIN DATA: TYPE S MORTAR - CLAY

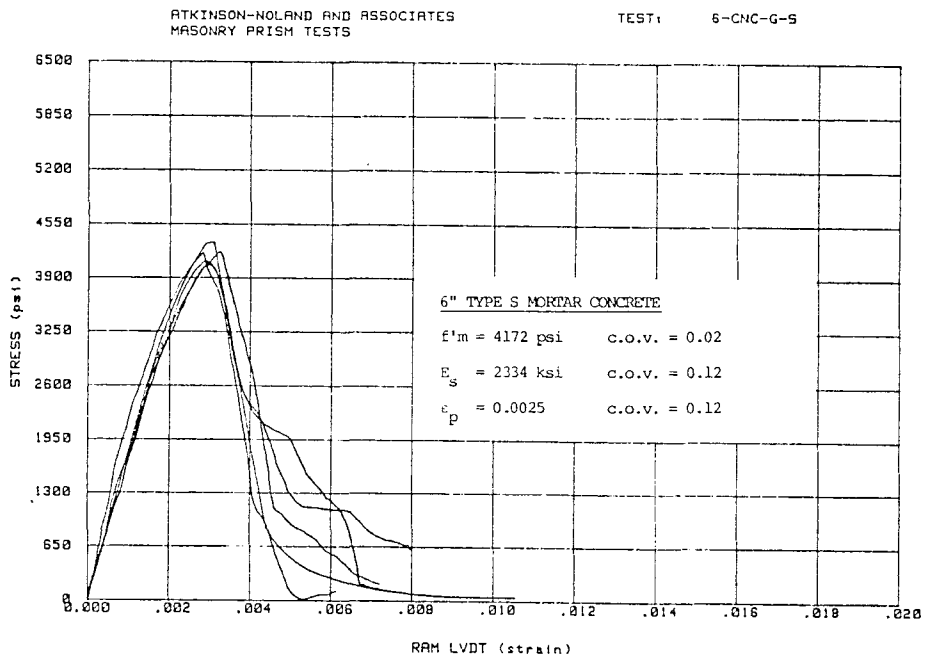


FIGURE 4.14 STRESS-STRAIN DATA: TYPE S MORTAR - CONCRETE

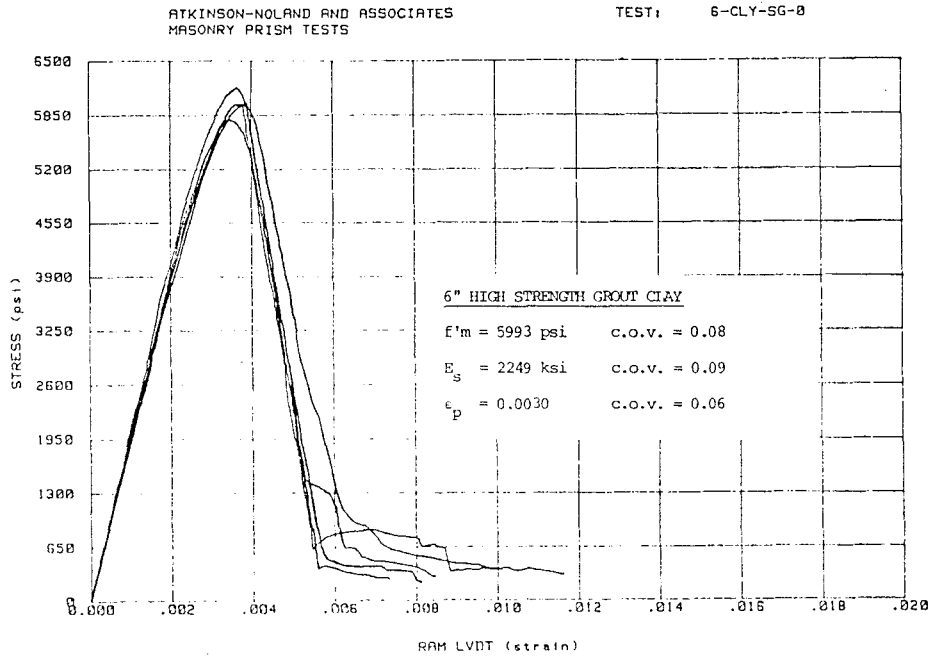


FIGURE 4.15 STRESS-STRAIN DATA: HIGH STRENGTH GROUT - CLAY

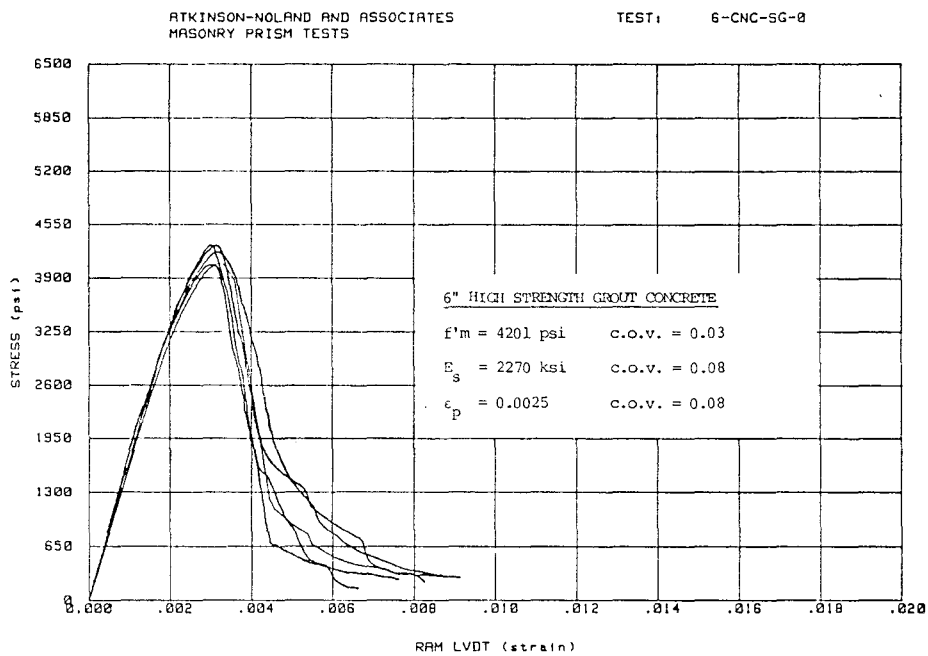


FIGURE 4.16 STRESS-STRAIN DATA: HIGH STRENGTH GROUT - CONCRETE

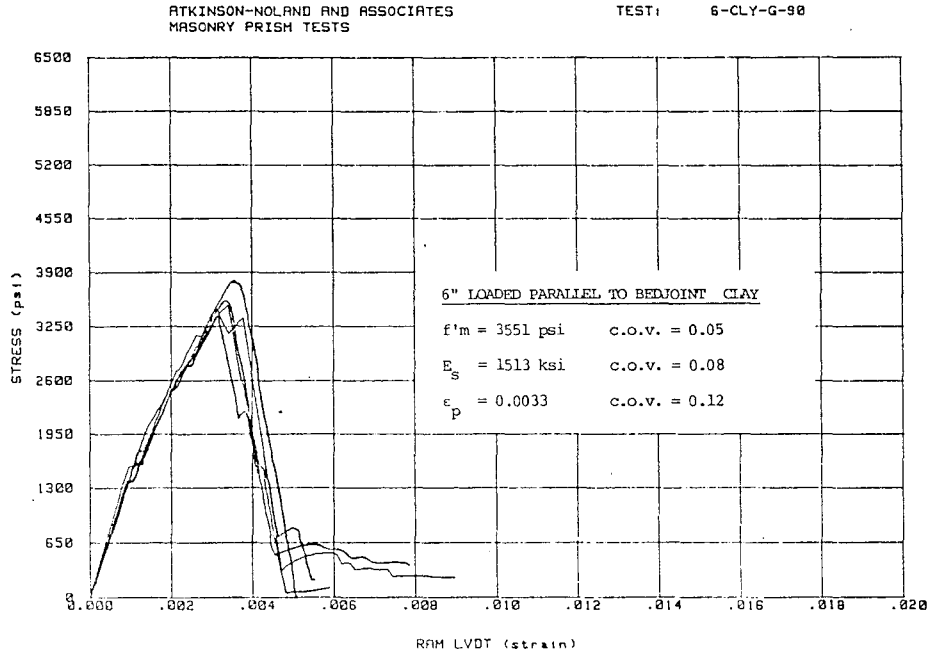


FIGURE 4.17 STRESS-STRAIN DATA: LOAD // TO BEDJOINT - CLAY

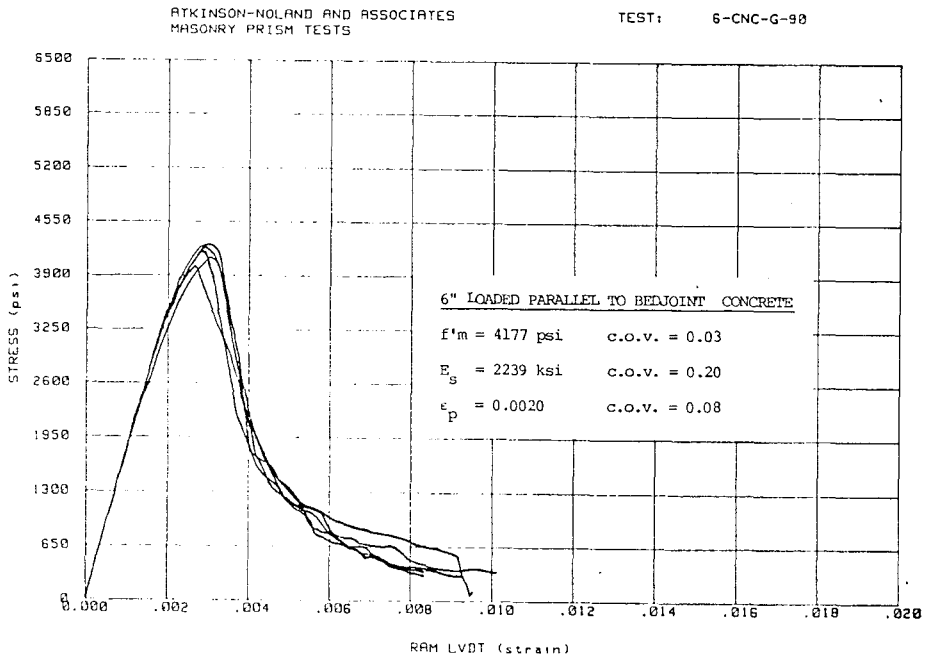


FIGURE 4.18 STRESS-STRAIN DATA: LOAD // TO BEDJOINT - CONCRETE

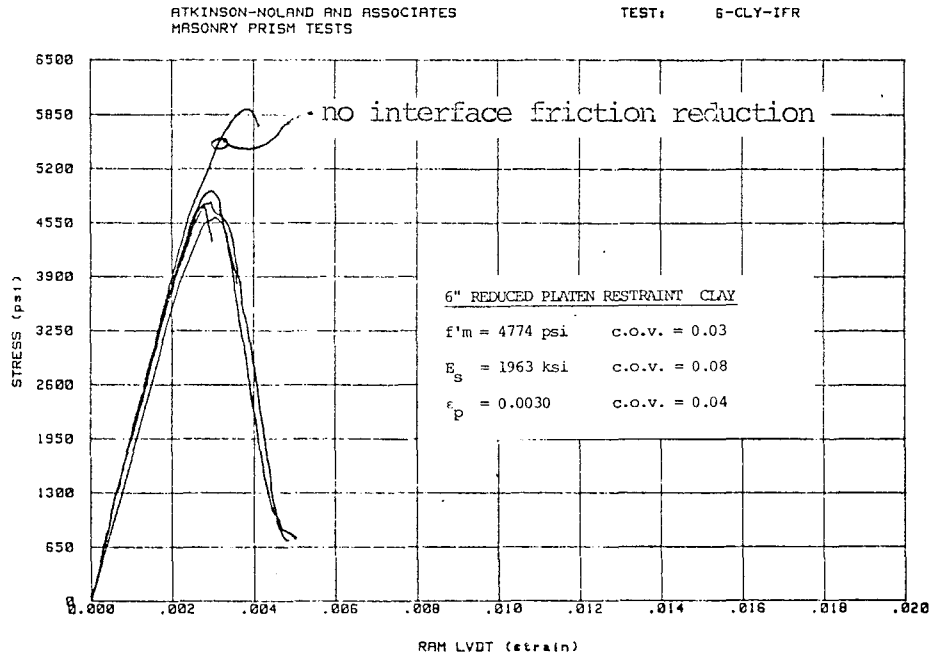


FIGURE 4.19 STRESS-STRAIN DATA: REDUCED PLATEN RESTRAINT - CLAY

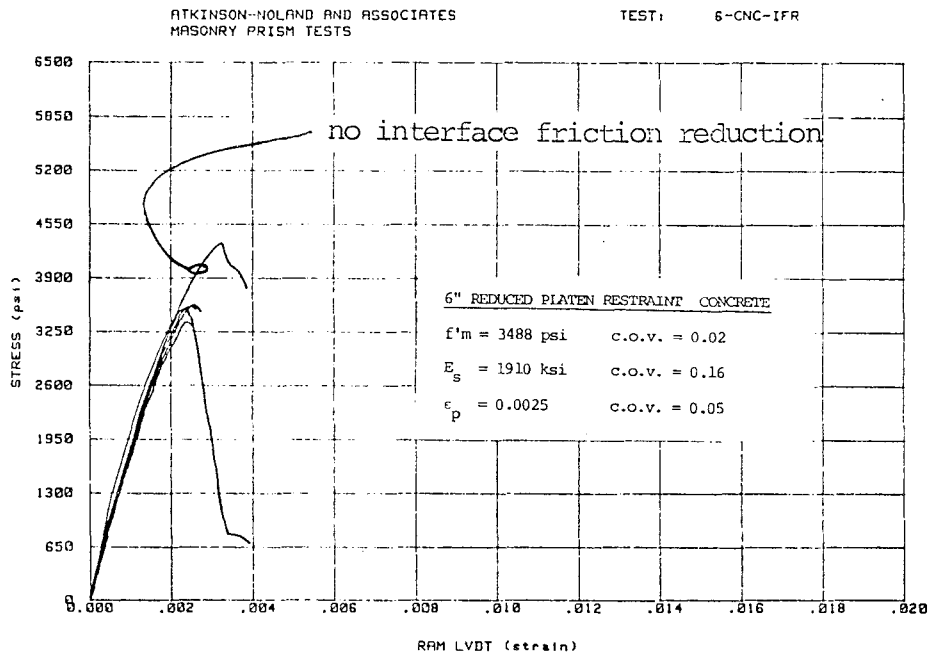


FIGURE 4.20 STRESS-STRAIN DATA: REDUCED PLATEN RESTRAINT - CONCRETE

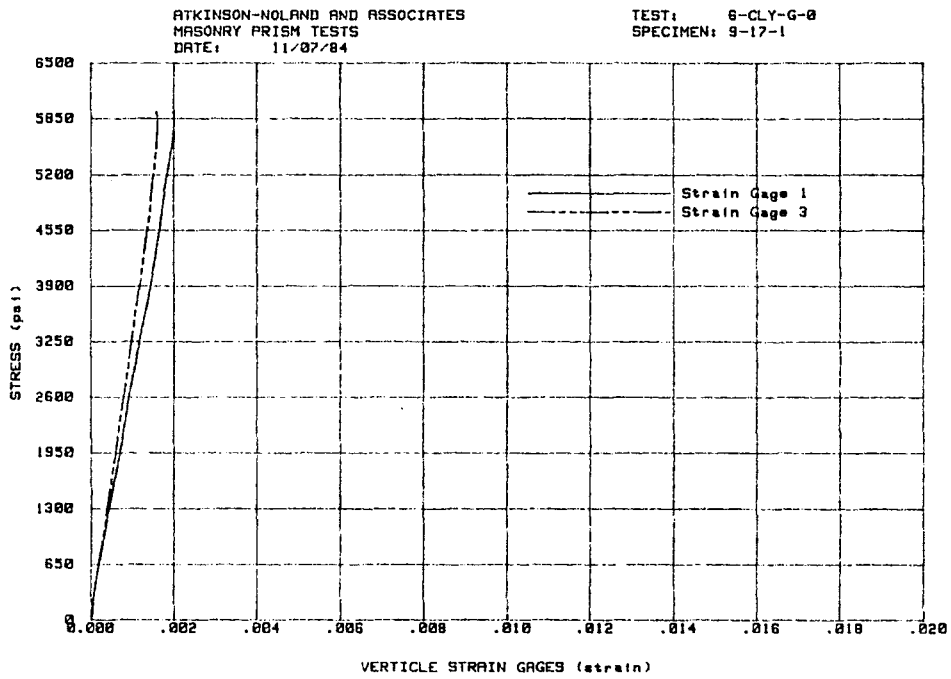


FIGURE 4.21 EXAMPLE OF VERTICAL STRAIN GAGE DATA

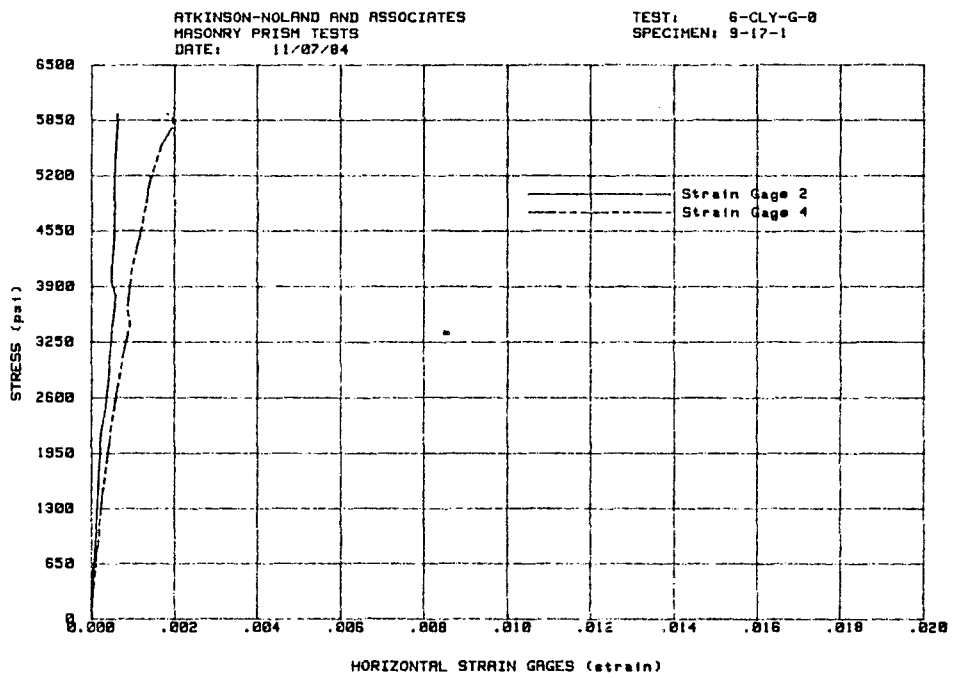


FIGURE 4.22 EXAMPLE OF HORIZONTAL STRAIN GAGE DATA

ATKINSON-NOLAND AND ASSOCIATES
MASONRY PRISM TESTS
DATE: 11/07/84

TEST: 8-CLY-G-8
SPECIMEN: 9-17-1

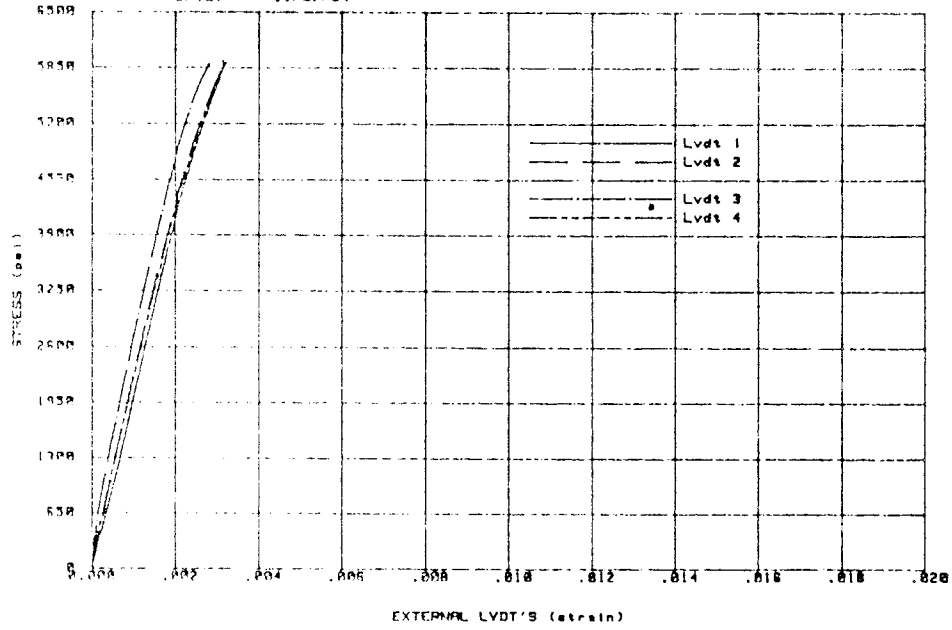
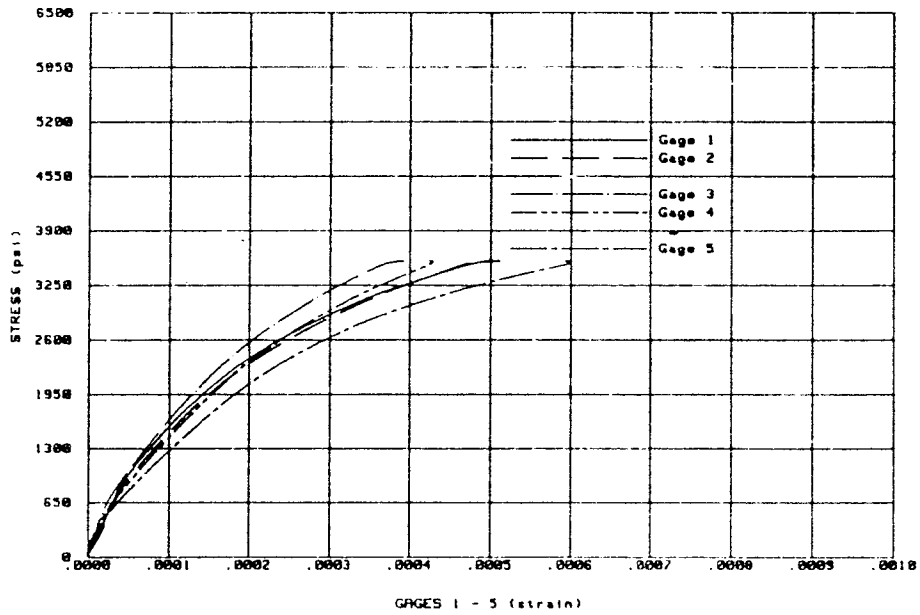


FIGURE 4.23 EXAMPLE OF EXTERNAL LVDT DATA

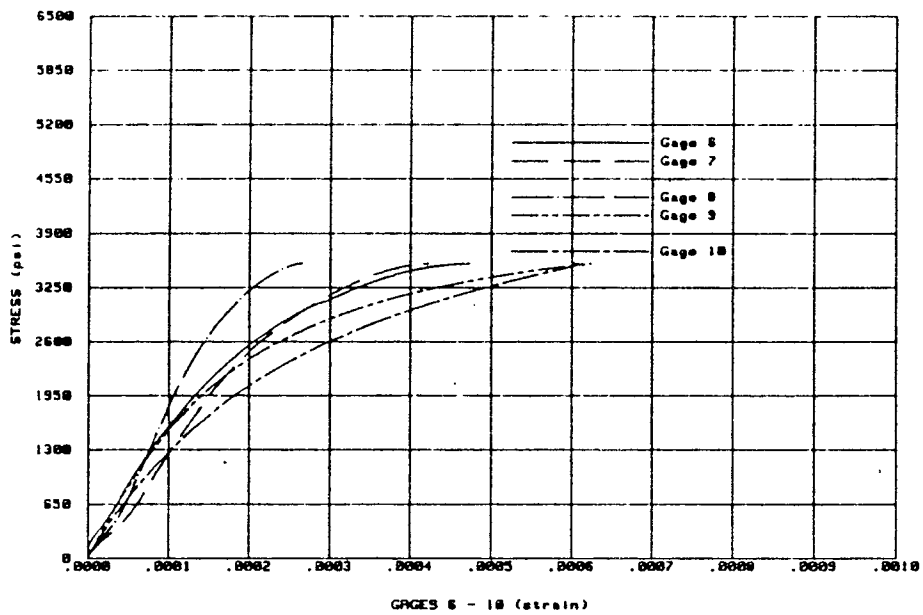
ATKINSON-NOLAND AND ASSOCIATES
MASONRY PRISM TESTS

TEST: 6-CNC-IFR
SPECIMEN: 12-18-4



ATKINSON-NOLAND AND ASSOCIATES
MASONRY PRISM TESTS

TEST: 6-CNC-IFR
SPECIMEN: 12-18-4



4.24 EXAMPLE OF STRAIN GAGE DATA FROM REDUCED PLATEN CONSTRAINT TESTS

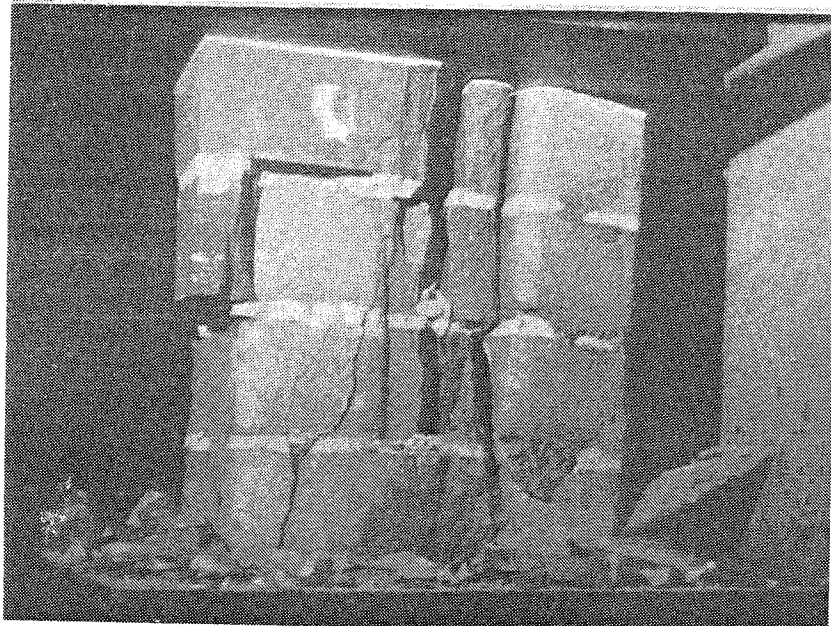
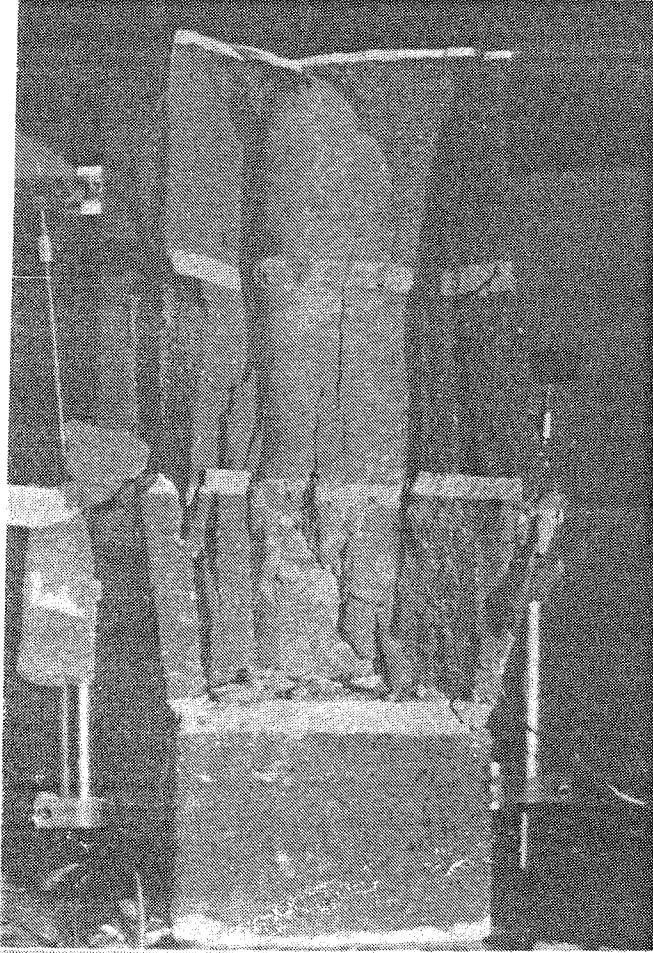
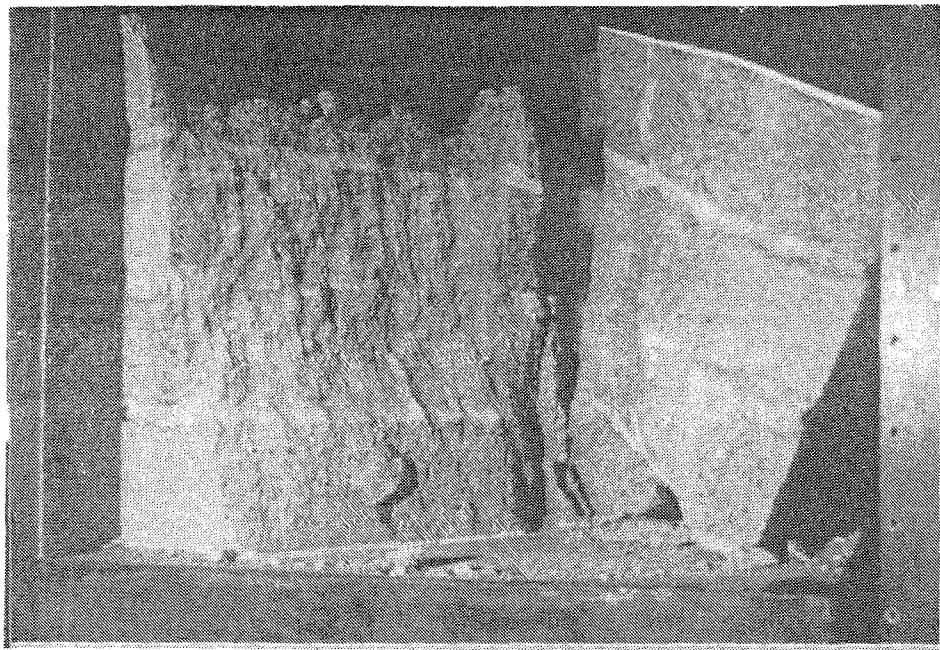
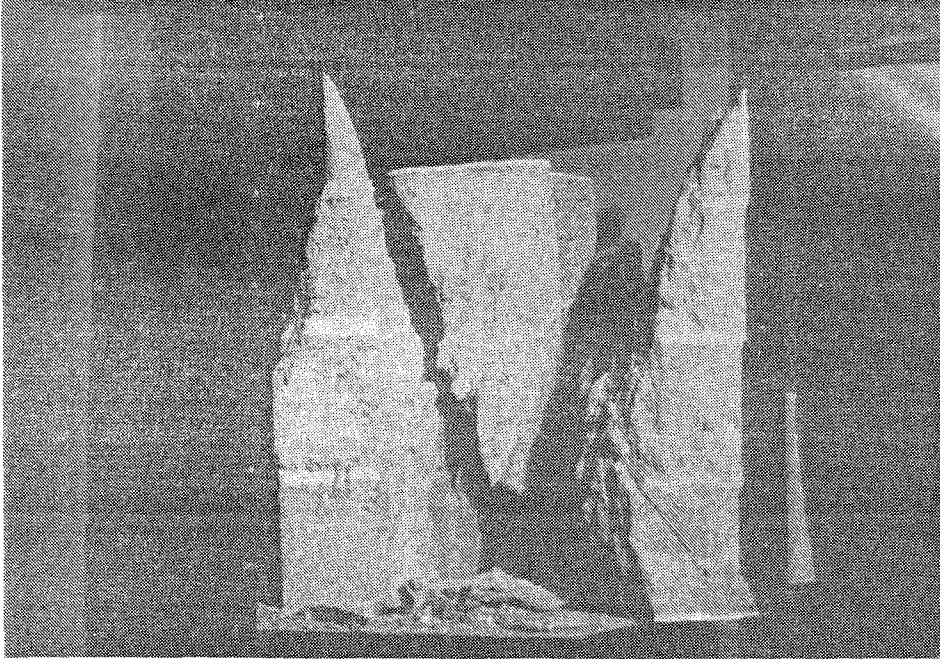


FIGURE 4.25 CLAY PRISM FAILURES.



4.26 CONCRETE PRISM FAILURES

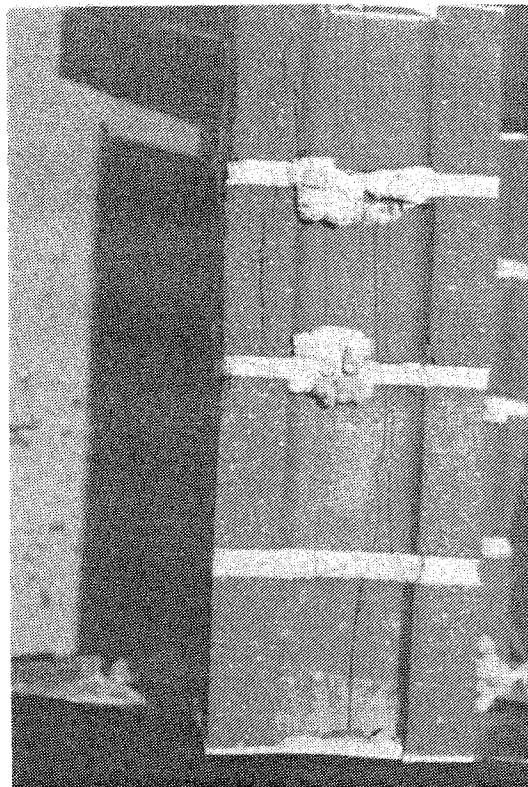


FIGURE 4.27 FAILURE OF CLAY PRISM WITH
REDUCED PLATEN CONSTRAINT

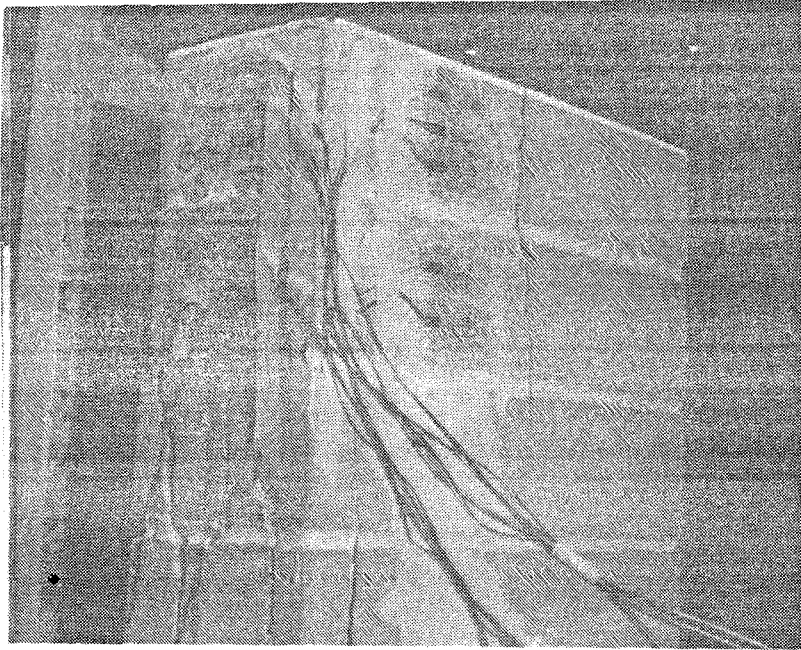


FIGURE 4.28 FAILURE OF CONCRETE PRISM
WITH REDUCED PLATEN CONSTRAINT

is the average of four LVDTs. In some cases, the value of peak strain reported in Table 4.1 will be less than the apparent value in Figures 4.1-4.20, since the average of the external LVDT's was not always in exact agreement with the corrected ram LVDT.

4.1.2. SECANT MODULUS AND SLOPE OF FALLING BRANCH

The secant modulus E_s is the slope of a line passing through the origin and a point on the stress-strain curve corresponding to 50% of the ultimate strength. The secant modulus was taken from the average LVDT curves, not the RAM LVDT curve. Also shown in Table 4.1 is the ratio of the secant modulus to the ultimate strength (E_s/f'_m) which is presented for comparison with code specified values of elastic modulus for working stress design.

The slope of the falling branch was measured by visually estimating the best fit straight line on the falling portion of the curves in Figures 4.1-4.20. The slope of the falling branch on the uncorrected RAM LVDT curves was very nearly vertical in many cases. As a result, the slope of the falling branch on the corrected curves was often only slightly less than the stiffness of the machine itself (approximately 3400 ksi for a nominally 6 x 16 x 16 inch prism). It should be recognized that measurements of the falling branch characteristics of a material are limited by the deformation characteristics of the test machine itself, and if a material has an unloading curve stiffer than that of the machine, actual material behavior may be masked by

machine response. Specifically, the reported corrected falling branch slope for such a material would be nearly equal to the measured machine stiffness. Thus the values of falling branch slope in Table 4.1 may, in some cases, underestimate the actual material properties.

4.1.3 RESIDUAL STRENGTH

The "residual strength" is a fictitious quantity suggested by the shape of the stress strain curves: the slope of the falling branch decreases as axial strain increases, approaching, but never attaining, a level of constant stress. A visual estimate of this constant stress is reported here as the "residual strength". It is included for purposes of comparison with the modified Kent-Park Model [35], which includes a similar parameter.

4.1.4 TOUGHNESS

The "toughness" is the area under the stress-strain curve at a specified level of strain. At peak strain, the toughness (T) is reported in units of psi. The toughness was also calculated at 150% of peak strain and 200% of peak strain, and is reported here as a percent of T.

4.1.5 POISSON'S RATIO

The numbers reported as Poisson's ratio were arrived at by taking the ratio of lateral to vertical strain, measured by strain gages (see Fig.3.6), at 50% of the ultimate load. The strains so measured represent strain "at-a-point" in a unit, and not global prism strain.

4.1.6 COMPONENT MATERIALS

The ultimate strengths of the units, mortar, and grout are presented for ease of comparison. They are discussed in more detail in Sections 3.2, 3.3, and 3.4 respectively.

4.2 FAILURE MODES

4.2.1. GROUTED PRISMS

Grouted clay prisms developed vertical tensile cracks on the wide and narrow faces throughout all four units, though most prominently in the middle units. In addition, all grouted clay prisms had vertical cracks at the corners, running from the interior corners of the grout core to the exterior corner of the unit face (also noted by Brown [6]). In most cases the faceshells debonded cleanly from the grout core. The grout core itself failed in compression in a manner typical of plane concrete cylinders. See Figure 4.25.

Grouted concrete prisms occasionally exhibited the same vertical splitting behavior of the clay prisms, but in more cases they failed in shear, with diagonal cracks crossing grout and block alike. In general, the faceshells did not split off from the grout core. See Figure 4.26.

4.2.2 UNGROUTED PRISMS

UngROUTED prisms failed with vertical tensile splitting on the narrow face. In concrete prisms, failure was confined predominantly to the middle two units.

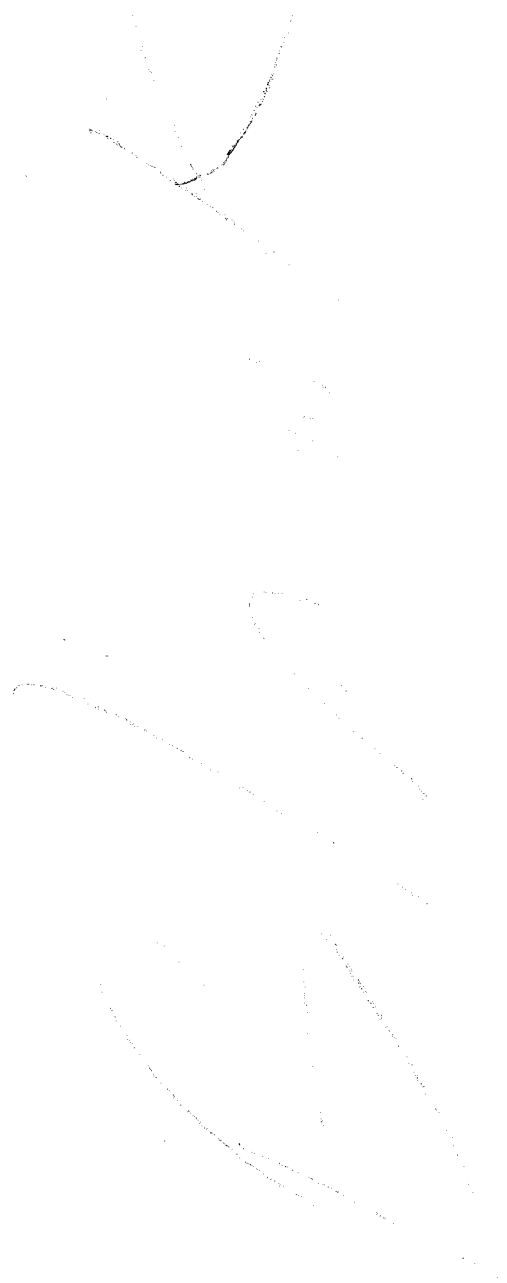
4.2.3 PRISMS LOADED PARALLEL TO THE BED JOINT

Clay prisms loaded parallel to the bedjoint failed in a brittle manner, with crushing confined to the unit faceshell adjacent to the center, ungrouted core of the units. The grout cores and the parts of the prism above and below the central core remained undamaged.

The concrete prisms failed in the same manner as those loaded normal to the bedjoint, except that the faceshells consistently debonded from the horizontal grout cores.

4.2.4 PRISMS WITH REDUCED PLATEN CONSTRAINT

The clay prisms with reduced platen restraint failed by uniform vertical splitting throughout the prism height. (Figure 4.27) Concrete prisms did not fail in shear, as did their restrained counterparts, but vertical splitting was not as uniform as in the clay prisms. Two concrete prism failed primarily in the lower two units. (Figure 5.28). All prisms, both clay and concrete, tested with reduced platen restraint developed a single vertical crack in the center of the wide face of the prism (Figure 4.28).



5. DISCUSSION OF RESULTS

5.1 INTRODUCTION

The prism test results given in Chapter Four reflect a high degree of repeatability, with a minimum of variation introduced by experimental error. The experimental methods used, documented in Chapter 3 and references 30, 46, and 47, are based on ASTM standards, but exercise further control in critical areas to minimize errors introduced by workmanship. The procedures were very successful in providing uniform specimens, and were considered to be essential to maintaining confidence in the test results.

The following sections 5.2 - 5.10, discuss the results of each series of prism tests. Of primary importance is the relative effect of different parameters on clay and concrete masonry prism behavior. As stated in Section 1.3, an exhaustive parameter study was not attempted here, as such studies have already been undertaken separately for clay and concrete masonry, and are available in the literature [6,8,19]. In Sections 5.11 and 5.12, a general comparison of the stress strain characteristics of clay and concrete masonry is made, and the implications on design are discussed.

5.2 EFFECT OF UNIT SIZE

The effect of unit size on ultimate strength of prisms is illustrated in Figure 5.1 where the ratio of prism strength to unit strength is plotted relative to unit width (Fig. 5.1). Grouted and ungrouted clay unit prism strengths

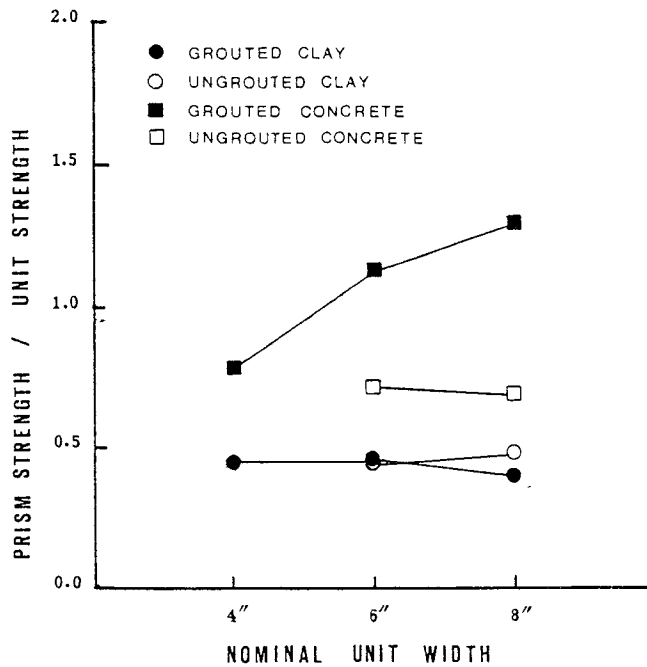


FIGURE 5.1 PRISM STRENGTH VS. UNIT SIZE FOR GROUTED AND UNGROUTED PRISMS

were constant at an average of 44% of the unit strength, regardless of unit size. UngROUTED concrete prism strength was also virtually independent of unit size, with prism strength averaging 70% of unit strength. Grouted concrete prism strengths, however, show a strong dependence on unit size, increasing as unit size increases. For 6" and 8" prisms, the prism strength actually exceeds the unit strength. Table 3.1 shows that the ratio of grouted area to gross area increases with unit size, suggesting a relationship between grouted area and prism strength, however, the relationship is not directly proportional.

5.3 EFFECT OF GROUTING

Figure 5.1 also illustrates the effect of grouting on

compressive strength of clay and concrete prisms. Grouting had a minor effect on the strength of clay prisms. Six inch prisms showed no change in strength due to grouting, and eight inch prisms showed a 17% decrease in strength. Lateral unit strains, as reflected by Poisson's ratio in Table 4.1, increased by 82% from ungrouted to grouted six inch prisms strength. Results concur in part with those of Brown and Whitlock [6] who found that for Type N mortar six inch prisms showed no change in strength due to grouting and eight inch prisms showed a 32% decrease in (net area) strength. They also reported an increase in unit lateral strain with the presence of grout. Concrete prisms showed a dramatic increase in strength with the addition of grout. While ungrouted concrete prisms attained 70% of unit strength, grouted 6" prisms attained 113% of unit strength and 8" prisms attained at 130% of unit strength. These results are not in agreement with the results of Hamid and Drysdale [8] who reported a decrease in prism strength from 80% of the unit strength to 60% of the unit strength with the addition of grout. Even when grout strength exceeded unit strength, as was the case in this project, they reported a loss of strength with grouting.

The conflicting results for concrete prisms suggest a complex failure mechanism which is dependent on the relative deformational properties of unit and grout. Apparently, the combination of concrete unit and grout used in this study was such that the tensile splitting failure mechanism no

longer applied, and the materials behaved more homogeneously than in previous studies.

5.4 EFFECT OF MORTAR TYPE

The stress-strain curves for grouted prisms are identical for prisms constructed with Type N mortar and Type S mortar. This was true for both clay and concrete prisms, and agrees with more comprehensive tests reported by Drysdale & Hamid [8] and Self [37]. While mortar strength may have a significant effect on modular brick prism strength, [3], it does not appear to be a significant parameter in the compressive behavior of grouted hollow unit masonry.

5.5 EFFECT OF GROUT STRENGTH

A comparison of Figures 4.1, 4.2, 4.15, and 4.16 shows little difference in the behavior of prisms made with different grouts. The clay prisms showed a 4% increase in prism strength for a 15% increase in grout strength. The concrete prisms showed a 3% increase in prism strength for a 5% increase in grout strength. Stiffness and peak strain were unaffected.

The increase in concrete prism strength with increasing grout strength, though slight, was more efficient than the increase in clay prism strength. This is consistent with the results discussed in Sections 5.1 and 5.2 which indicate that the properties of the concrete prisms in this project were much more dependent on grout properties than were the

clay prisms. However, it should be noted that while the increase in prism strength relative to the increase in grout strength was greater for concrete prisms, the 5% increase in grout strength was attained at the considerable expense of increasing the grout cement content by 100% (See Section 3.4). In this light, increasing grout strength may not be considered to be an efficient means of increasing prism strength.

5.6 EFFECT OF BOND PATTERN

Results of the tests on running bond prisms show a strength decrease from stack bond prisms of 18% for clay and 11% for concrete prisms. These results support the results obtained by previous researchers. Maurenbrecher [27] tested solid clay brick prisms, and reported strength reductions of 6% - 13% between running bond prisms and stack bond prisms. Hegemier [19] reported a 16% strength reduction for running bond grouted concrete block prisms.

Initial stiffness (secant modulus) was also less for running bond prisms than for stack bond prisms, decreasing 16% for clay and 11% for concrete.

5.7 EFFECT OF LOADING DIRECTION

The behavior of the prisms loaded parallel to the bedjoint was very different for the clay and concrete prisms. The concrete prisms, like those loaded perpendicular to the bedjoint, failed in shear with the grout and unit acting together as one material. Thus, for the combination

of materials and two loading direction investigated, concrete prisms behaved isotropically. Clay prisms loaded parallel to the bedjoint showed a significant loss of strength and stiffness, and failed in a more brittle, explosive manner than those loaded perpendicular to the bedjoint. Unlike the concrete units, clay units have three cavities: two large grouted cavities and one smaller ungrouted cavity in the center of the unit. (See Figure 3.1). When loaded parallel to the bedjoint, failure occurred in the brick faceshells next to the central ungrouted core, leaving the grout unloaded and unfailed. Stress-strain curves show a jagged loading curve with a small step occurring between 1400 and 1800 psi for all prisms. The step may be the result of one web failing before the other. The unloading portion of the curve was also jagged.

5.8 EFFECT OF REDUCED PLATEN RESTRAINT

It is well known that the lateral frictional restraint of steel platens on prism ends confines the end units and produces failure modes different from those observed in full size walls [5,17,41]. Previous researchers [2,5,17,19,25,41] have shown that reducing the frictional end restraint can change the failure mode from shear to vertical tensile splitting, and significantly reduce the ultimate load capacity of a prism. Theoretically, eliminating end restraint should result in a more uniform stress state in the test prism thus creating a better model of a masonry wall in

compression.

From each set of five clay or concrete prisms tested with reduced platen restraint, four prisms were tested with the greased teflon interface, and one control prism was tested in the standard manner with no teflon interface. The stress-strain curves are shown in Figures 4.19 and 4.20, and the lateral strain measurements are shown in Figure 4.24 and in Appendix A.

Comparison of the stress-strain curve for the control prism with the others in Figures 4.19 & 4.20 shows the reduction in ultimate strength that results from reducing platen restraint. The ultimate strength was reduced 17% for clay prisms and 15% for concrete prisms. Examination of the stress-strain curves shows, however, that the peak strain and secant modulus were unaffected by reduced platen restraint.

The stress-lateral strain curves for unrestrained prisms do not indicate that the lateral strain distribution in the end units is similar to the lateral strain distribution in the middle units. As in the case of the control prism, the end units had less measured lateral strain at a given load than the middle units.

In general, the stress-lateral strain curves were erratic for the unrestrained prisms, a problem noted by previous researchers [41]. However, a few trends were visible. The stress-strain curves for the concrete prisms were generally smoother and less erratic than for the clay prisms. Also,

all prisms displayed less lateral strain on the narrow face than on the wide face at a given load.

Many of the lateral strain curves for both clay and concrete indicated a short period of compressive straining in the end-unit gages at low loads. (The plots show absolute values of recorded data, so the compressive straining looks like a relaxation of tensile strain followed by a discontinuity in the stress-strain curve.) This behavior has been recognized before by Lepetsos [25], who attributed the compressive strain to the closing of diagonally oriented microcracks under the gage. This does not explain why the effect is isolated in the end unit. Both clay and concrete control prisms displayed this behavior, so the effect is not isolated to unrestrained prisms.

The unrestrained clay prisms exhibited another interesting phenomenon. At about half of the ultimate load, the stress-lateral strain diagrams have a short horizontal step, indicating a sudden large lateral expansion. The step occurred in a middle unit on three prisms and an end unit on one prism. This behavior is observed in all lateral strain gages attached to the unit and thus represents material behavior rather than transducer produced effects. The step was not isolated to either the wide or narrow face. The concrete prisms exhibited no such behavior.

Several problems encountered in testing the unrestrained prisms should be noted. The greased teflon sheets have a coefficient of friction on the order of 0.014 [2], so

they are quite successful in reducing the frictional restraint of the platens. However, the loss of restraint creates new problems. Despite good end-parallelism and careful placement in the test machine, the greased-end prisms slid sideways between the platens well before ultimate load was reached. To prevent this, four steel bars were bolted to the top platen leaving less than 1/16" clearance around the prism. This prevented major lateral movement of the prism by restraining it along one edge after a small slip occurred. The lateral forces generated by this restraint were significant, as in two cases the failure of a clay prism sheared off a 1/8" diameter steel bolt holding the restraint bar in place. As a result of these problems, the reduced friction prism tests took significantly more time and effort than the restrained (normal) prism tests. In addition, the slip-restraint bars introduced new unknowns into the prism test, and may have had an undesirable effect on the axial stress distribution.

5.9 FAILURE MODES

There was a significant difference in the failure modes of the grouted clay and concrete prisms. In general, concrete prisms failed in shear with the grout and units acting together, while the clay prisms failed by vertical tensile splitting with the unit face shells separating from the grout cores. This difference in failure mode is reflected in the parameter studies discussed in the preceding sections. Figure 5.1 shows that for the clay prisms, ultimate

strength is directly proportional to unit strength, while grouted concrete prism strength is more dependent on the grouted area. While clay prisms fail at less than half of their unit strength the concrete prisms exceeded their unit strengths, depending primarily on the relatively high grout strength. Thus unit properties governed clay prism failure while grout crushing strength governed concrete prism behavior.

5.10 AGREEMENT OF RESULTS WITH PREVIOUS WORK

In general, observed prism behavior coincided with the experience of previous researchers. The one significant exception was the increase in strength attained by grouting hollow concrete prisms. While previous work [8] has shown that grouting can decrease the net area strength by increasing the lateral strain in the unit, the concrete prisms in this project showed no such increase in strain or decrease in strength. It is suggested that the concrete units and grout used in this study had very similar properties and thus the failure mechanism, which is usually dependent on the interaction of dissimilar materials, was different than for previously tested prisms. Clay prisms, on the other hand, behaved as expected, since grout strength and stiffness did not match that of the units.

5.11 SHAPE OF THE STRESS-STRAIN CURVES

The parameters discussed in Sections 5.2 - 5.8 primarily affected prism strength, f'_m ; the shape of the stress-

strain curves was not significantly altered. The shape can be roughly qualified in terms of the elastic modulus, the strain at peak, and the area under the curve. These values are plotted in histograms for clay and concrete prisms together and individually in Figures 5.2 - 5.5. (Results from the reduced-platen-restraint series and the load-parallel-to-bedjoint series are not included.)

The elastic modulus is consistent for the clay prisms, but varies somewhat with $f'm$ for the concrete prisms, giving a flat distribution. The distribution for both materials is skewed, with the relatively high coefficient of variation of 0.22.

The peak strain was very consistent for both materials, with a mean of 0.0026 for each. The scatter was larger for clay prisms, but the combined results appear to have a normal distribution, and have a coefficient of variation of 0.16.

Figures 5.4 and 5.5 show the area under the stress-strain curve at strain levels of 1-1/2 and 2 times the peak strain respectively. The area is expressed as a percentage of the area under the curve at peak strain. The histograms show that the area under the curves is very consistent and is equivalent for both clay and concrete.

In general, the stress-strain characteristics of clay and concrete masonry, when considered independently of $f'm$, are virtually identical.

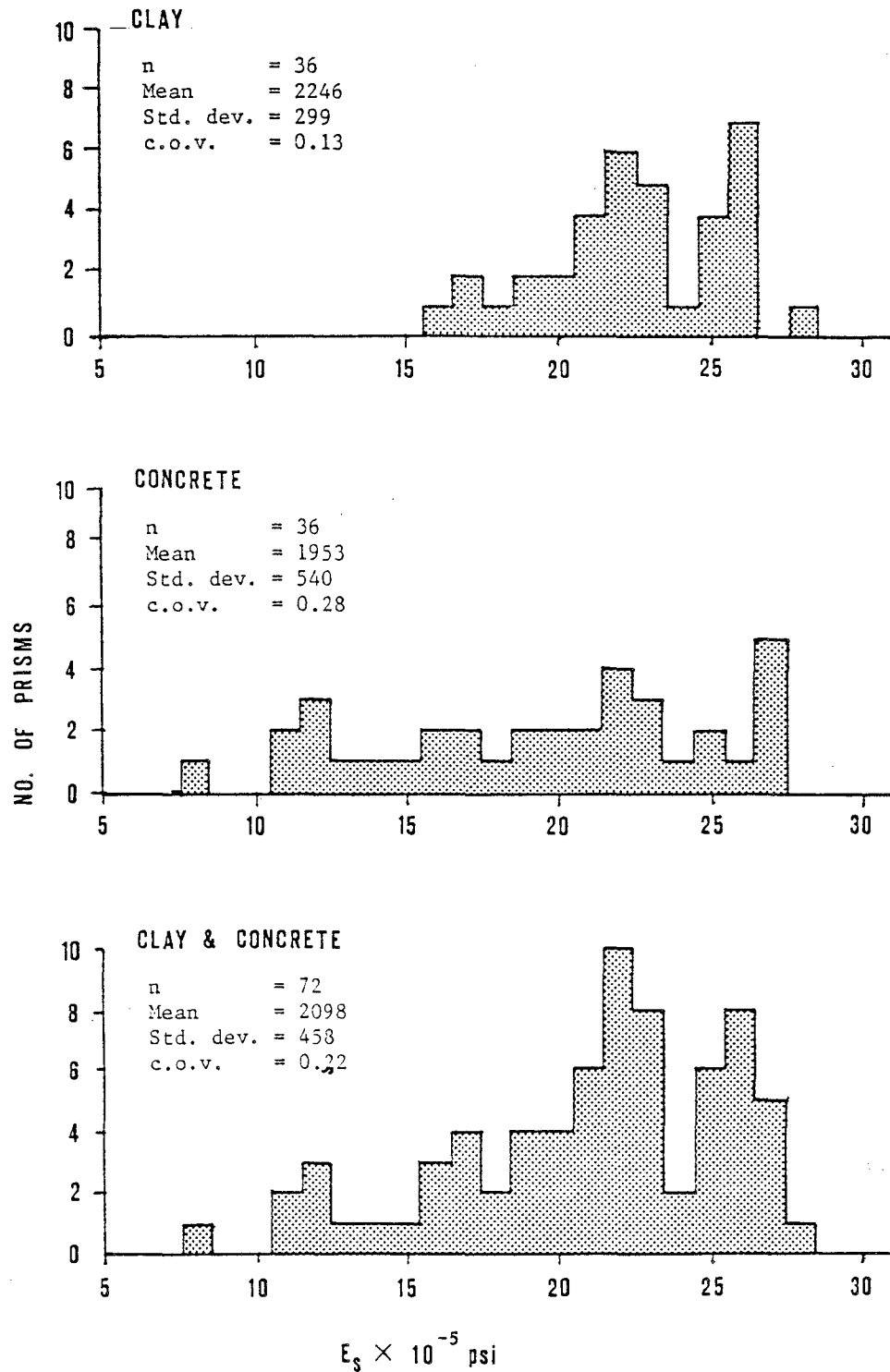


FIGURE 5.2 DISTRIBUTION OF SECANT MODULUS DATA FOR CLAY AND CONCRETE PRISMS

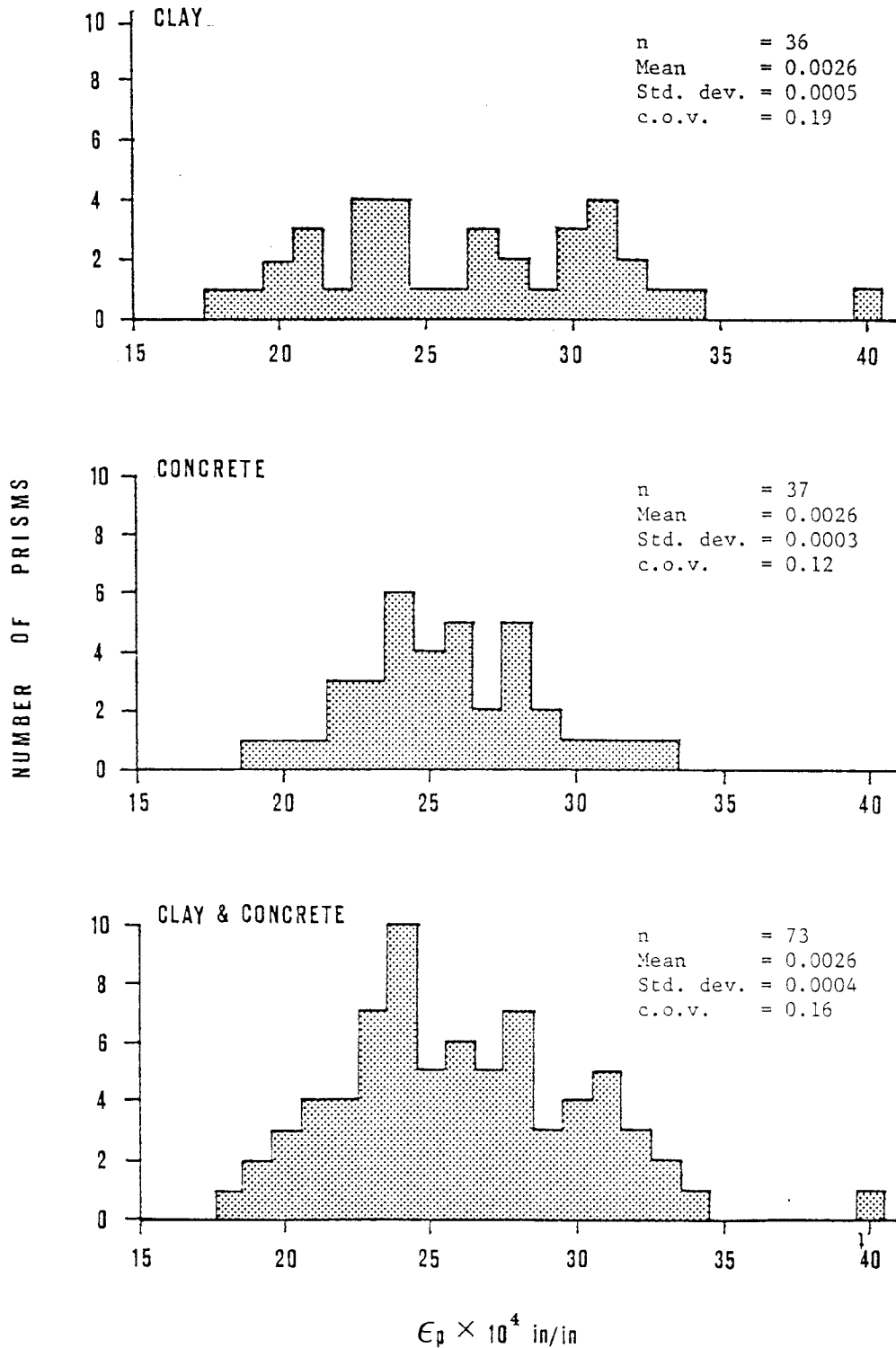


FIGURE 5.3 DISTRIBUTION OF PEAK STRAIN DATA FOR CLAY AND CONCRETE PRISMS

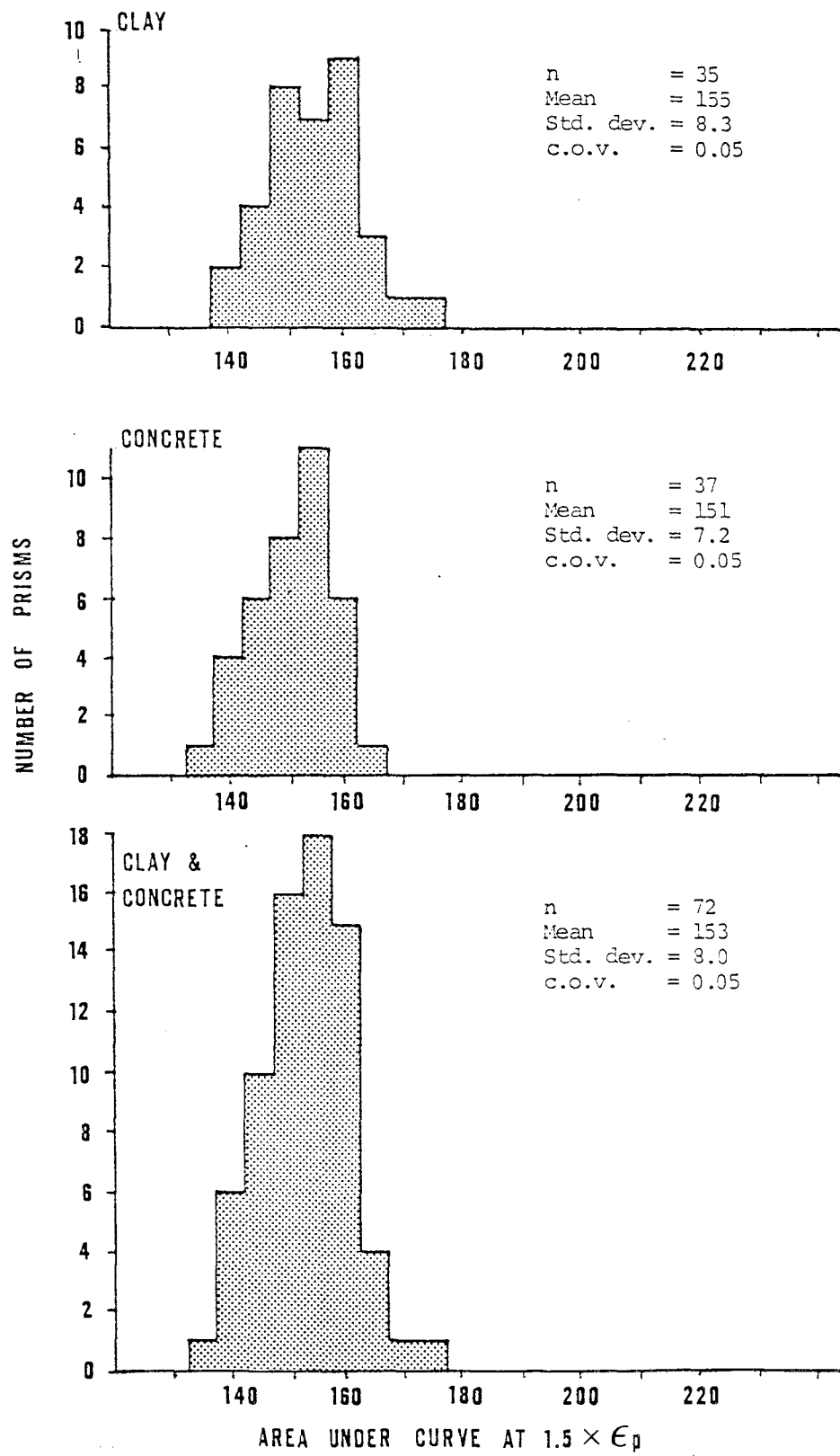


FIGURE 5.4 DISTRIBUTION OF AREA-UNDER-CURVE AT $1.5 \times \epsilon_p$ FOR CLAY AND CONCRETE PRISMS

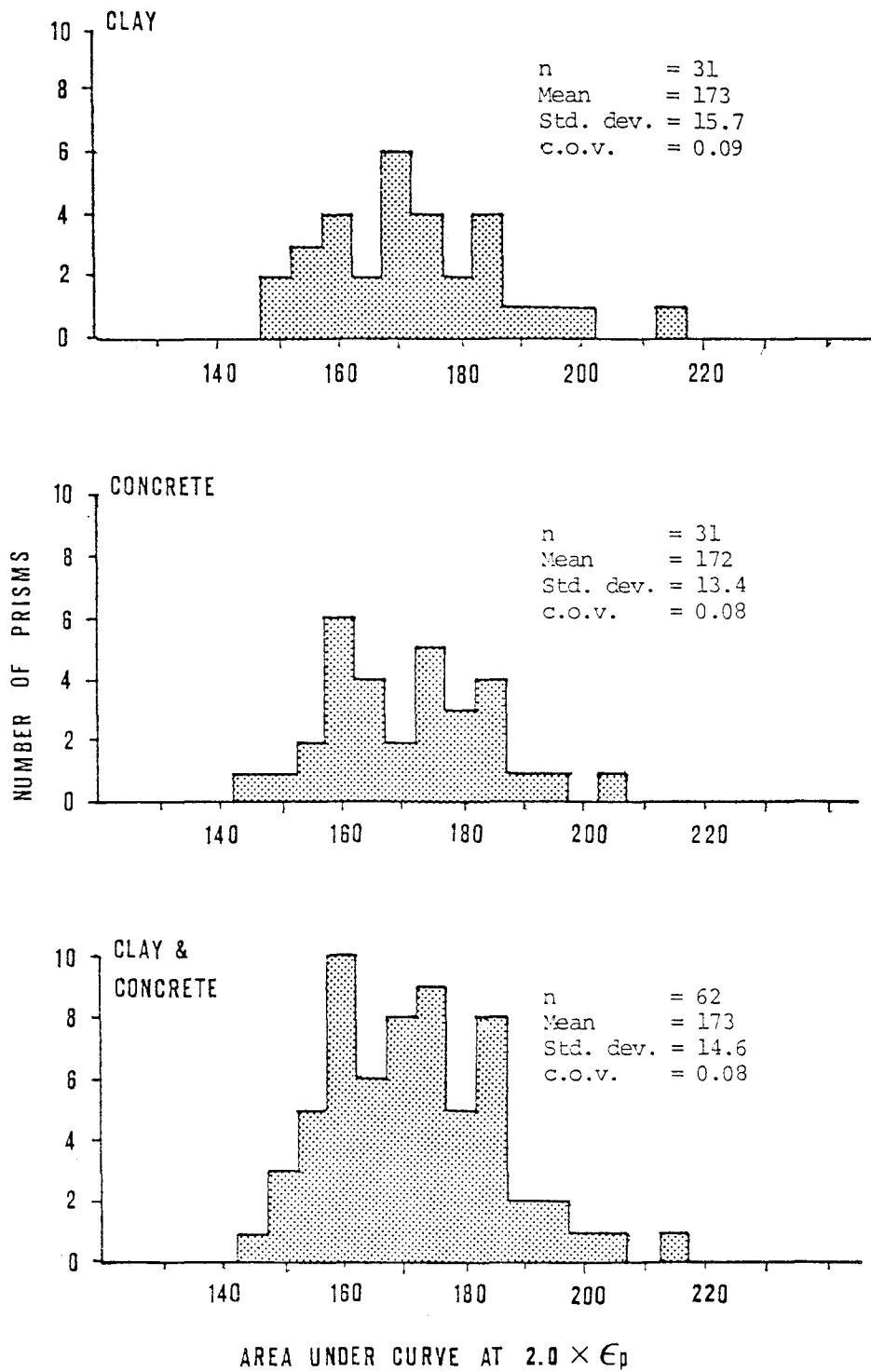


FIGURE 5.5 DISTRIBUTION OF AREA-UNDER-CURVE AT $2.0 \times \epsilon_p$ FOR CLAY AND CONCRETE PRISMS

5.12 IMPLICATIONS ON DESIGN

The parameter studies discussed in Sections 5.2-5.8 were directed primarily towards understanding how variations in constituent materials and prism configuration could affect masonry prism behavior. This is an important subject which has been investigated in some detail, for concrete and clay separately, by previous researchers [6,8,19]. For purposes of design, however, a designer need only know the value of $f'm$ and enough about the stress-strain behavior of masonry to derive the other parameters applicable to a problem. The sections that follow discuss the implication of the stress-strain relationships determined in this study on assumptions used in working stress and ultimate strength design.

5.12.1 WORKING STRESS DESIGN

Current design standards provide working stress design methods for designing masonry buildings. The only material properties required for designing masonry in compression are the ultimate strength, $f'm$, and the elastic modulus for the linear portion of the stress-strain curve. In the code, the quantity $f'm$ is supplied either by a table of unit strengths and mortar types, or by laboratory tests of prisms. The elastic modulus is then determined as a function of $f'm$. ($E_m = 1000 f'm$ for inspected masonry and $E_m = 500 f'm$ for uninspected masonry).

Assuming that $f'm$ is known, it remains only to find a value for the elastic modulus. Figure 5.2 suggests that the

elastic modulus is relatively variable, (COV = 0.22), and using a constant value for clay and concrete may not be warranted. When the elastic modulus is considered to be a function of f'_m , ($E_s = k f'_m$), the correlation is improved. The values of E_s/f'_m given in Table 4.1 show a mean value of 439 for clay prisms and 557 for concrete prisms. The combined mean is 498 with a coefficient of variation of 0.18. While there is some difference in the values of E_s/f'_m for clay and concrete, using a single value for both clay and concrete may be justified for design. Given the inherent variability in each material a more accurate specification would not be warranted. Thus, if a reliable means of obtaining f'_m is used, the assumption that clay and concrete hollow masonry behave identically is justified for working stress design of masonry in compression.

5.12.2 ULTIMATE STRENGTH DESIGN

Ultimate strength design methods require a more complete understanding of material stress-strain behavior than working stress design methods. In particular, the shape of the stress-strain curve beyond ultimate strength and the ultimate strain are required. In Table 4.1, the area under the curve at three levels of strain is given to quantify the shape of the stress-strain curve. The strain at ultimate strength is also listed. The peak strain is relatively consistent for both clay and concrete, with a mean value for all prisms of 0.0026 in/in (cov = 0.16) (See Figure 5.4). The area under the curve at peak strain varies directly with

the ultimate strength, but beyond peak strain the area increases in the same proportions for both clay and concrete prisms. (See Figure 5.5)

Before developing a stress block for masonry, the influence of other factors on the shape of the stress-strain curve such as load rate and duration [11] and strain gradient effects, must be understood. However, the data provided by this preliminary investigation suggests that clay and concrete hollow unit masonry need not be differentiated for purposes of developing the stress block for ultimate strength design.

CHAPTER 6 CONCLUSIONS

6.1 SUMMARY

The primary objective of this project was to investigate the extent to which clay and concrete hollow unit masonry have similar engineering characteristics. Parallel groups of clay and concrete masonry prisms were tested in uniaxial compression to evaluate the complete stress-strain characteristics of the two materials. Ten series of tests, each consisting of five clay and five concrete prisms, were conducted to determine the influence of unit size, grouting, mortar strength, grout strength, bond pattern, load direction, and platen restraint on the relative behavior of clay and concrete masonry.

The effect of these parameters and the resulting implications on design methods for clay and concrete masonry are summarized in the conclusions listed below.

6.2 CONCLUSIONS

- (1) The clay and concrete prisms tested in this project did not display the same type of failure mechanisms. While clay prisms consistently failed as a result of vertical tensile splitting, concrete prisms often displayed shear failures.
- (2) Although clay and concrete masonry prisms loaded in compression may exhibit different failure mechanisms, the shape of the complete stress-strain curves of these two materials were essentially identical. This implies that clay and concrete hollow unit masonry may

be regarded as one material for purposes of both working stress and ultimate strength design.

- (3) The influence of bond pattern and mortar strength on prism strength and stiffness was similar for clay and concrete prisms.
- (4) The influence of unit size (% grouted area), grouting, and grout strength was different for clay and concrete prisms, since the interaction of unit and grout was different for each material.
- (5) The influence of loading direction on prism behavior was different for clay and concrete prisms, but resulted from differences in unit geometry rather than material properties.
- (6) The influence of reduced platen restraint on strength and stiffness of clay and concrete prisms was the same, however the lateral strain behavior of the clay units differed somewhat from that in the concrete units.

6.3 RECOMMENDATIONS FOR FUTURE STUDIES

This study has provided a basis for the suggestion that clay and concrete masonry behave as similar engineering materials for purposes of design. However, further work must be done to quantify this work and to extend conclusions to other types of stress - states experienced by masonry. Areas of possible concentration are suggested below.

- (1) An analytical model for the curves in this and other related studies should be developed. The applicability

of the Kent-Park model for concrete [21] and the modified Kent-Park model [35] for concrete masonry to both clay and concrete masonry should be investigated.

- (2) The effect of combined bending and axial load on the stress strain curve should be quantified and compared for clay and concrete masonry.
- (3) Partially-grouted prisms should be investigated.
- (4) A comparison of the behavior of clay and concrete shear walls in shear, in-plane and out-of-plane bending should be made.

REFERENCES

1. Anonymous, "Masonry Test of Grout Aid", Masonry Industry, February 1967
2. Atkinson, R. H., Noland, J.L., Abrams, D.P., and McNary, S., "A Deformation Failure Theory for Stack-Bond Brick Masonry Prisms in Compression", Proceedings, Third North American Masonry Conference, Arlington, Texas, June 1985.
3. Baur, J., Noland, J.L., and Chinn, J., "Compression Tests of Clay-Unit Stackbond Prisms", Proc. 1st North American Masonry Conf., Boulder, Colorado, August 1978.
4. Becica, I.J., and Harris, H.G., "Behavior of Hollow Concrete Masonry Prisms Under Axial Load and Bending", TMS Journal, January-June 1983, pp. T1-T26.
5. Brown, R. H., "Prediction of Brick Masonry Prism Strength from Reduced Constraint Brick Tests", Masonry: Past & Present, ASTM, Philadelphia, 1975, pp. 171-194.
6. Brown, R. H. and Whitlock, A.R., "Compressive Strength of Grouted Hollow Brick Prisms", Masonry: Materials, Properties, and Performance, ASTM STP 778, J. G. Borchelt, Ed., American Society for Testing & Materials, 1982, pp. 99-117.
7. Chuknunenye, A. O., and Hamid A. A. "Behavior of Concrete Block Prisms Under Concentric Loading: An Analytical Approach", Structural Masonry Laboratory Report No. MS 85/1, Drexel University, 1985.
8. Drysdale, R.G. and Hamid, A.A., "Behavior of Concrete Block Masonry Under Axial Compression", ACI Journal, June 1979, pp. 707-716.
9. Drysdale, R.G. and Hamid, A.A., "Tension Failure Criteria for Plain Concrete Masonry", Proc. ASCE, Vol. 110, ST2 Feb. 1984.
10. Drysdale, R.G. and Hamid, A.A., "Capacity of Concrete Block Masonry Prisms Under Eccentric Compressive Loading", ACI Journal, March-April 1983, pp. 102-108.
11. Englekirk, R.E., and Hart, G.C., Earthquake Design of Concrete Masonry Buildings: Volume 2, Strength Design of One-to-Four Story Buildings, Prentice-Hall Inc., 1984.

12. Fattal, S.G. and Cattaneo, L.E., "Structural Performance of Masonry Walls Under Compression and Flexure", National Bureau of Standards Building Science Series No. 73, June 1976.
13. Frey, D.J., "Effect on Constituent Proportions on Uniaxial Compressive Strength of Two Inch Cube Specimens of Masonry Mortars", M.S. Thesis, University of Colorado, Boulder, 1975.
14. Hamid, A.A. and Drysdale, R.G., "Concrete Masonry Under Combined Shear and Compression Along the Mortar Joints", ACI Journal, Sept.-Oct. 1980, pp. 314-320.
15. Hamid, A.A. and Drysdale, R.G., "Proposed Failure Criteria for Concrete Block Masonry Under Biaxial Stresses", Proc. ASCE, Vol. 107, No ST8, Aug. 1981, pp. 1675-1687.
16. Hamid, A.A. and Drysdale, R.G., "Suggested Failure Criteria for Grouted Concrete Masonry Under Axial Compression", ACI Journal, Oct. 1979, pp. 1047-1061.
17. Hanada, K.T., "Effects of Height and End Lateral Restraints on Clay Unit Prisms", M.S. Thesis, University of Colorado, 1978.
18. Hatzinikolas, M., Longworth, J., and Warwarak, J., "Failure Modes for Eccentrically Loaded Concrete Block Masonry Walls", ACI Journal, No. 77-28, July-August 1980, pp. 258-263.
19. Hegemier, G.A., Krishnamoorthy, G., Nunn, R.O., and Moorthy, T.V., "Prism Tests for the Compressive Strength of Concrete Masonry", Proc. First North American Masonry Conference, Boulder, Colorado, August 1978.
20. Hodgkinson, H.R. and Davies, S., "The Stress Strain Relationships of Brickwork when Stressed in Directions Other than Normal to the Bed Face", Proceedings 6th IBMAC, Rome 1982.
21. Kent, P.C., and Park, R., "Flexural Members with Confined Concrete", Journal of the Structural Division, ASCE, 97: ST7, 1969-1990, July 1971.
22. Khalil, M.R.A., "Stress-Strain Behavior of Clay and Concrete Masonry," M.S. Thesis, Univ. of Calgary, June 1979.

23. Kingsley, G.R., Tulin, L.G., and Noland, J.L., "Parameters Influencing the Quality of Grout in Hollow Clay Masonry", Proceedings, 7th International Brick Masonry Conference, Melbourne, Australia, February, 1985.
24. Kingsley, G. R., Tulin, L.G., and Noland, J.L., "The Influence of Water Content and Unit Absorption Properties on Grout Compressive Strength and Bond Strength in Hollow Clay Masonry", Proceedings Third NAMC, Texas, June 1985.
25. Lepetsos, G.N., "An Investigation into the Distribution of Strains of Masonry Prisms", Senior Project (Unpublished., University of Colorado, Boulder, Colorado 1984.
26. Maurenbrecher, A.H.P., "Compressive Strength of Eccentrically Loaded Masonry Prisms", Proc. 3rd Canadian Masonry Symposium, Edmonton, Canada June 1983, pp. 10.110.13.
27. Maurenbrecher, A.H.P., "Effect of Test Procedures on Compressive Strength of Masonry Prisms", Proceedings: 2nd Canadian Masonry Symposium, Ottawa, Canada, 1980, pp. 119-132.
28. Miller, D.E., Noland, J.L., and Feng, C.C., "Factors Influencing the Compressive Strength of Hollow Clay Unit Prisms", Proc. 5th Int. Brick Masonry Conference, Washington, D.C., 1979.
29. Miller, M.E., Nunn, R.O., and Hegemier, G.A., "The Influence of Flaws, Compaction, and Admixture on Strength and Elastic Moduli of Concrete Masonry", National Science Foundation Report No. UCSD/AMES/TR-78-2, August 1978.
30. Noland, J.L., "Proposed Test Method for Determining Compressive Strength of Clay-Unit Prisms", for Western States Clay Products Assoc. by Atkinson-Noland & Assoc., Inc., Boulder, Colorado, June 1982.
31. Nunn, R.O., Miller, M.E., and Hegemier, G.A., "Grout-Block Bond Strength in Concrete Masonry", National Science Foundation Report No. UCSD/AMES/TR-78001, March 1978.
32. Pedreschi, R.F. and Sinha, B.P., "The Stress/Strain Relationship of Brickwork" Proceedings 6th IBMAC, Rome, 1982.

33. Powell, B. and Hodgkinson, H.R., "The Determination of Stress/Strain Relationship of Brickwork", Proceedings 4th IBMAC.
34. Priestley, M.J.N., "Ductility of Unconfined and Confined Concrete Masonry Shear Walls," The Masonry Society Journal, Vol. 1, No. 2, July December, 1981, pp T28-T39.
35. Priestley, M.J.N. and Elder, D.M., "Stress-Strain Curves for Unconfined & Confined Concrete Masonry", ACI Journal, No.80-19, May-June 1983.
36. Ridinger, W., "Effect of Unit and Mortar Properties on Compressive Strength of Hollow Clay Unit Prisms", M.S. Thesis, University of Colorado, Boulder, 1979.
37. Self, M.V., "Structural Properties of Load-Bearing Concrete Masonry", Masonry: Past & Present, ASTM STP 589, American Society for Testing and Materials, 1975, pp. 233-254.
38. Scrivener, J.C. and Williams, D., "Compressive Behavior of Masonry Prisms", University of Canterbury, New Zealand, 1971.
39. Uniform Building Code, 1985.
40. Uniform Building Code Standards, 1982.
41. Watstein, D., "Relation of Unrestrained Compressive Strength of Brick to Strength of Masonry", Journal of Materials, JMLSH, Vol. 6, No. 2, June 1971, pp. 304-319.
42. Yokel, F.Y., Mathey, R.G., and Dijkers, R.D., "Strength of Masonry Walls Under Compressive and Transverse Loads", Building Science Series 34, National Bureau of Standards, Washington, D.C., 1971.
43. Yokel, F.Y., Mathey, R.G., and Dijkers, R.D., "Compressive Strength of Slender Concrete Masonry Walls", National Bureau of Standards Building Science Series No. 33, December 1970.
44. Yong, P.M.F., "Grouting of Concrete Masonry" New Zealand Ministry of Works and Development Report No. 5-83/7, 1983.
45. Yorkdale, BIA Hollow Brick Masonry Testing Program, Unpublished, 1973.

46. "Construction of Masonry Prisms", Atkinson-Noland & Associates and the Dept. of Civil Engineering, University of Colorado, Boulder, May 1985.
47. "Preparation and Testing of Two-Inch Mortar Cubes", Atkinson-Noland & Associates, and the Dept. of Civil Engineering, University of Colorado, Boulder, May 1984.

2

1

1

APPENDIX
INDIVIDUAL TEST RESULTS

The stress-strain curves derived from the externally mounted LVDT data are presented in Sections A.1 - A.9 for each prism tested. See Figure 3.6 for the locations of LVDT's 1, 2, 3, and 4. Section A.10 contains the lateral strain data from the reduced platen constraint tests. See Figure 3.7 for the location of the strain gages for the reduced platen constraint tests.

2

3

4

5

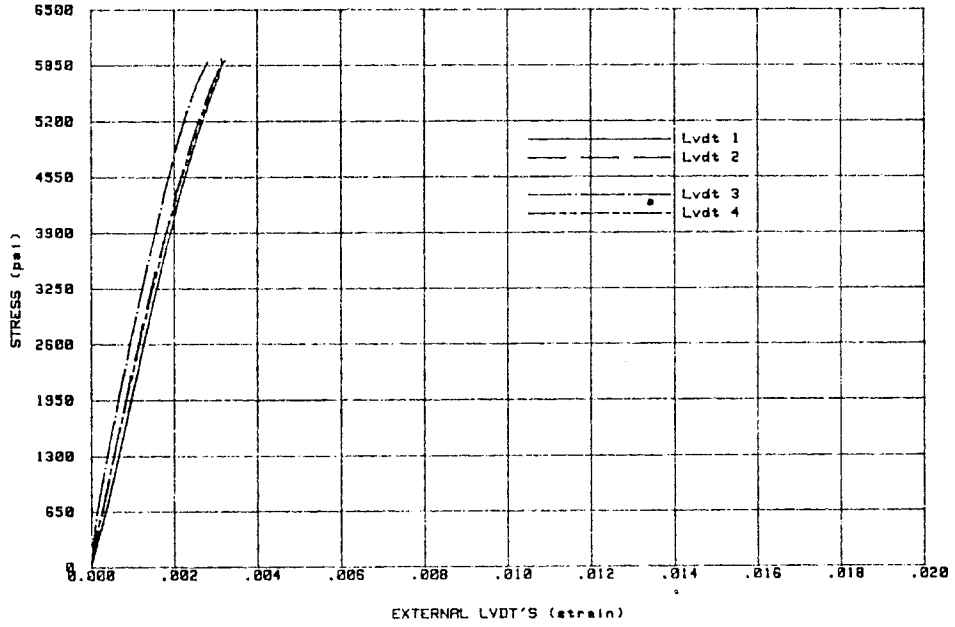
6

A.1 SERIES 1

UNIT WIDTH	6"
GROUT	STANDARD
MORTAR	TYPE H
BOND PATTERN	STACK BOND
LOAD DIRECTION	NORMAL TO BEDJOINT

ATKINSON-NOLAND AND ASSOCIATES
MASONRY PRISM TESTS
DATE: 11/07/84

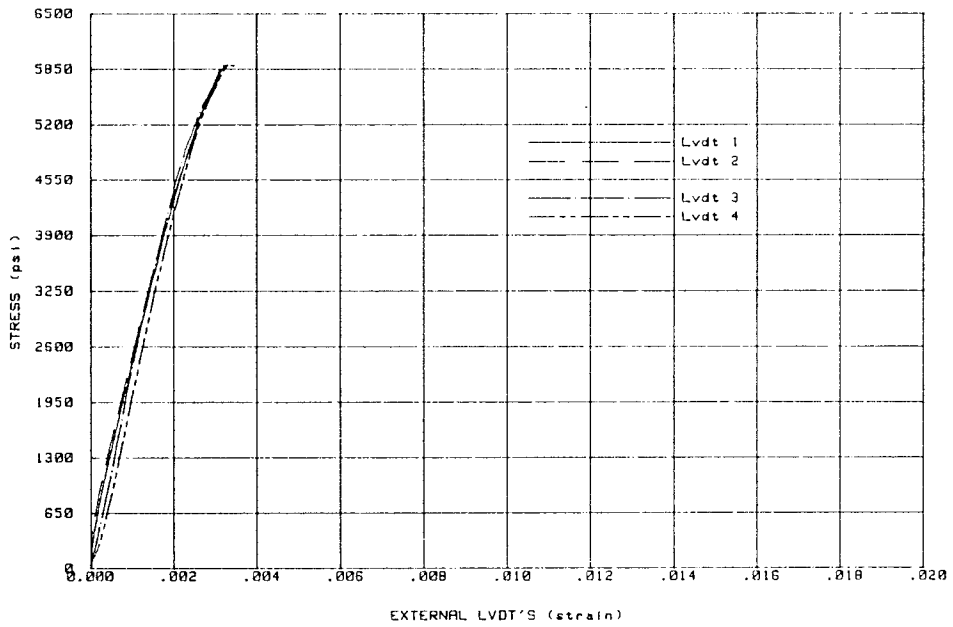
TEST: 6-CLY-G-0
SPECIMEN: 9-17-1



CLAY 1

ATKINSON-NOLAND AND ASSOCIATES
MASONRY PRISM TESTS

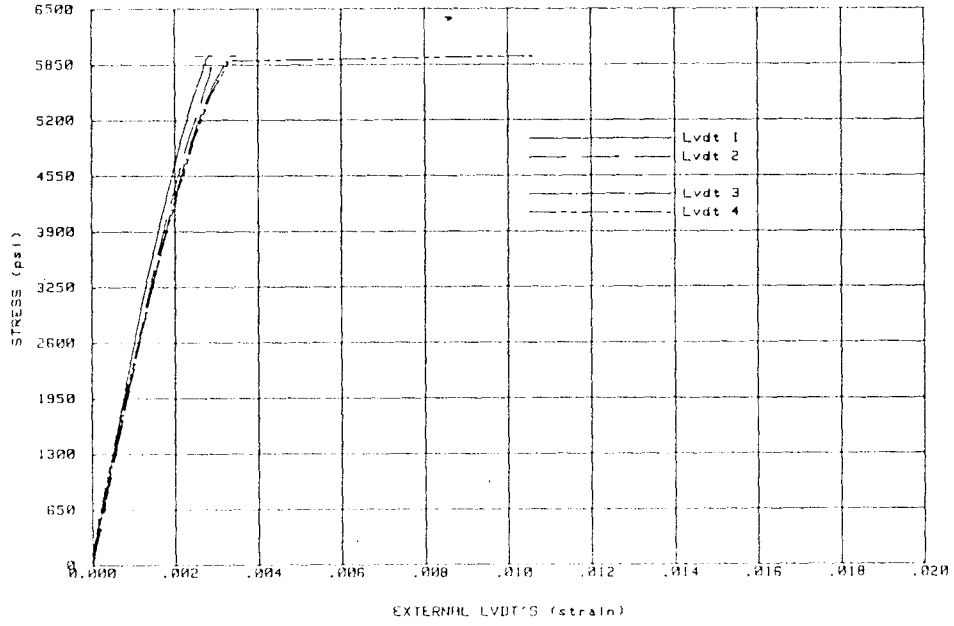
TEST: 6-CLY-G-0
SPECIMEN: 9-17-3



CLAY 2

ATKINSON-NOLAND AND ASSOCIATES
MASONRY PRISM TESTS
DATE: 11/02/84

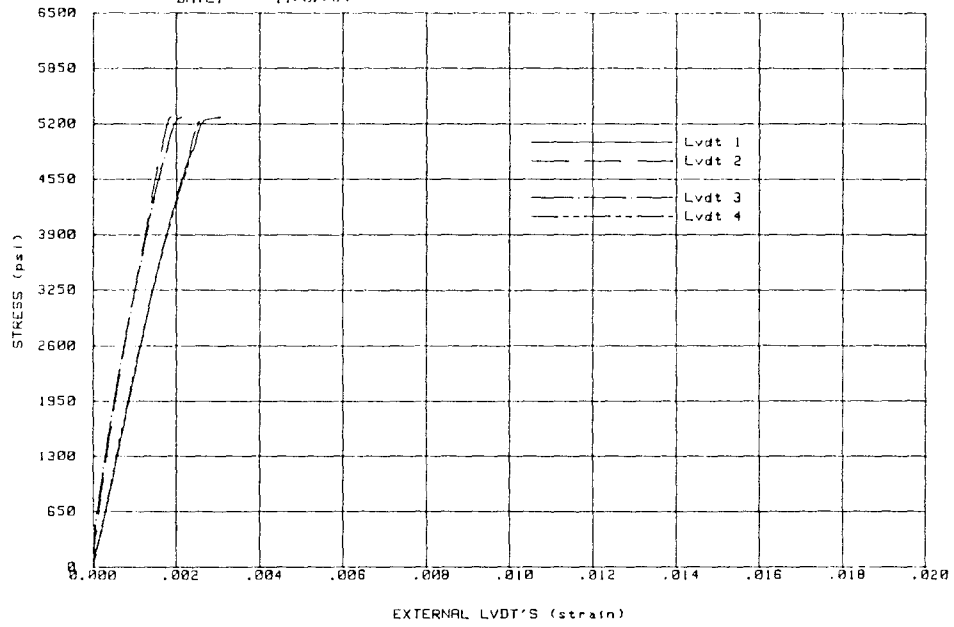
TEST: 6-CLY-G-0
SPECIMEN: 9-17-4



CLAY 3

ATKINSON-NOLAND AND ASSOCIATES
MASONRY PRISM TESTS
DATE: 11/02/84

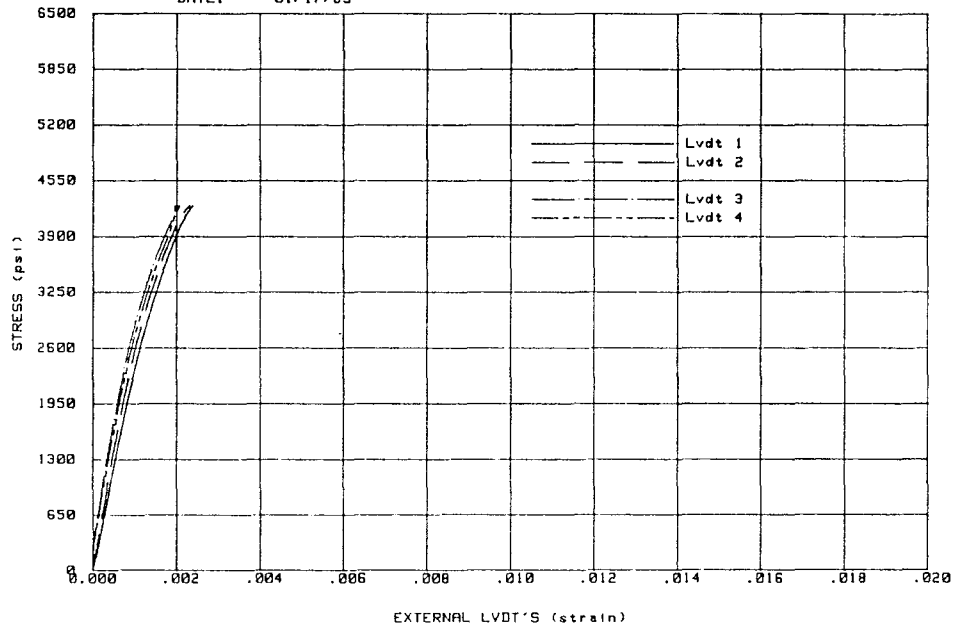
TEST: 6-CLY-G-0
SPECIMEN: 9-17-5



CLAY 4

ATKINSON-NOLAND AND ASSOCIATES
MASONRY PRISM TESTS
DATE: 01/17/85

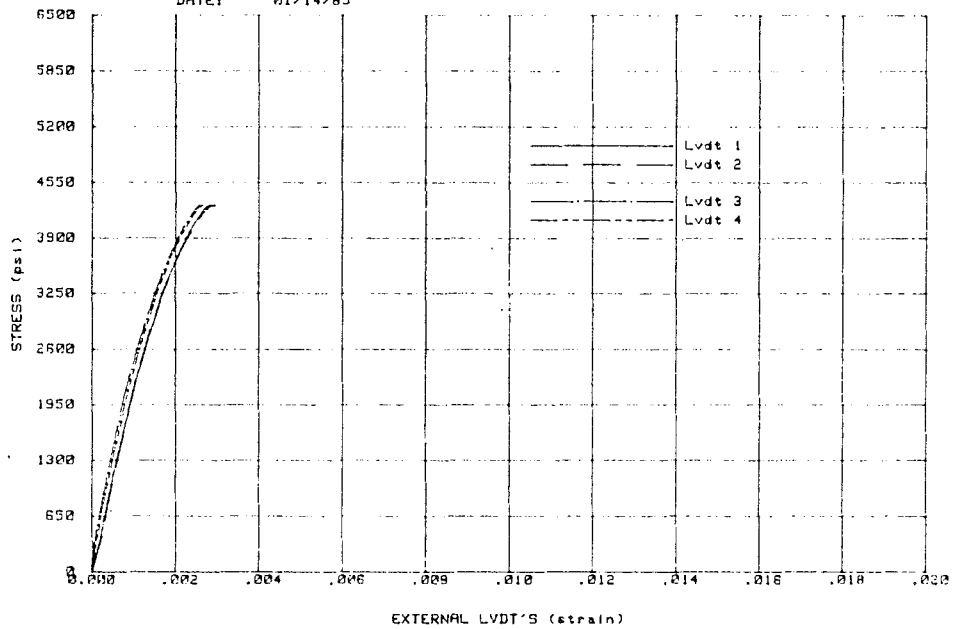
TEST: 6-CNC-G-2
SPECIMEN: 11-6-1



CONCRETE 1

ATKINSON-NOLAND AND ASSOCIATES
MASONRY PRISM TESTS
DATE: 01/14/85

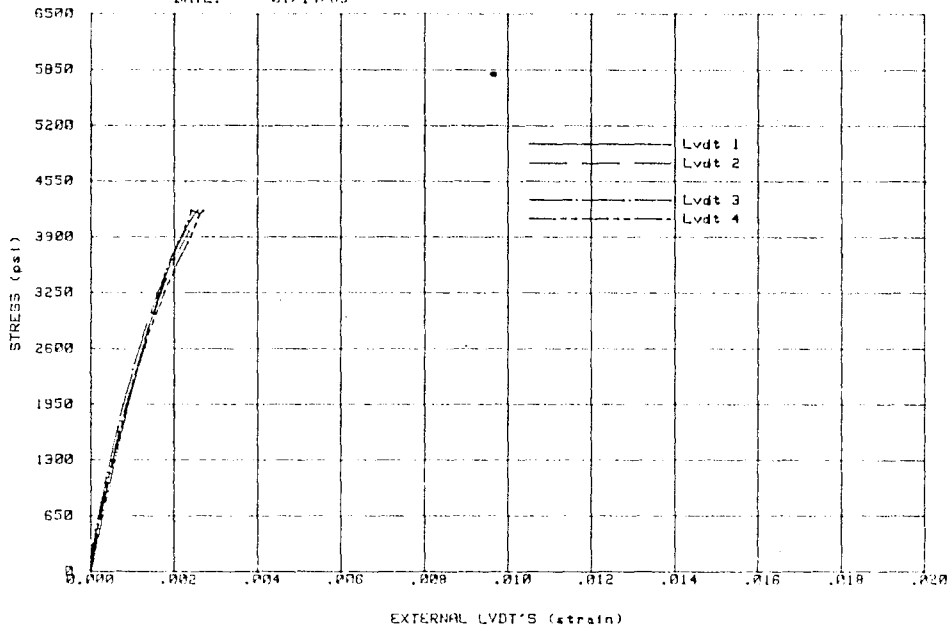
TEST: 6-CNC-G-2
SPECIMEN: 11-6-2



CONCRETE 2

ATKINSON-NOLAND AND ASSOCIATES
MASONRY PRISM TESTS
DATE: 01/14/85

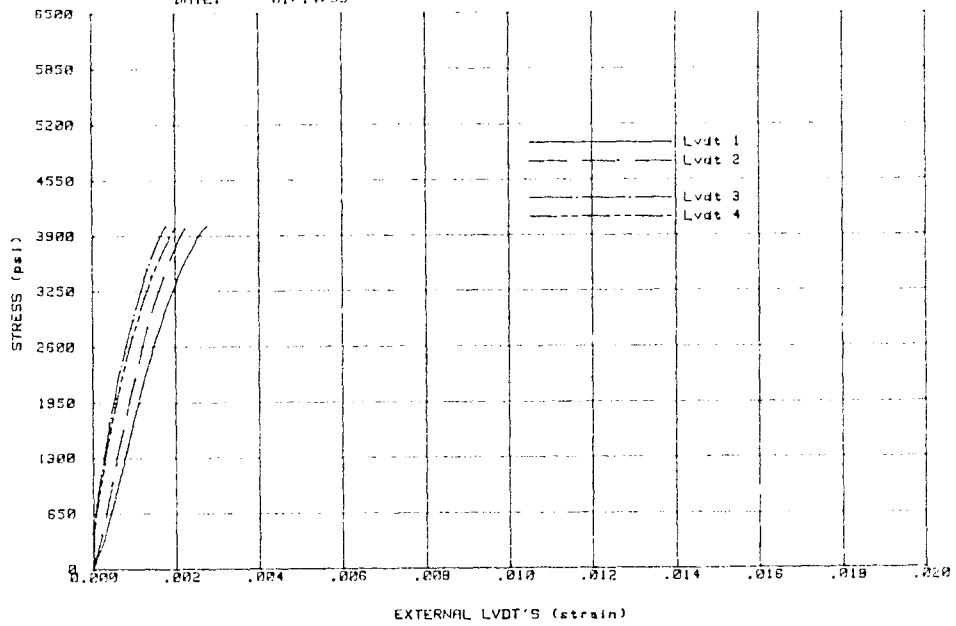
TEST: 6-CNC-G-2
SPECIMEN: 11-6-3



CONCRETE 3

ATKINSON-NOLAND AND ASSOCIATES
MASONRY PRISM TESTS
DATE: 01/14/85

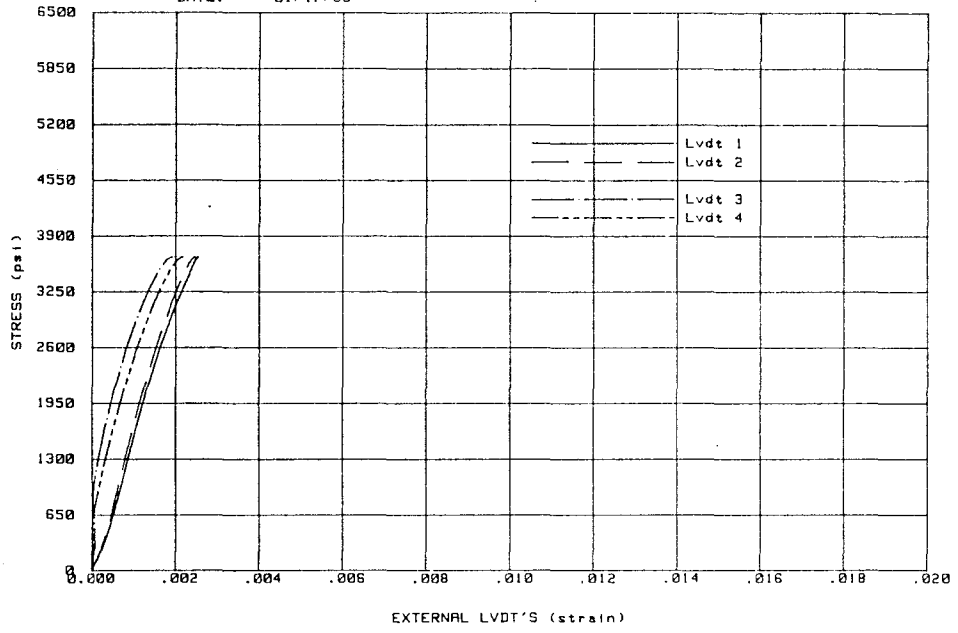
TEST: 6-CNC-G-2
SPECIMEN: 11-6-4



CONCRETE 4

ATKINSON-NOLAND AND ASSOCIATES
MASONRY PRISM TESTS
DATE: 01/17/85

TEST: 5-CNC-G-2
SPECIMEN: 11-6-5



CONCRETE 5

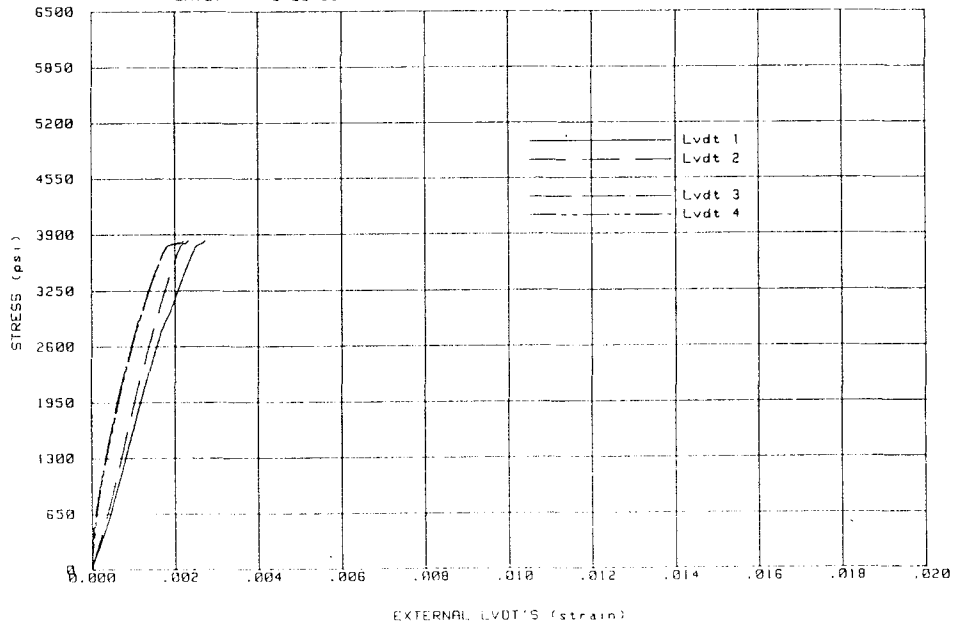
Reproduced from
best available copy.

A.2 SERIES 2

UNIT WIDTH	4"
GROUT	STANDARD
MORTAR	TYPE N
BOND PATTERN	STACK BOND
LOAD DIRECTION	NORMAL TO BEDJOINT

ATKINSON-NOLAND AND ASSOCIATES
MASONRY PRISM TESTS
DATE: 2/26/85

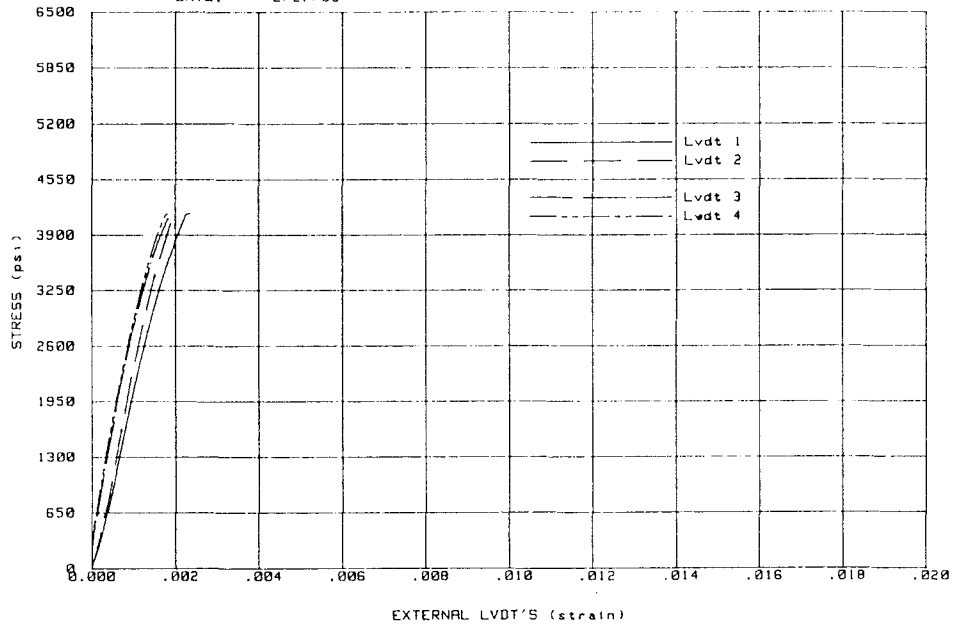
TEST: 4-CLY-G
SPECIMEN: 12-10-6



CLAY 1

ATKINSON-NOLAND AND ASSOCIATES
MASONRY PRISM TESTS
DATE: 2/27/85

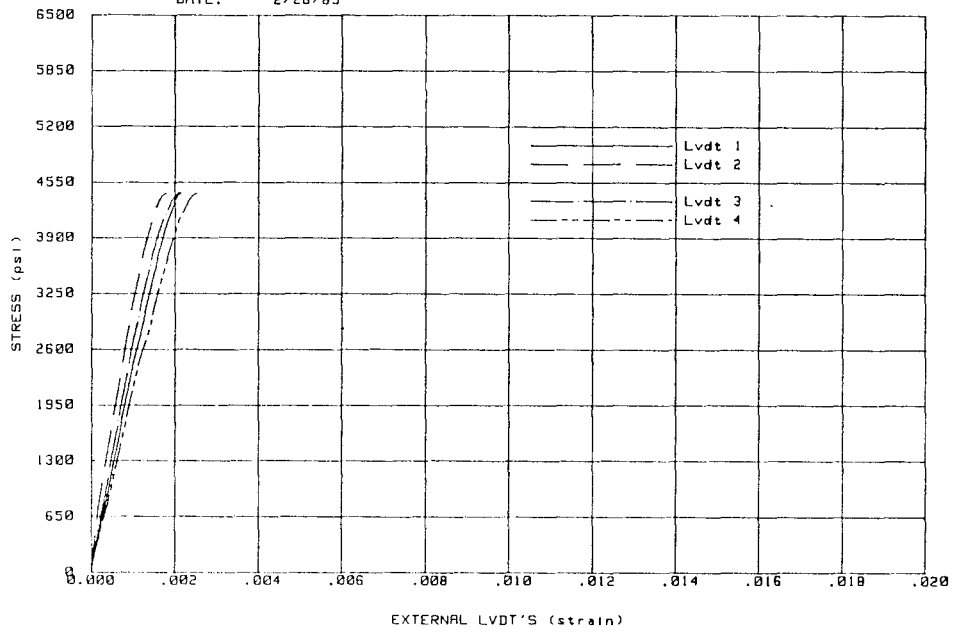
TEST: 4-CLY-G
SPECIMEN: 12-19-7



CLAY 2

ATKINSON-NOLAND AND ASSOCIATES
MASONRY PRISM TESTS
DATE: 2/26/85

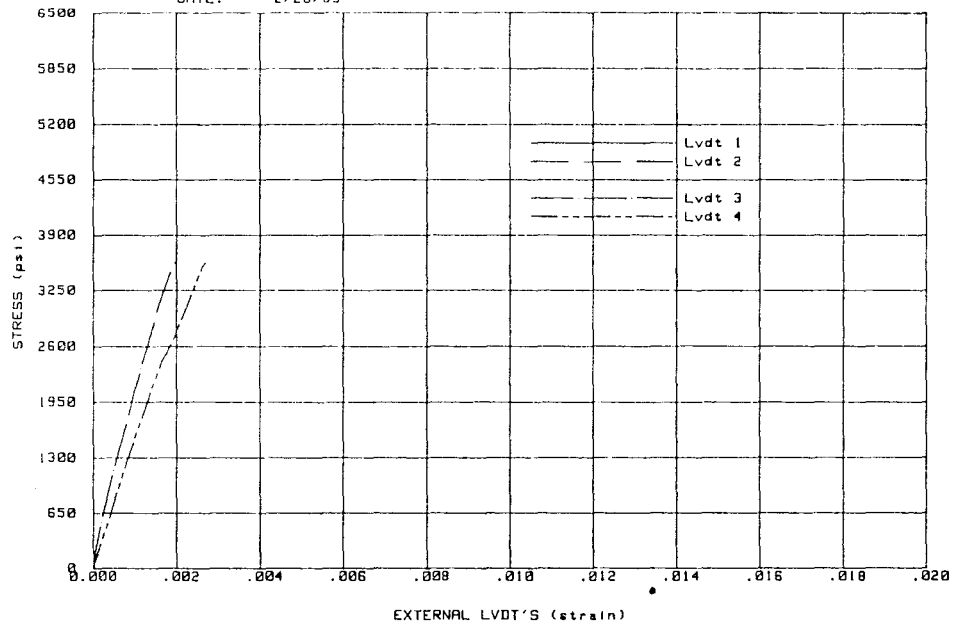
TEST: 4-CLY-G
SPECIMEN: 12-19-8



CLAY 3

ATKINSON-NOLAND AND ASSOCIATES
MASONRY PRISM TESTS
DATE: 2/26/85

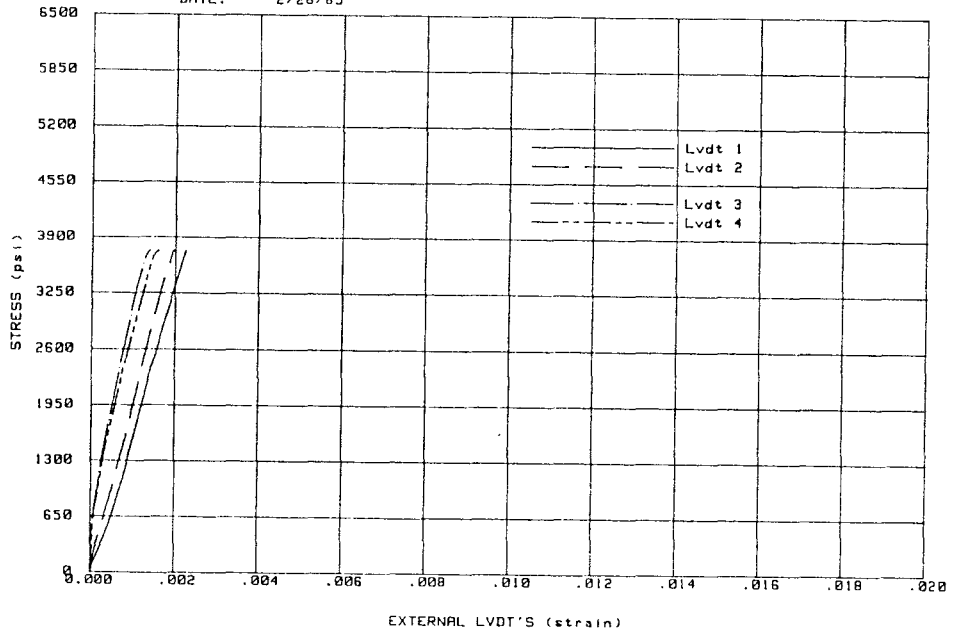
TEST: 4-CLY-G
SPECIMEN: 12-19-9



CLAY 4

ATKINSON-NOLAND AND ASSOCIATES
MASONRY PRISM TESTS
DATE: 2/26/85

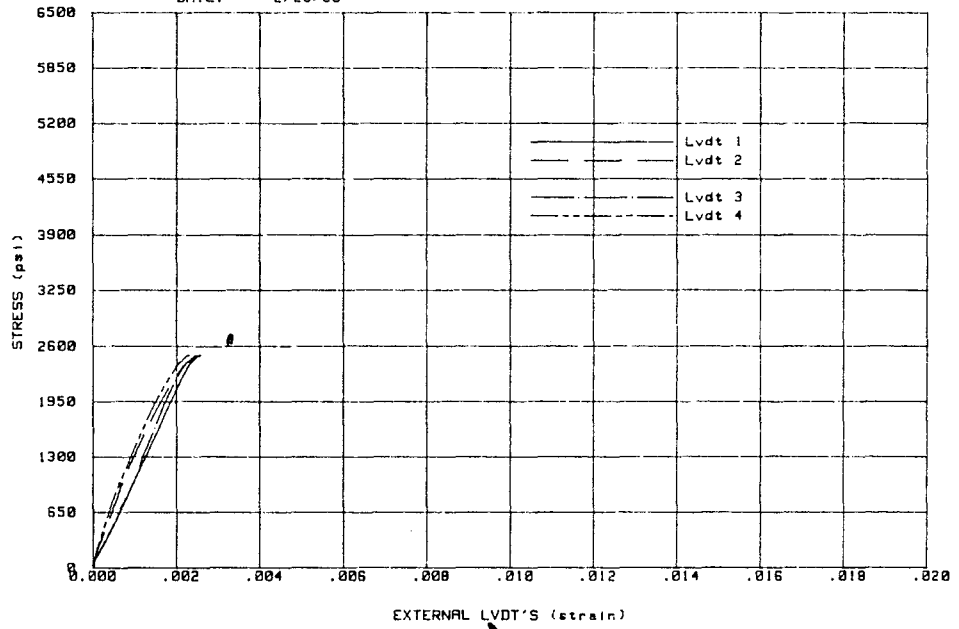
TEST: 4-CLY-G
SPECIMEN: 12-19-10



CLAY 5

ATKINSON-NOLAND AND ASSOCIATES
MASONRY PRISM TESTS
DATE: 2/26/85

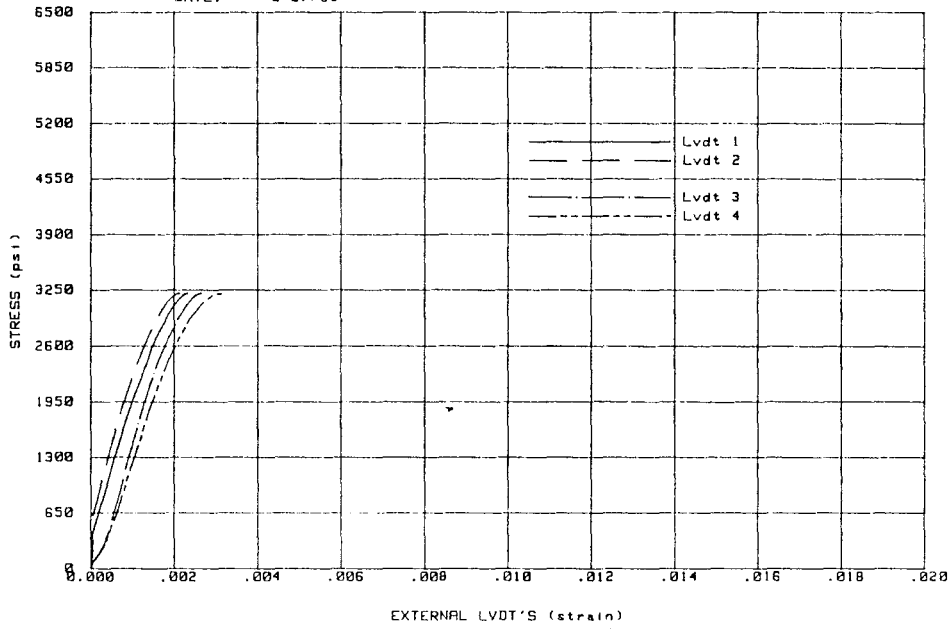
TEST: 4-CNC-G
SPECIMEN: 12-19-11



CONCRETE 1.

ATKINSON-NOLAND AND ASSOCIATES
MASONRY PRISM TESTS
DATE: 2/27/85

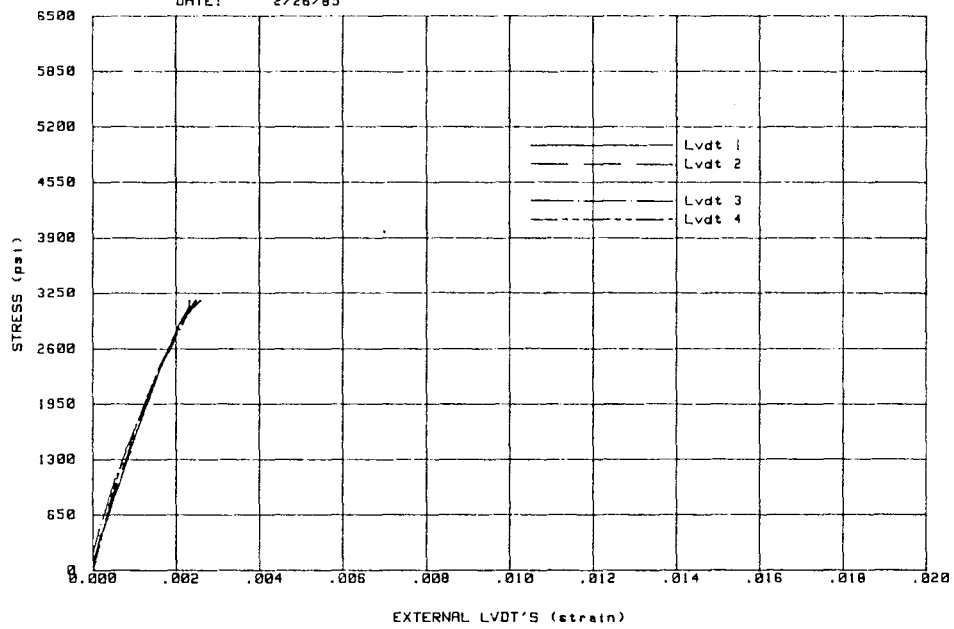
TEST: 4-CNC-G
SPECIMEN: 1-7-1



CONCRETE 2

ATKINSON-NOLAND AND ASSOCIATES
MASONRY PRISM TESTS
DATE: 2/26/85

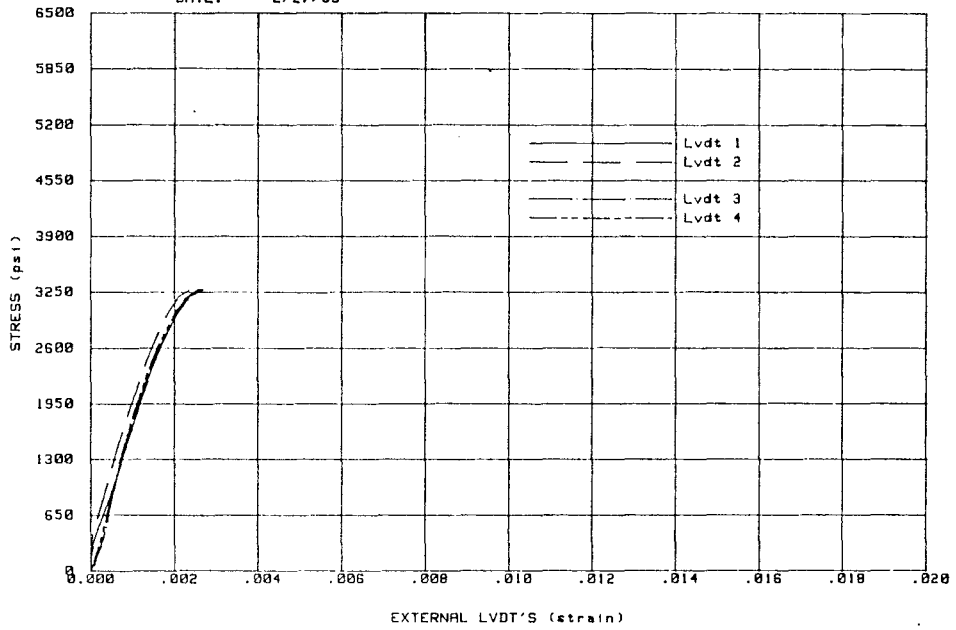
TEST: 4-CNC-G
SPECIMEN: 1-7-2



CONCRETE 3

ATKINSON-NOLAND AND ASSOCIATES
MASONRY PRISM TESTS
DATE: 2/27/85

TEST: 4-CNC-G
SPECIMEN: 1-7-3



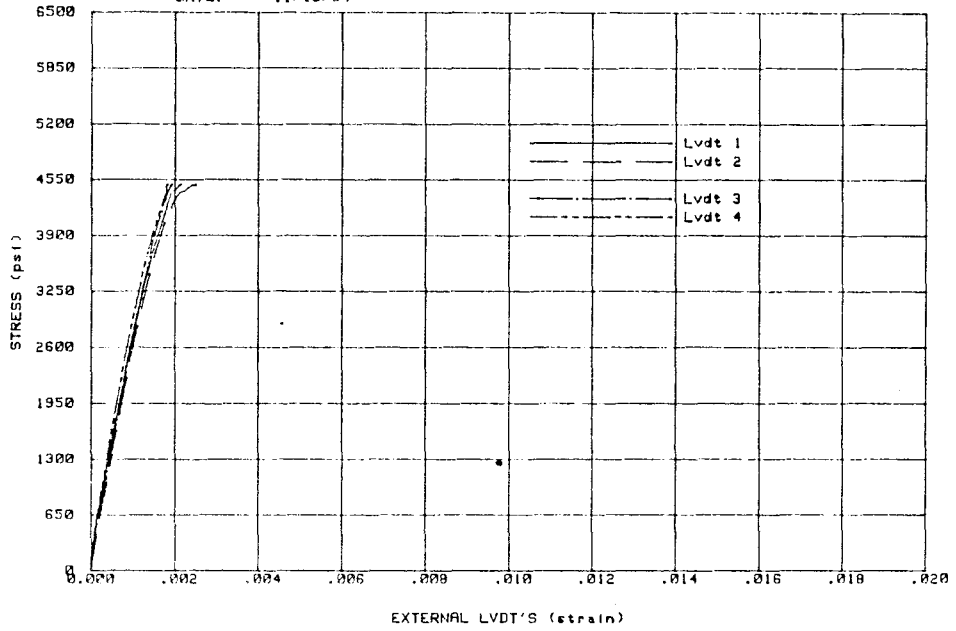
CONCRETE 4

A.3 SERIES 3

UNIT WIDTH	8"
GROUT	STANDARD
MORTAR	TYPE N
BOND PATTERN	STACK BOND
LOAD DIRECTION	NORMAL TO BEDJOINT

ATKINSON-NOLAND AND ASSOCIATES
MASONRY PRISM TESTS
DATE: 11/15/84

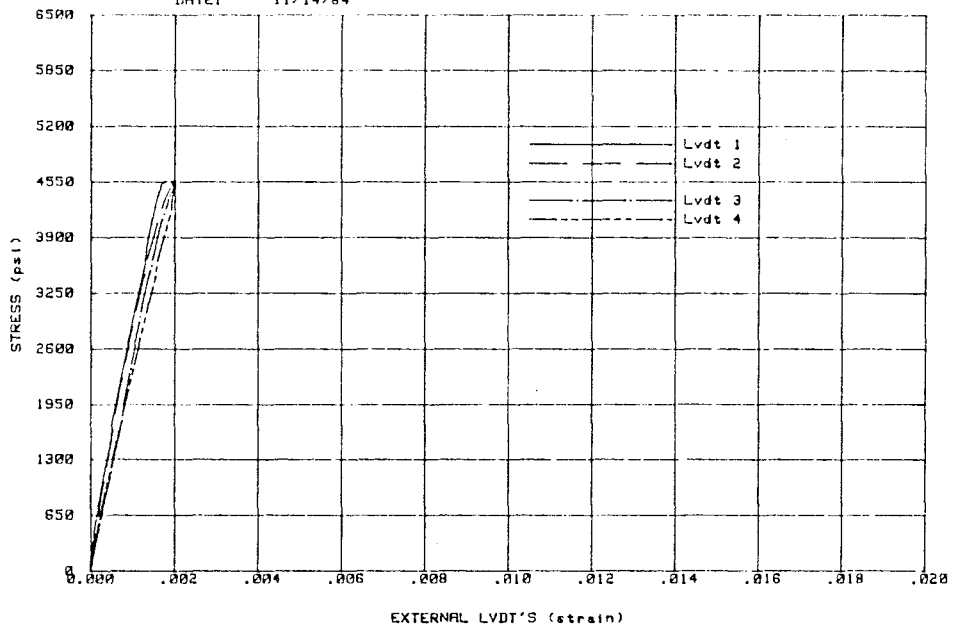
TEST: 8-CLY-G-0
SPECIMEN: 9-25-6



CLAY 1

ATKINSON-NOLAND AND ASSOCIATES
MASONRY PRISM TESTS
DATE: 11/14/84

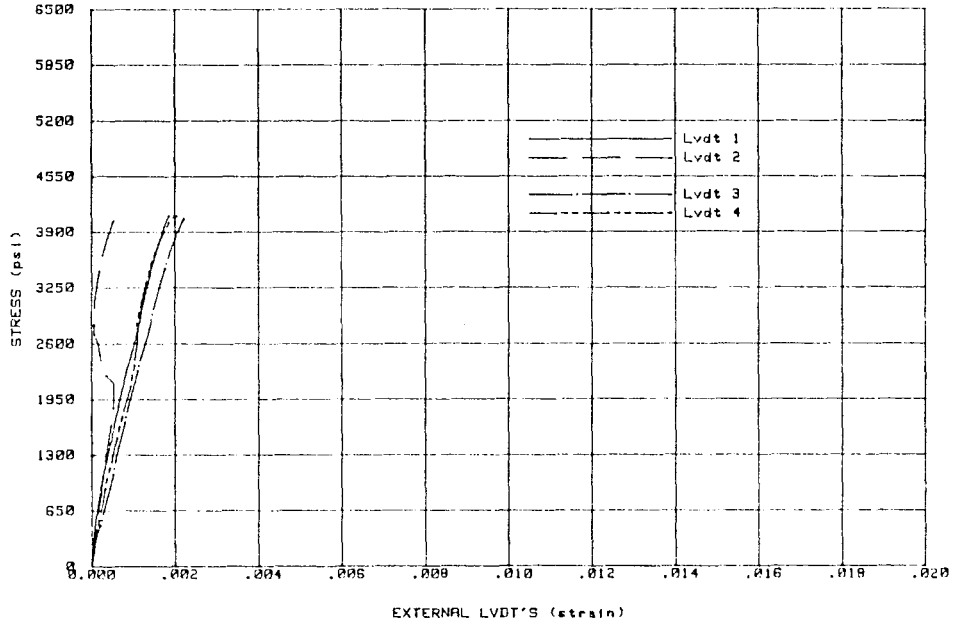
TEST: 8-CLY-G-0
SPECIMEN: 9-25-7



CLAY 2

ATKINSON-NOLAND AND ASSOCIATES
MASONRY PRISM TESTS
DATE: 11/14/84

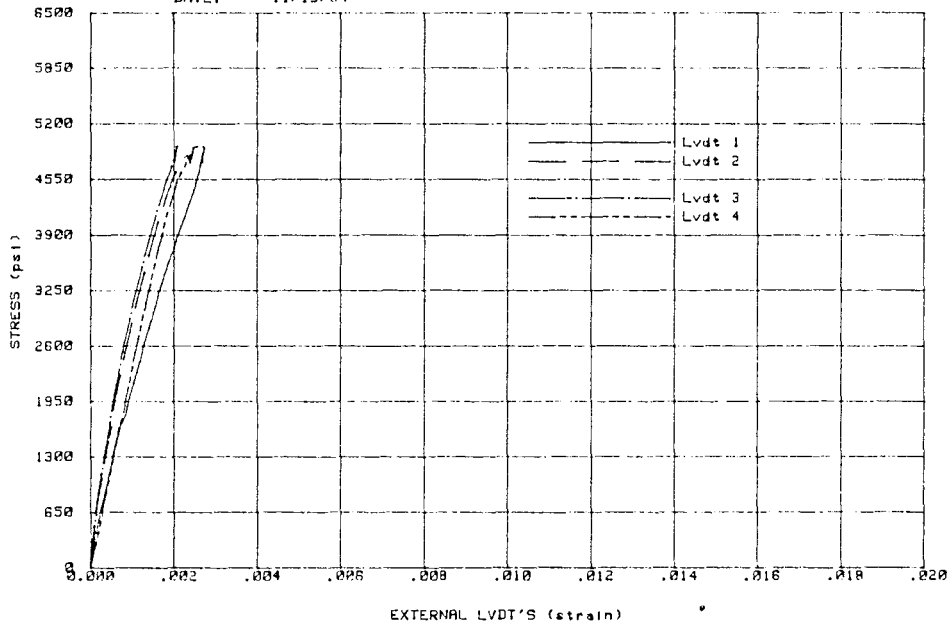
TEST: 8-CLY-G-0
SPECIMEN: 9-25-8



CLAY 3

ATKINSON-NOLAND AND ASSOCIATES
MASONRY PRISM TESTS
DATE: 11/15/84

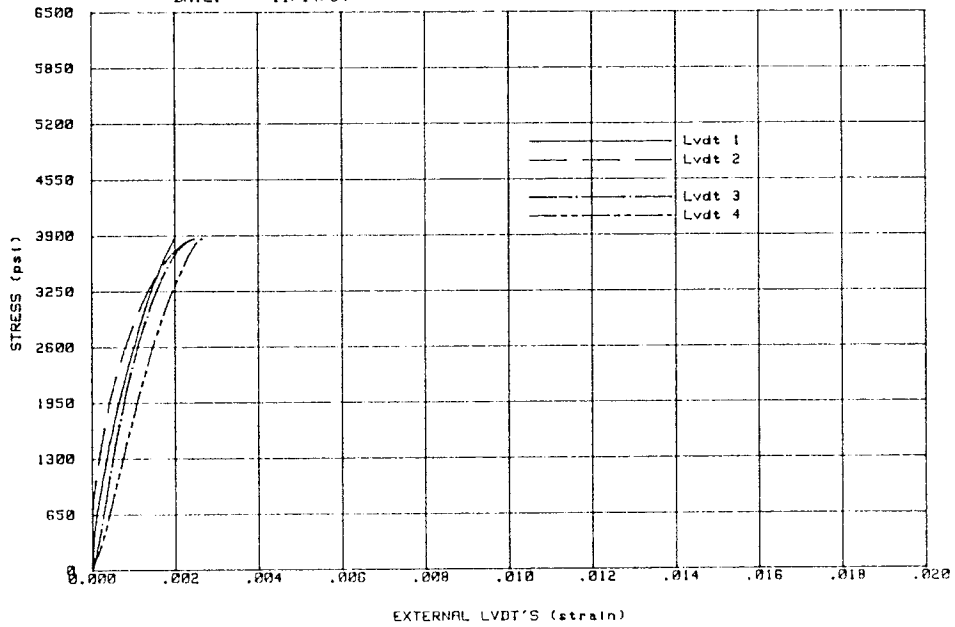
TEST: 8-CLY-G-0
SPECIMEN: 9-25-10



CLAY 4

ATKINSON-NOLAND AND ASSOCIATES
MASONRY PRISM TESTS
DATE: 11/14/84

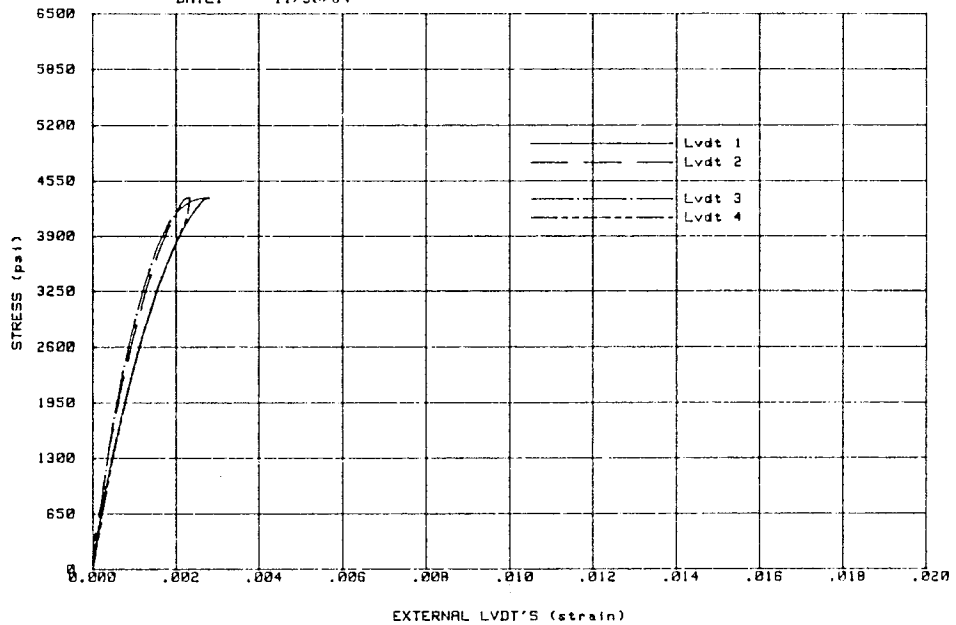
TEST: 8-CNC-G-0
SPECIMEN: 9-25-1



CONCRETE 1

ATKINSON-NOLAND AND ASSOCIATES
MASONRY PRISM TESTS
DATE: 11/30/84

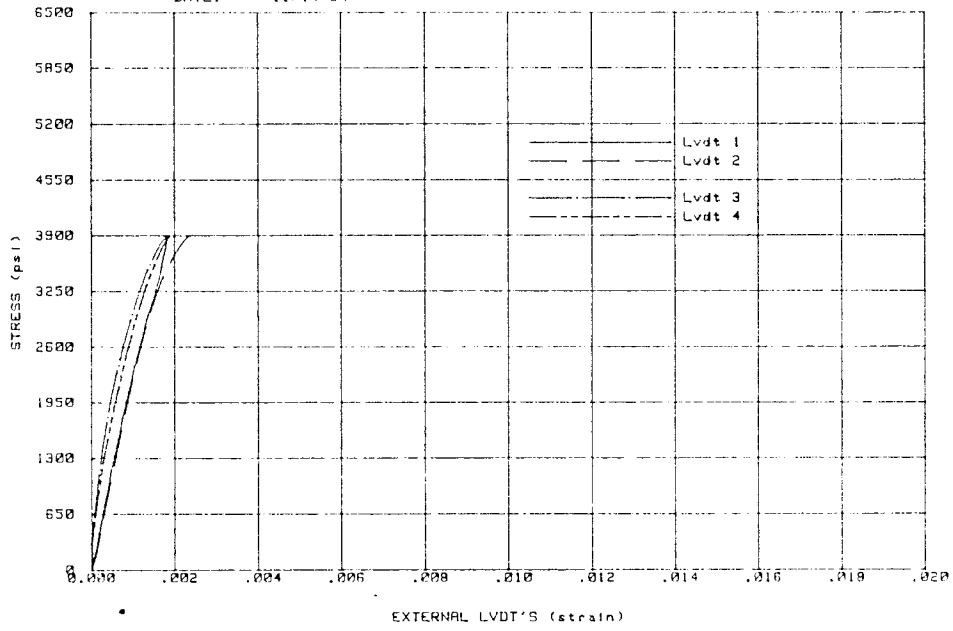
TEST: 8-CNC-G-0
SPECIMEN: 9-25-2



CONCRETE 2

ATKINSON-NOLAND AND ASSOCIATES
MASONRY PRISM TESTS
DATE: 11/14/84

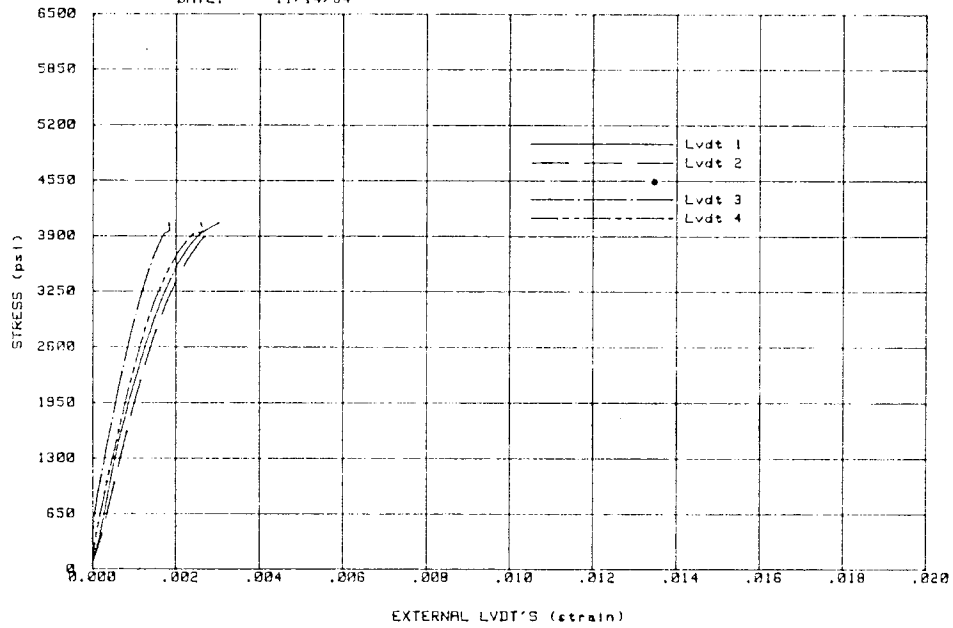
TEST: 8-CNC-G-0
SPECIMEN: 9-25-3



CONCRETE 3

ATKINSON-NOLAND AND ASSOCIATES
MASONRY PRISM TESTS
DATE: 11/14/84

TEST: 8-CNC-G-0
SPECIMEN: 9-25-4



CONCRETE 4

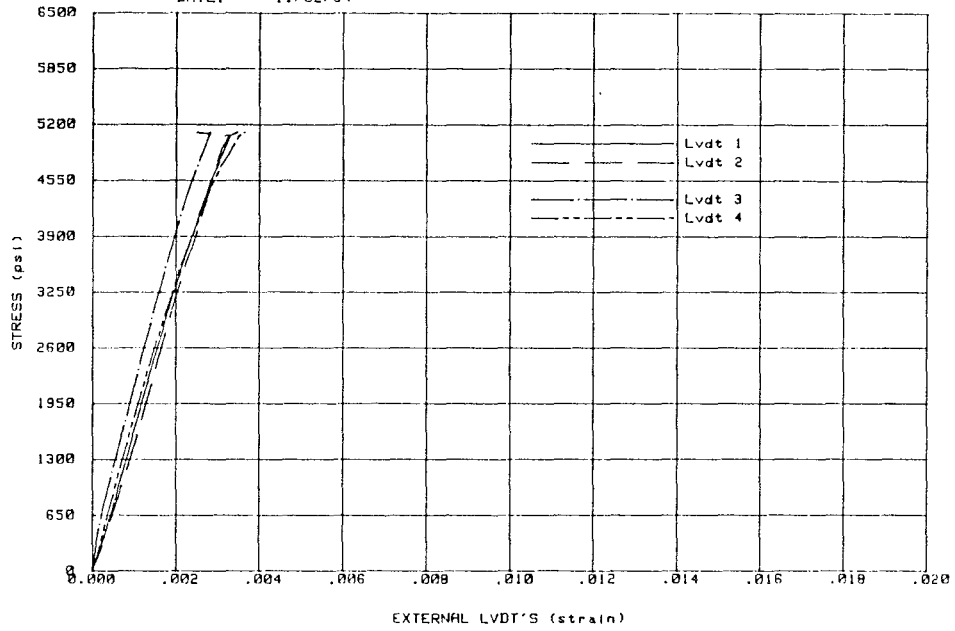
[Faint, illegible handwritten text]

A.4 SERIES 4

UNIT WIDTH	6"
GROUT	NONE
MORTAR	TYPE N
BOND PATTERN	STACK BOND
LOAD DIRECTION	NORMAL TO BEDJOINT

ATKINSON-NOLAND AND ASSOCIATES
MASONRY PRISM TESTS
DATE: 11/02/84

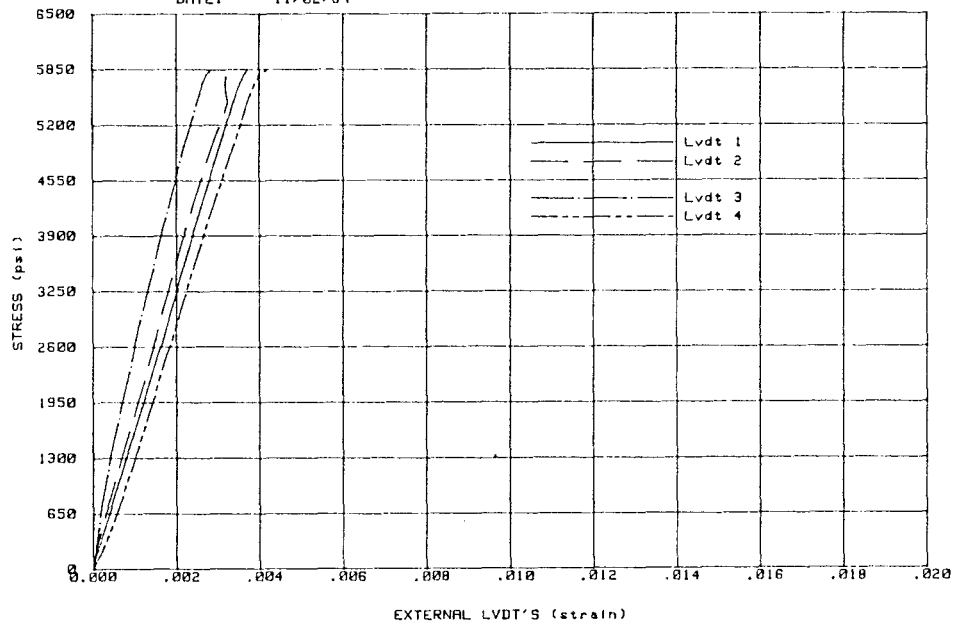
TEST: 6-CLY-NG-0
SPECIMEN: 9-18-6



CLAY 1

ATKINSON-NOLAND AND ASSOCIATES
MASONRY PRISM TESTS
DATE: 11/02/84

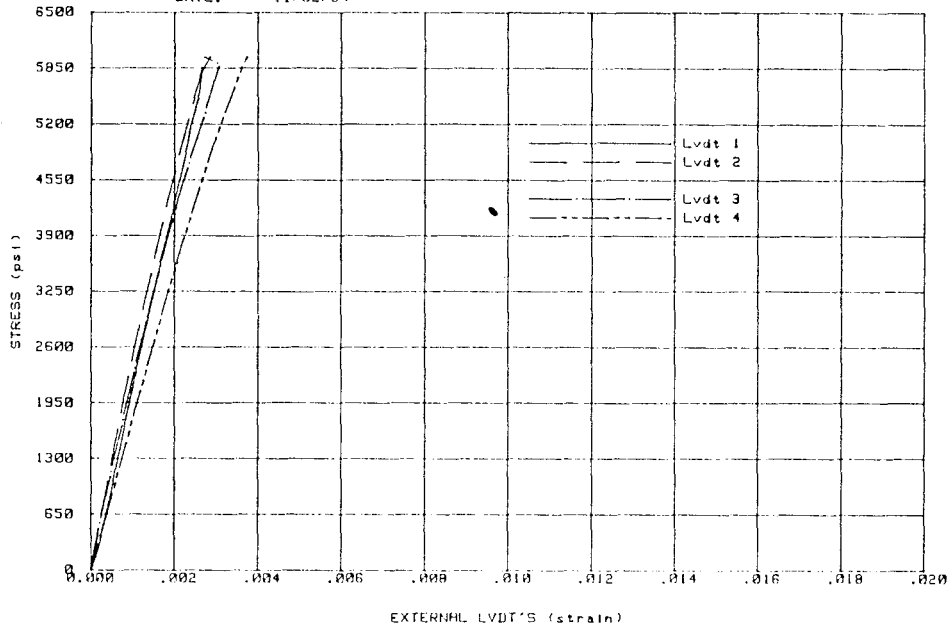
TEST: 6-CLY-NG-0
SPECIMEN: 9-18-7



CLAY 2

ATKINSON-NOLAND AND ASSOCIATES
MASONRY PRISM TESTS
DATE: 11/02/84

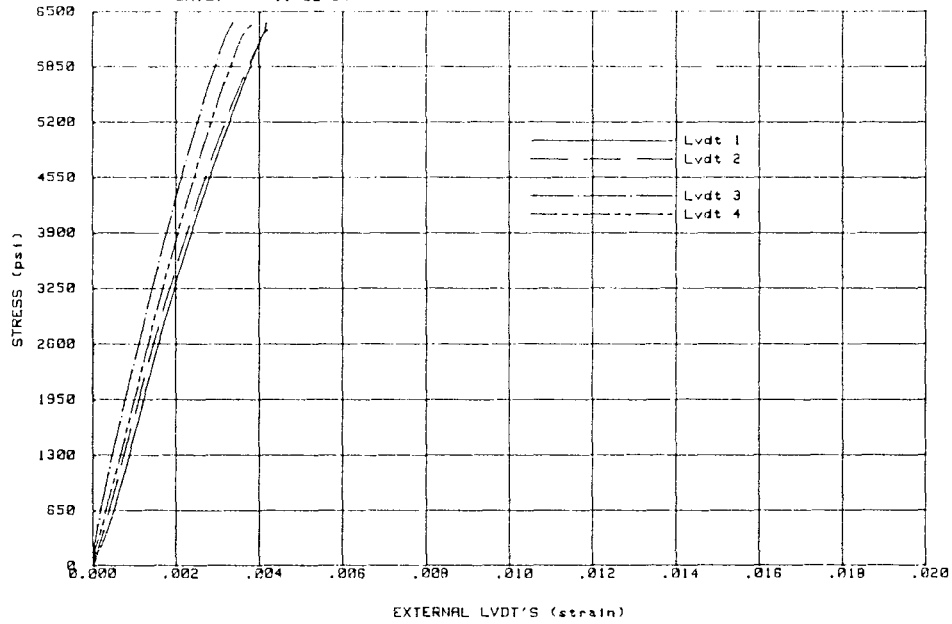
TEST: 6-CLY-NG-0
SPECIMEN: 9-18-8



CLAY 3

ATKINSON-NOLAND AND ASSOCIATES
MASONRY PRISM TESTS
DATE: 11/02/84

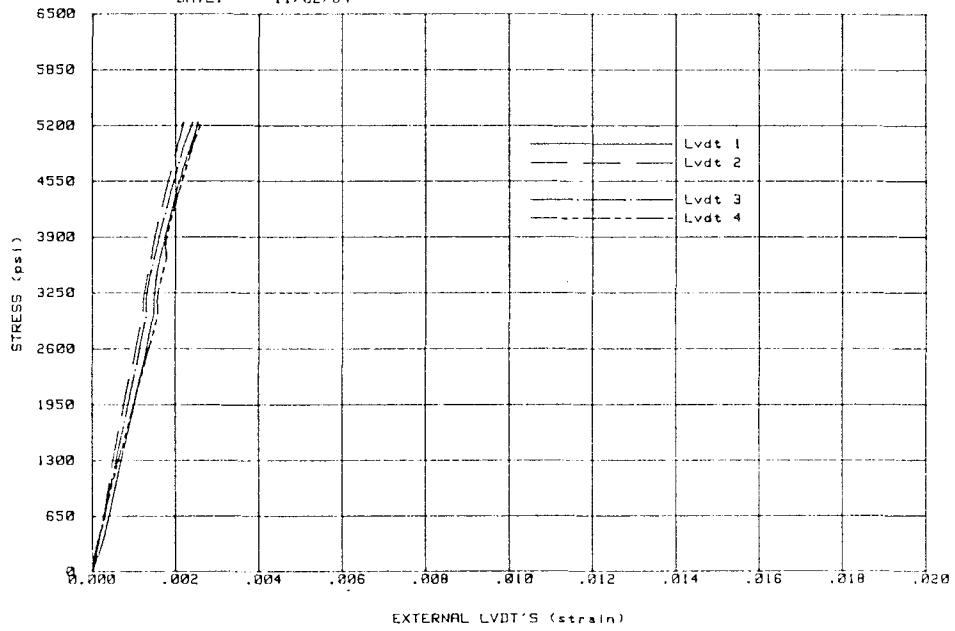
TEST: 6-CLY-NG-0
SPECIMEN: 9-18-9



CLAY 4

ATKINSON-NOLAND AND ASSOCIATES
MASONRY PRISM TESTS
DATE: 11/02/84

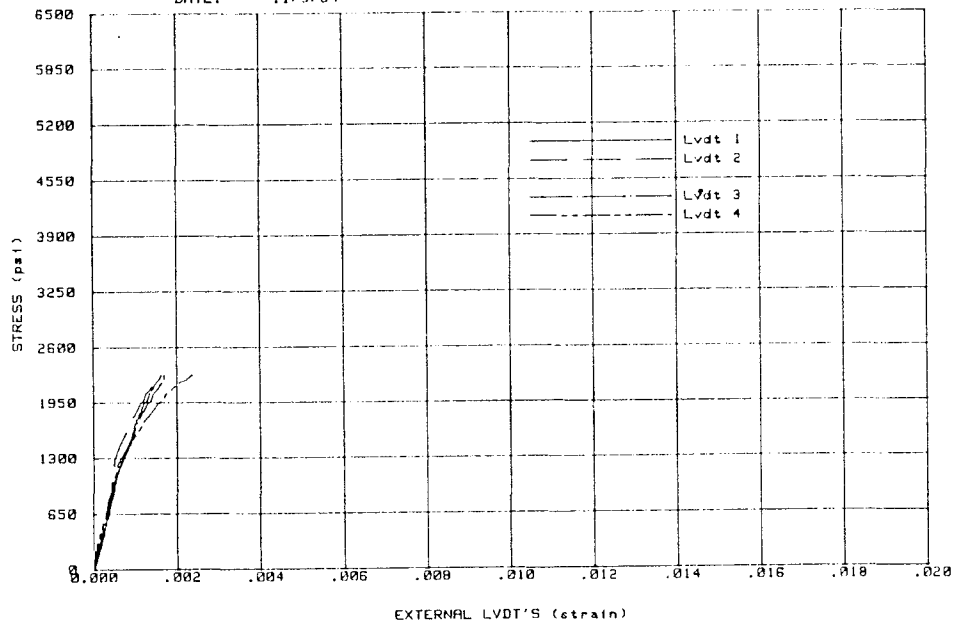
TEST: 6-CLY-NG-0
SPECIMEN: 9-18-10



CLAY 5

ATKINSON-NOLAND AND ASSOCIATES
MASONRY PRISM TESTS
DATE: 11/9/84

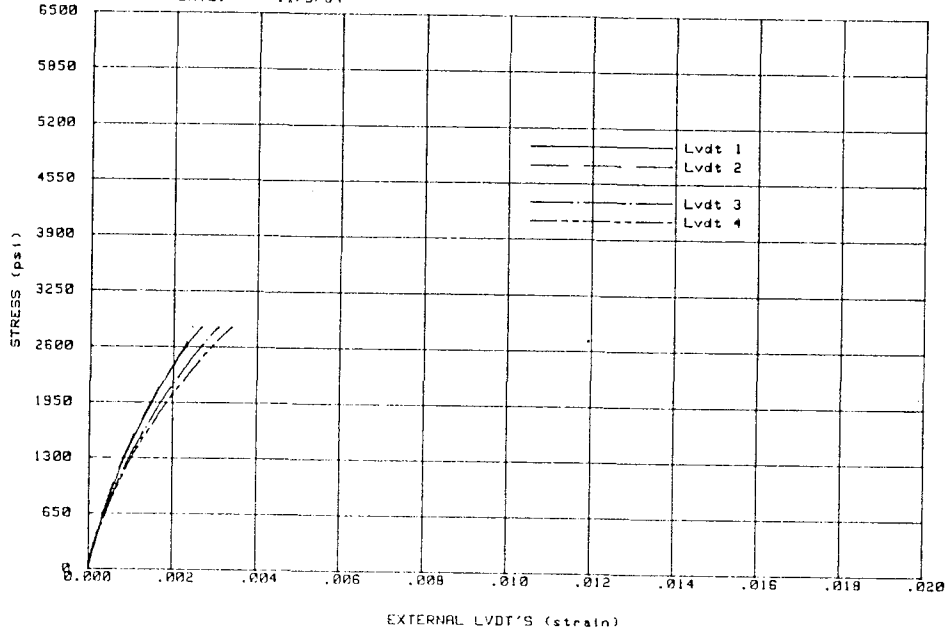
TEST: 6-CNC-NG-0
SPECIMEN: 9-18-1



CONCRETE 1

ATKINSON-NOLAND AND ASSOCIATES
MASONRY PRISM TESTS
DATE: 11/9/84

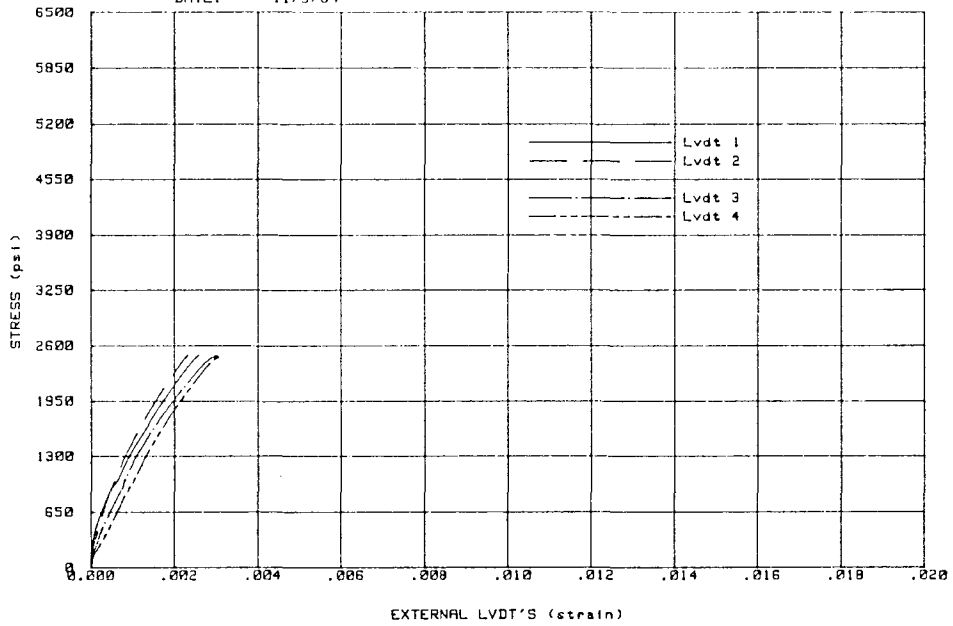
TEST: 6-CNC-NG-0
SPECIMEN: 9-18-2



CONCRETE 2

ATKINSON-NOLAND AND ASSOCIATES
MASONRY PRISM TESTS
DATE: 11/9/84

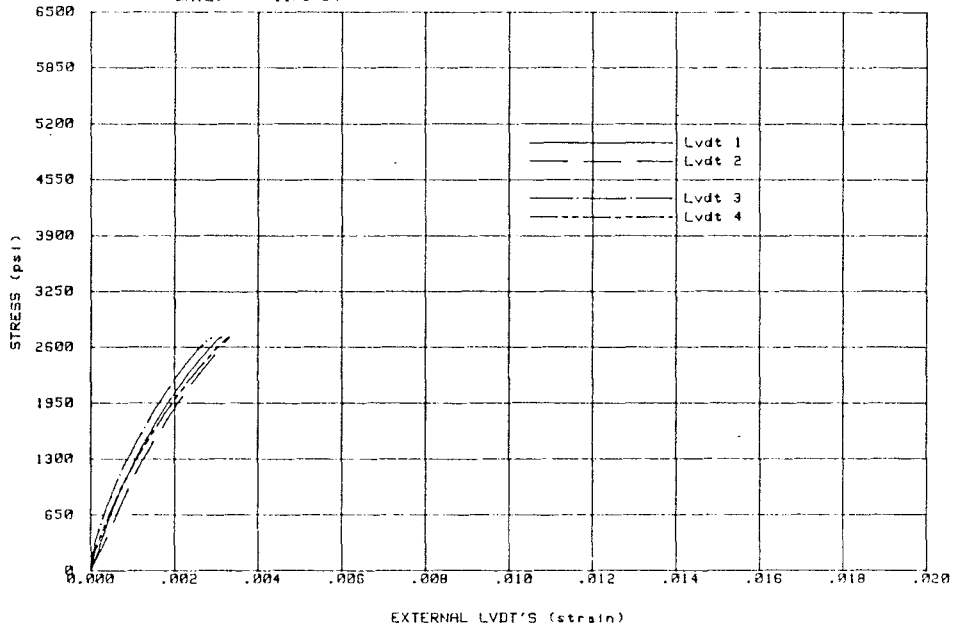
TEST: 6-CNC-NG-0
SPECIMEN: 9-18-3



CONCRETE 3

ATKINSON-NOLAND AND ASSOCIATES
MASONRY PRISM TESTS
DATE: 11/9/84

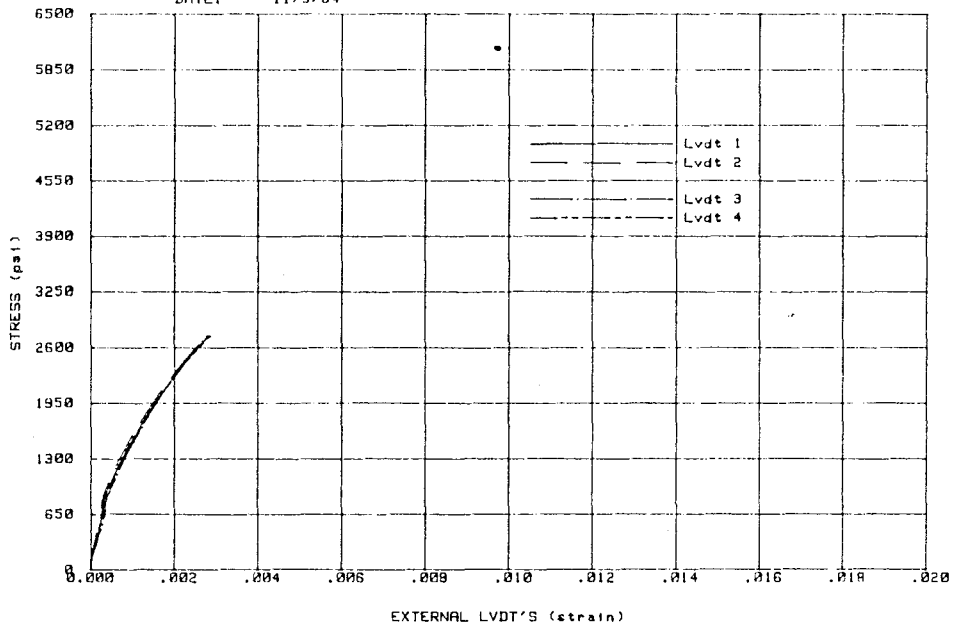
TEST: 6-CNC-NG-0
SPECIMEN: 9-18-4



CONCRETE 4

ATKINSON-NOLAND AND ASSOCIATES
MASONRY PRISM TESTS
DATE: 11/9/84

TEST: 6-CNC-NG-0
SPECIMEN: 9-18-5



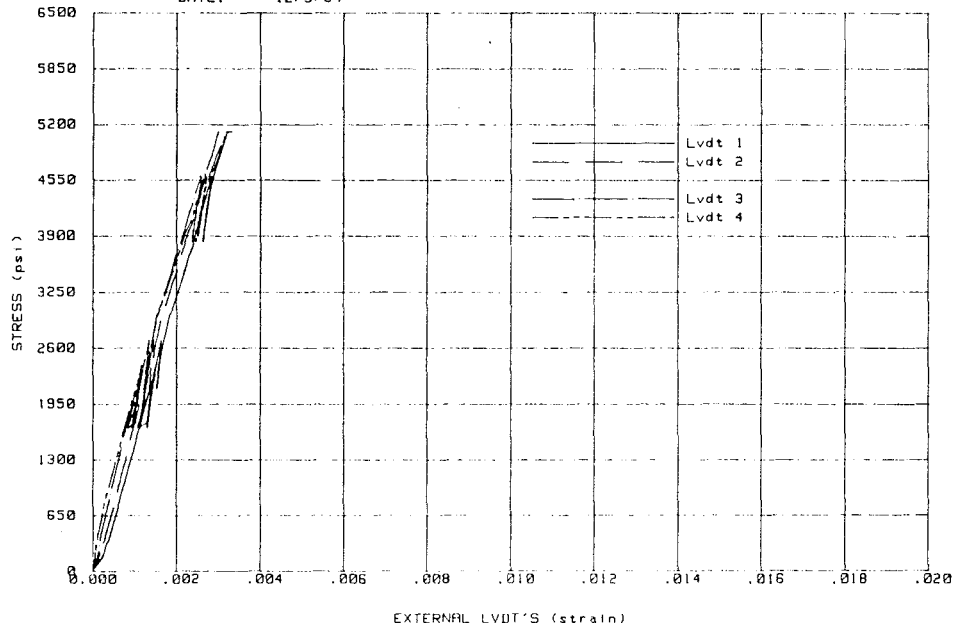
CONCRETE 5

A.5 SERIES 5

UNIT WIDTH	8"
GROUT	NONE
MORTAR	TYPE N
BOND PATTERN	STACK BOND
LOAD DIRECTION	NORMAL TO BEDJOINT

ATKINSON-NOLAND AND ASSOCIATES
MASONRY PRISM TESTS
DATE: 12/5/84

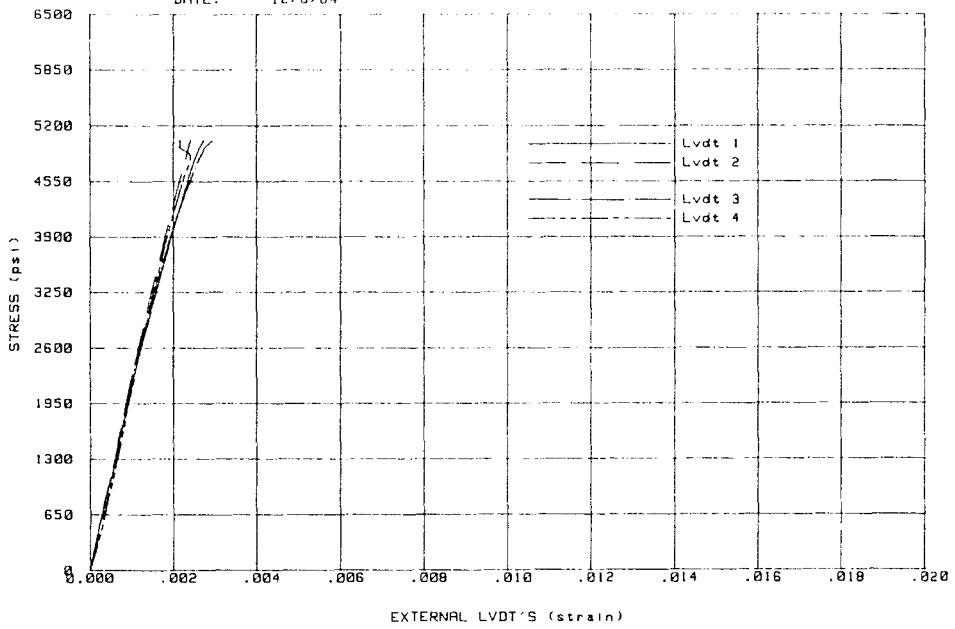
TEST: 8-CLY-NG-0
SPECIMEN: 10-2-1



CLAY 1

ATKINSON-NOLAND AND ASSOCIATES
MASONRY PRISM TESTS
DATE: 12/6/84

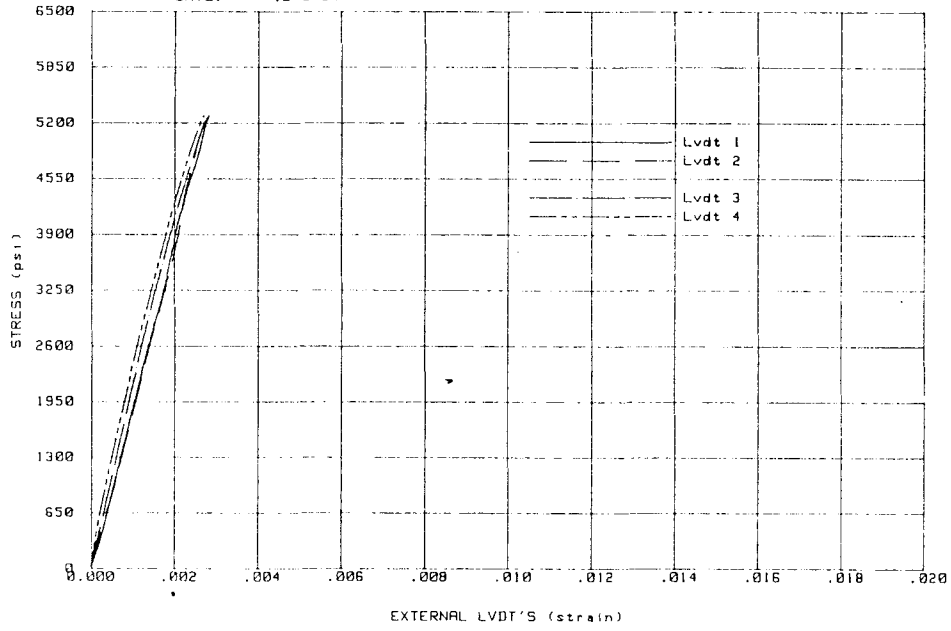
TEST: 8-CLY-NG-0
SPECIMEN: 10-2-2



CLAY 2

ATKINSON-NOLAND AND ASSOCIATES
MASONRY PRISM TESTS
DATE: 12/6/84

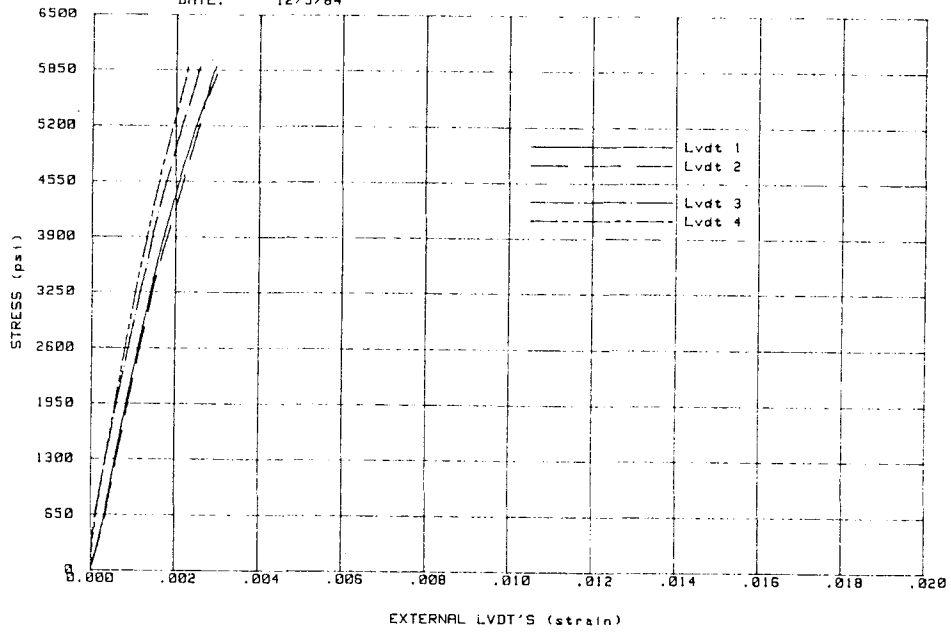
TEST: 8-CLY-NG-0
SPECIMEN: 10-2-3



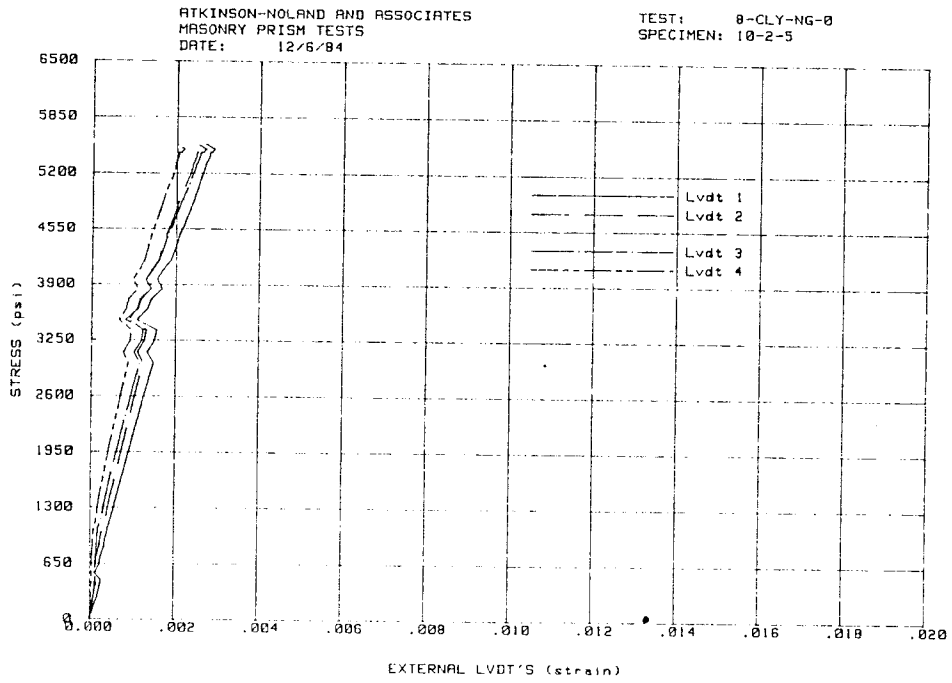
CLAY 3

ATKINSON-NOLAND AND ASSOCIATES
MASONRY PRISM TESTS
DATE: 12/5/84

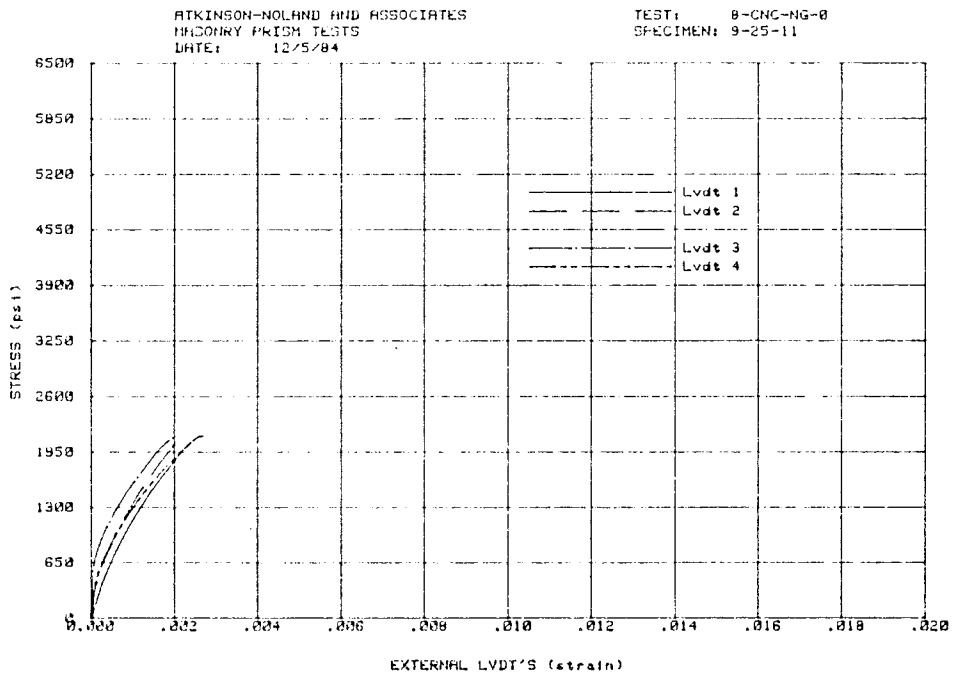
TEST: 8-CLY-NG-0
SPECIMEN: 10-2-4



CLAY 4



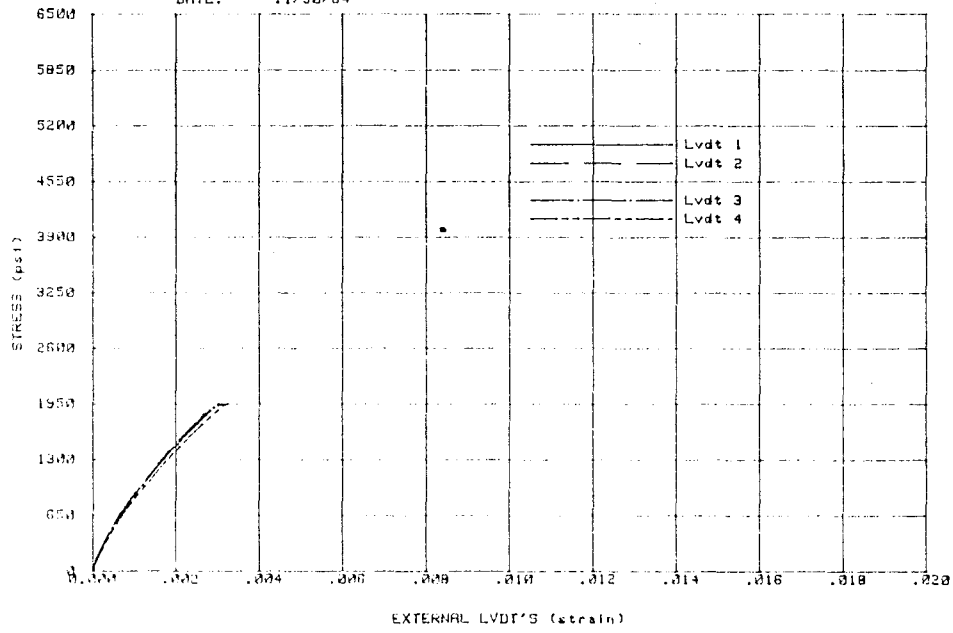
CLAY 5



CONCRETE 1

ATKINSON-NOLAND AND ASSOCIATES
MASONRY PRISM TESTS
DATE: 11/30/84

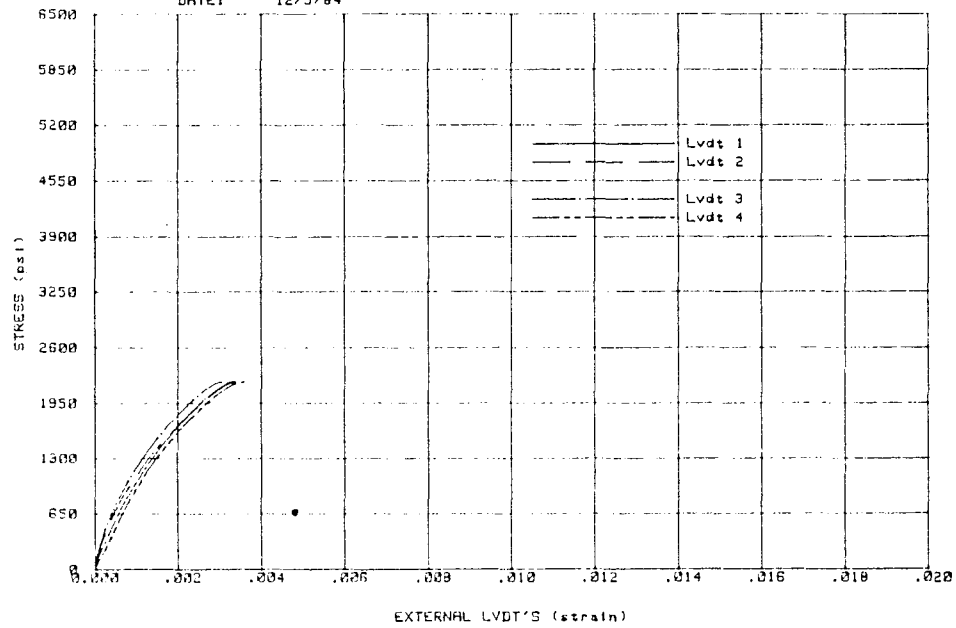
TEST: 8-CNC-NG-0
SPECIMEN: 9-25-12



CONCRETE 2

ATKINSON-NOLAND AND ASSOCIATES
MASONRY PRISM TESTS
DATE: 12/5/84

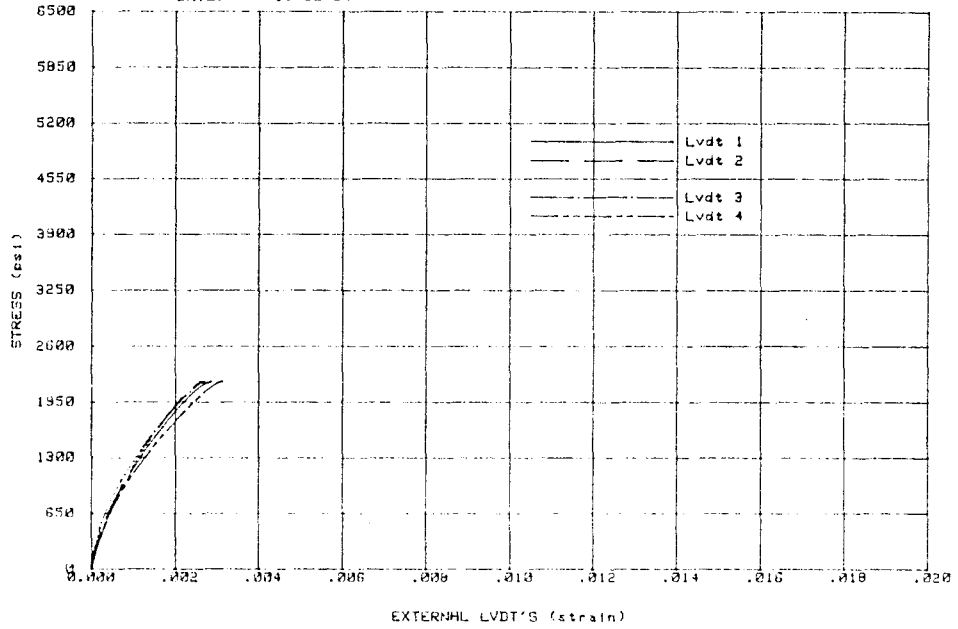
TEST: 8-CNC-NG-0
SPECIMEN: 9-25-13



CONCRETE 3

ATKINSON-NOLAND AND ASSOCIATES
MASONRY PRISM TESTS
DATE: 11/30/84

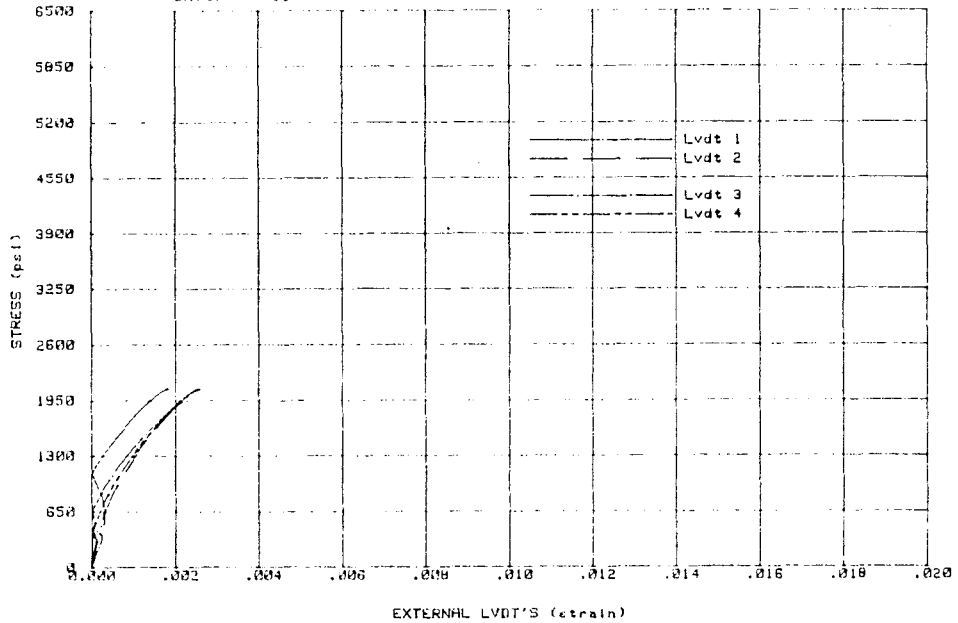
TEST: 8-CNC-NG-8
SPECIMEN: 9-25-14



CONCRETE 4

ATKINSON-NOLAND AND ASSOCIATES
MASONRY PRISM TESTS
DATE: 11/30/84

TEST: 8-CNC-NG-8
SPECIMEN: 9-25-15



CONCRETE 5

Reproduced from
best available copy.

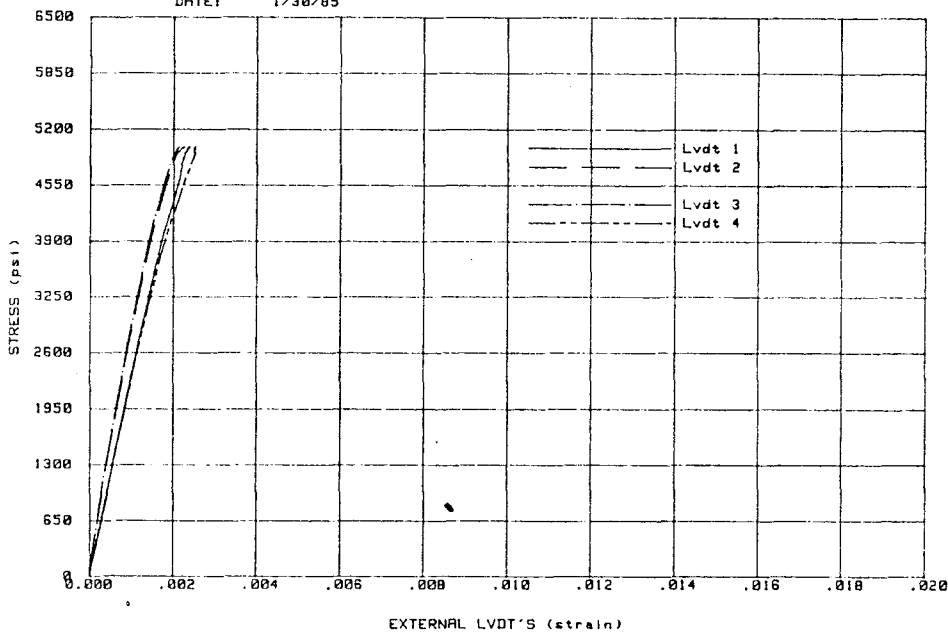
A.1.6 DETAILS B

UNIT WIDTH	6"
GROUT	STANDARD
MORTAR	TYPE M
BOND PATTERN	ROUGHENED SURF
LOAD DIRECTION	NORMAL TO SURFACE

Reproduced from
best available copy.

ATKINSON-NOLAND AND ASSOCIATES
MASONRY PRISM TESTS
DATE: 1/30/85

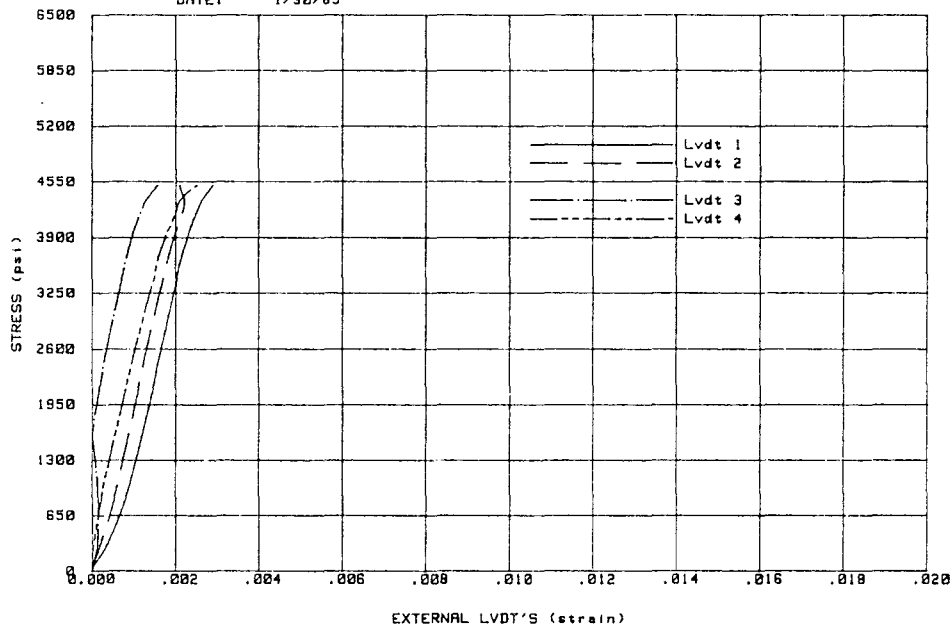
TEST: 6-CLY-G-R
SPECIMEN: 12-4-2



CLAY 1

ATKINSON-NOLAND AND ASSOCIATES
MASONRY PRISM TESTS
DATE: 1/30/85

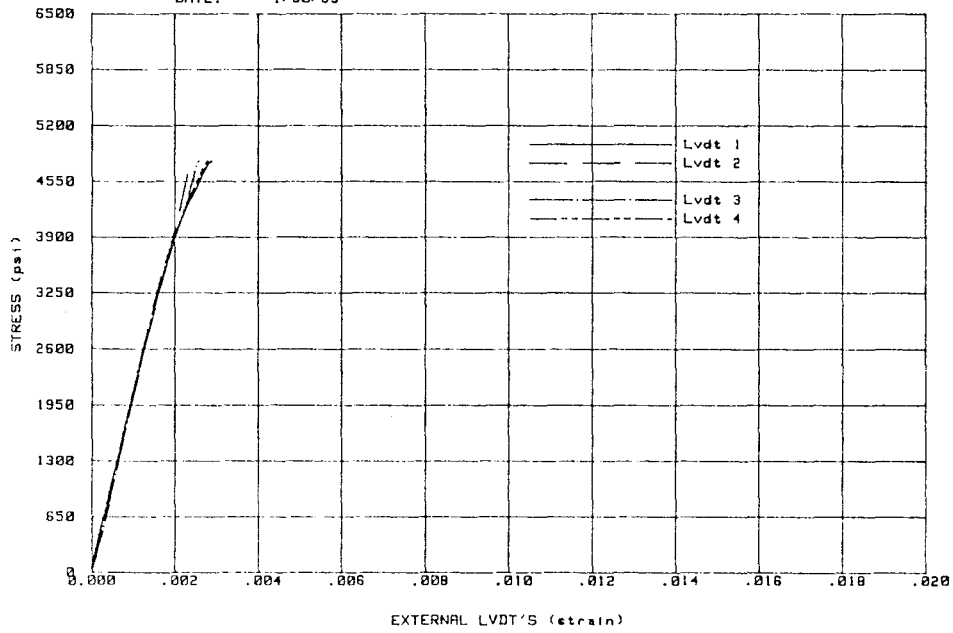
TEST: 6-CLY-G-R
SPECIMEN: 12-4-4



CLAY 2

ATKINSON-NOLAND AND ASSOCIATES
MASONRY PRISM TESTS
DATE: 1/30/85

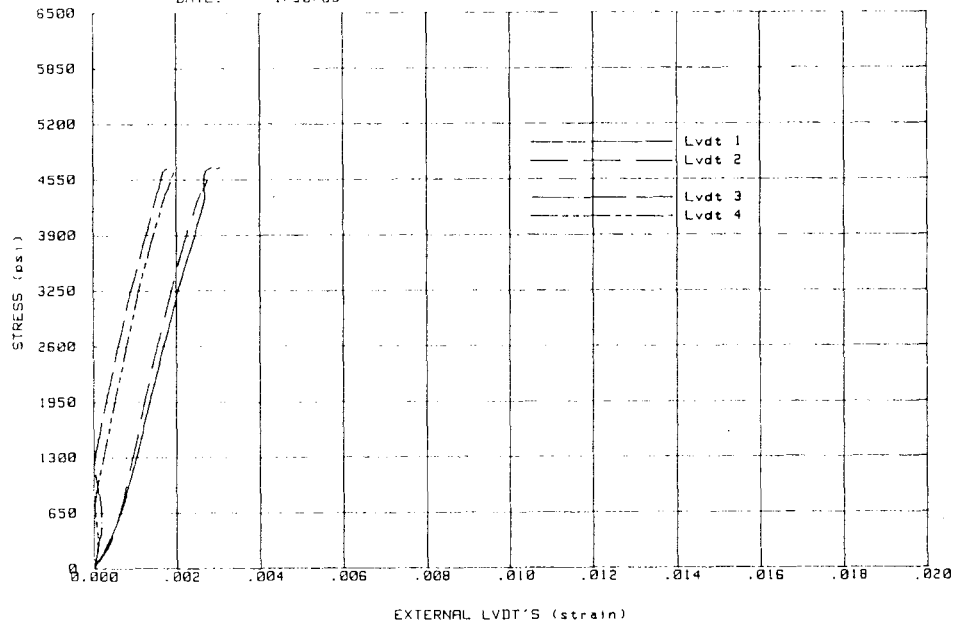
TEST: 6-CLY-G-R
SPECIMEN: 12-4-5



CLAY 3

ATKINSON-NOLAND AND ASSOCIATES
MASONRY PRISM TESTS
DATE: 1/30/85

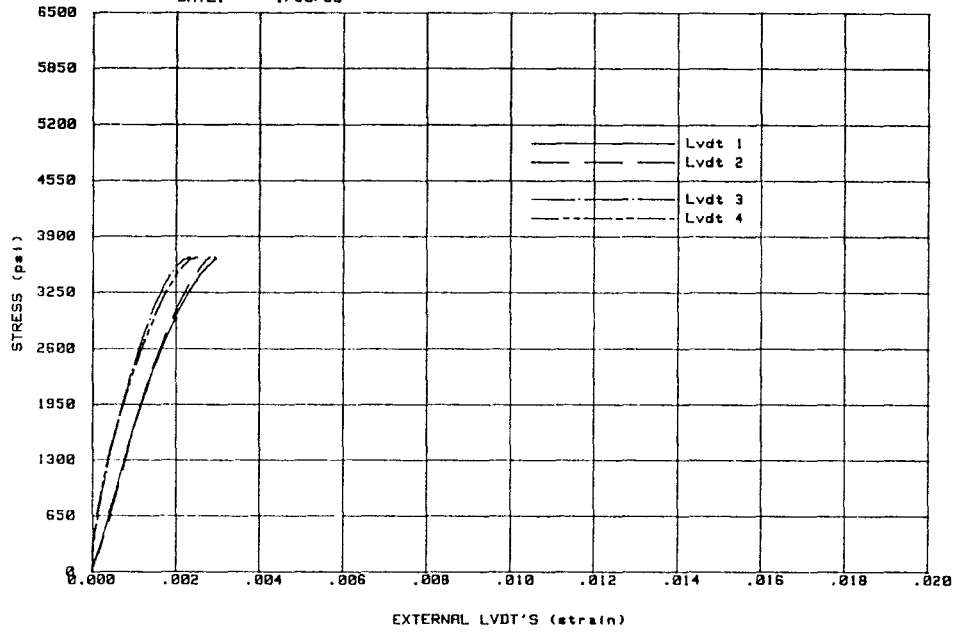
TEST: 6-CLY-G-R
SPECIMEN: 12-4-6



CLAY 4

ATKINSON-NOLAND AND ASSOCIATES
MASONRY PRISM TESTS
DATE: 1/30/85

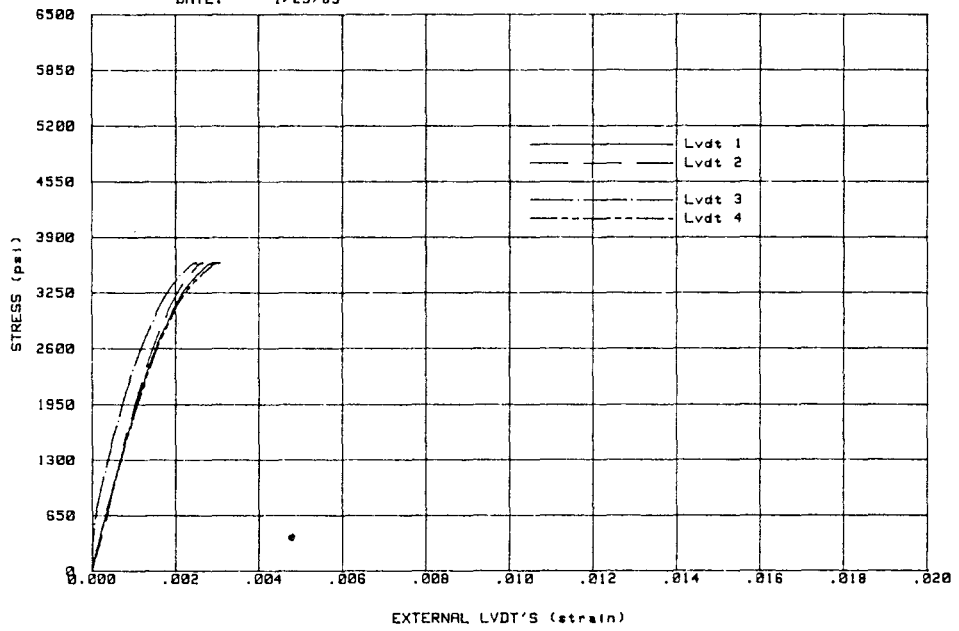
TEST: 6-CNC-G-R
SPECIMEN: 11-28-1



CONCRETE 1

ATKINSON-NOLAND AND ASSOCIATES
MASONRY PRISM TESTS
DATE: 1/29/85

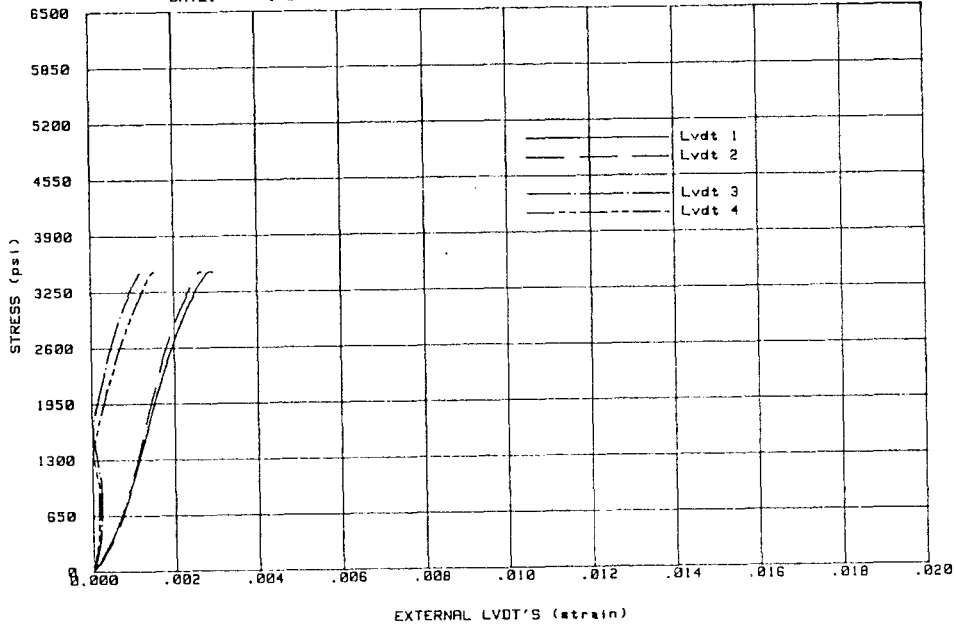
TEST: 6-CNC-G-R
SPECIMEN: 11-28-2



CONCRETE 2

ATKINSON-NOLAND AND ASSOCIATES
MASONRY PRISM TESTS
DATE: 1/29/85

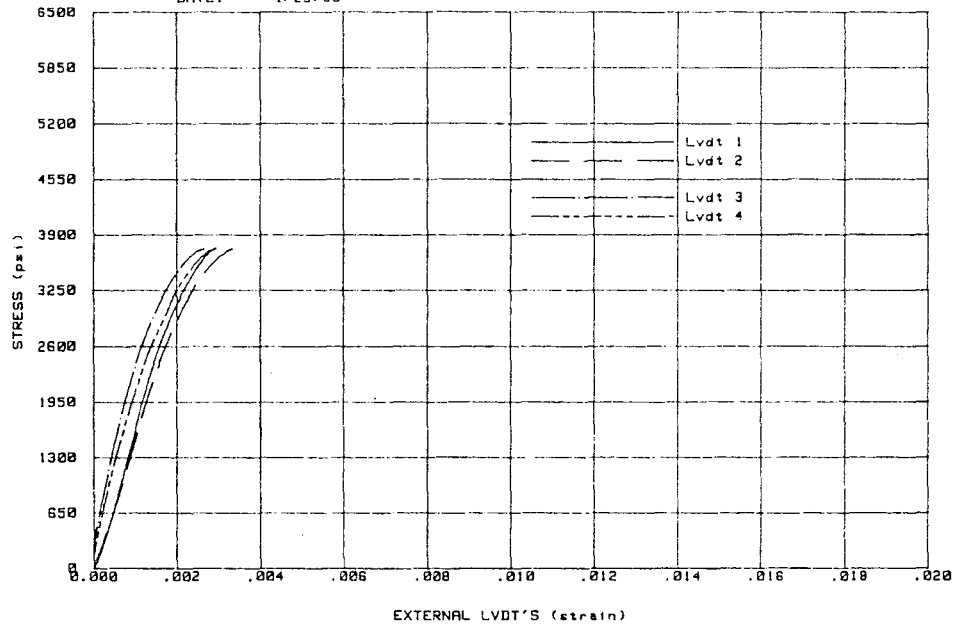
TEST: 6-CNC-G-R
SPECIMEN: 11-28-3



CONCRETE 3

ATKINSON-NOLAND AND ASSOCIATES
MASONRY PRISM TESTS
DATE: 1/29/85

TEST: 6-CNC-G-R
SPECIMEN: 11-28-4



CONCRETE 4

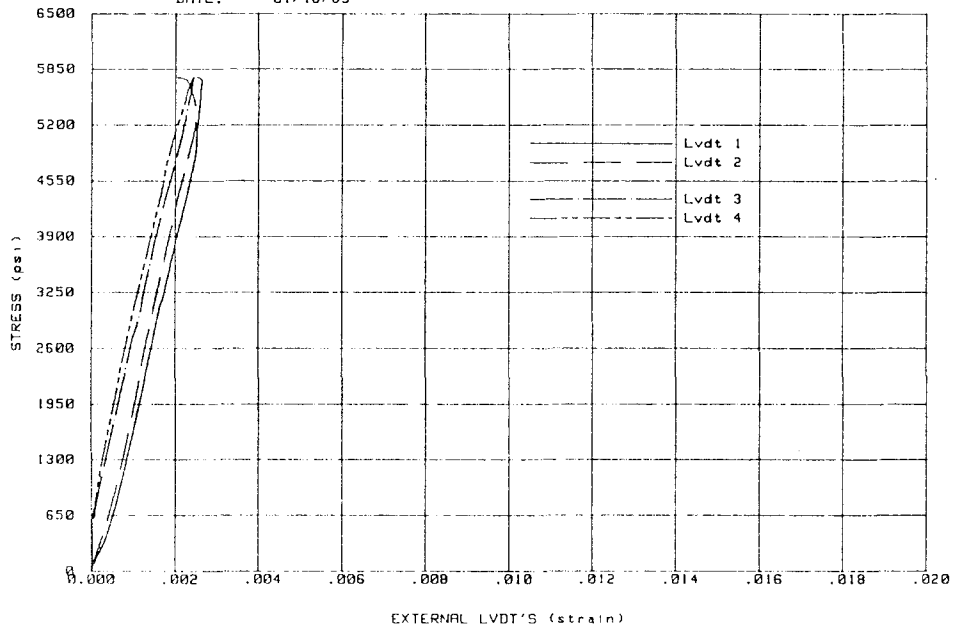
Handwritten scribbles or marks, possibly representing a signature or initials, located in the upper right quadrant of the page.

A.7 SERIES 7

UNIT WIDTH	6"
GROUT	STANDARD
MORTAR	TYPE S
BOND PATTERN	STACK BOND
LOAD DIRECTION	NORMAL TO BEDJOINT

ATKINSON-NOLAND AND ASSOCIATES
MASONRY PRISM TESTS
DATE: 01/18/85

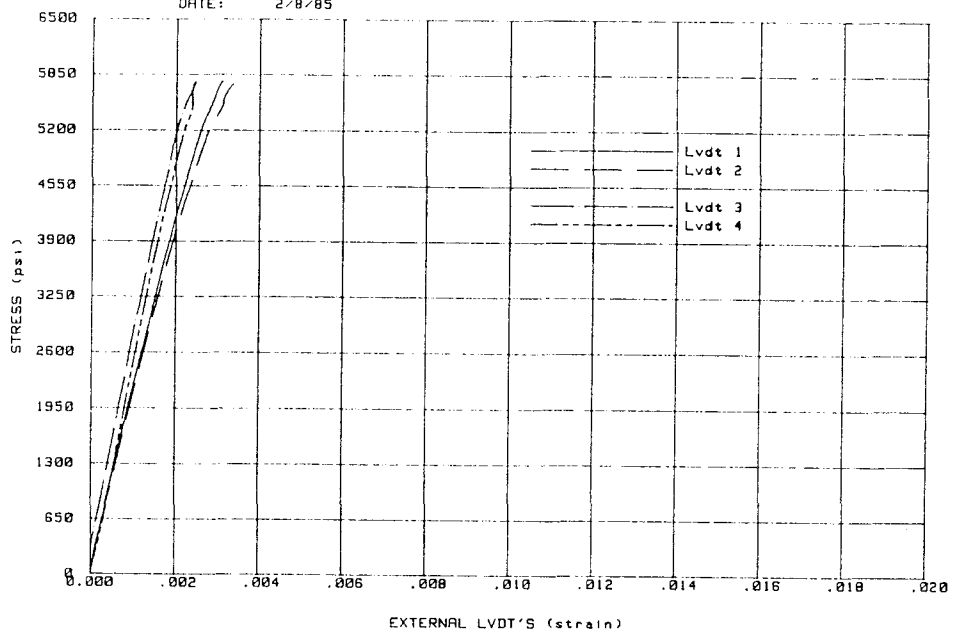
TEST: 6-CLY-G-5
SPECIMEN: 12-11-6



CLAY 1

ATKINSON-NOLAND AND ASSOCIATES
MASONRY PRISM TESTS
DATE: 2/8/85

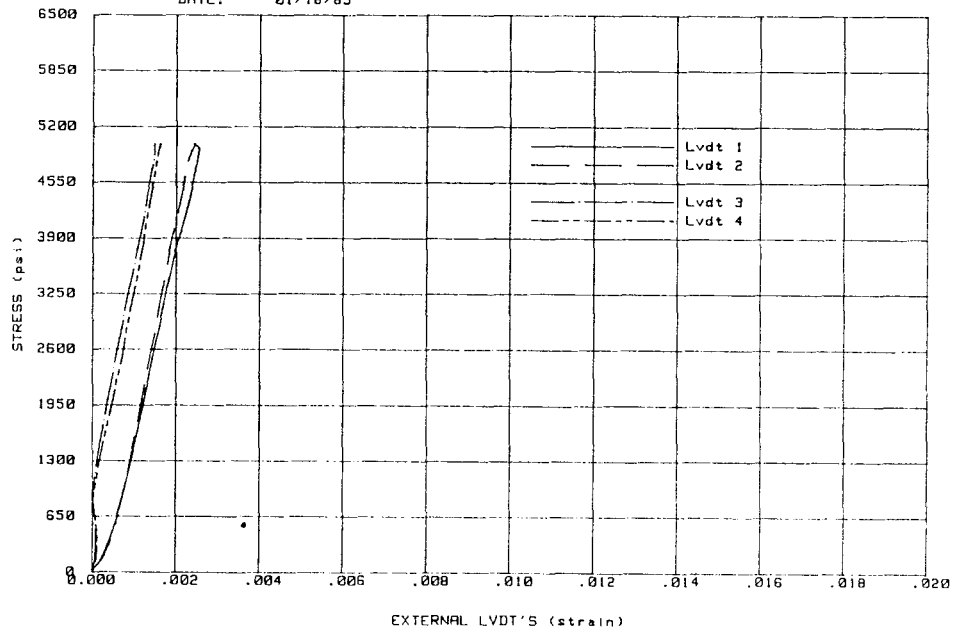
TEST: 6-CLY-G-5
SPECIMEN: 12-11-7



CLAY 2

ATKINSON-NOLAND AND ASSOCIATES
MASONRY PRISM TESTS
DATE: 01/18/85

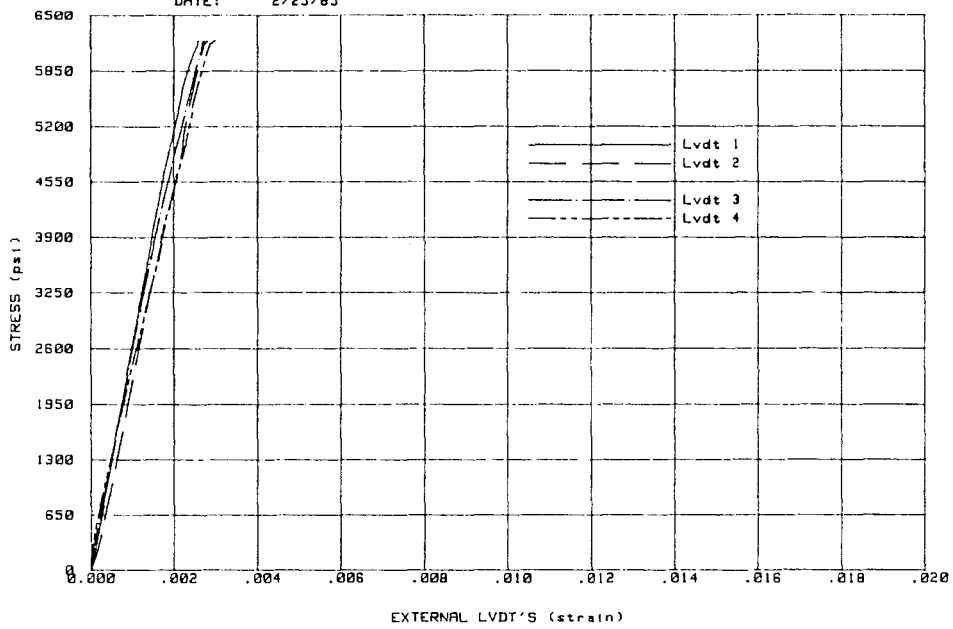
TEST: 6-CLY-G-S
SPECIMEN: 12-11-8



CLAY 3

ATKINSON-NOLAND AND ASSOCIATES
MASONRY PRISM TESTS
DATE: 2/25/85

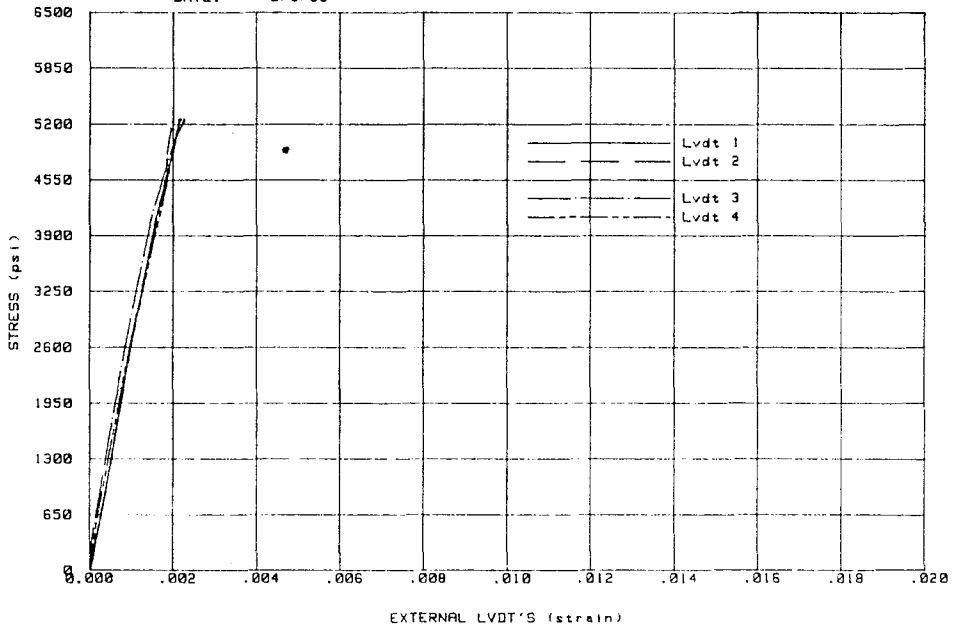
TEST: 6-CLY-G-S
SPECIMEN: 12-11-9



CLAY 4

ATKINSON-NOLAND AND ASSOCIATES
MASONRY PRISM TESTS
DATE: 2/8/85

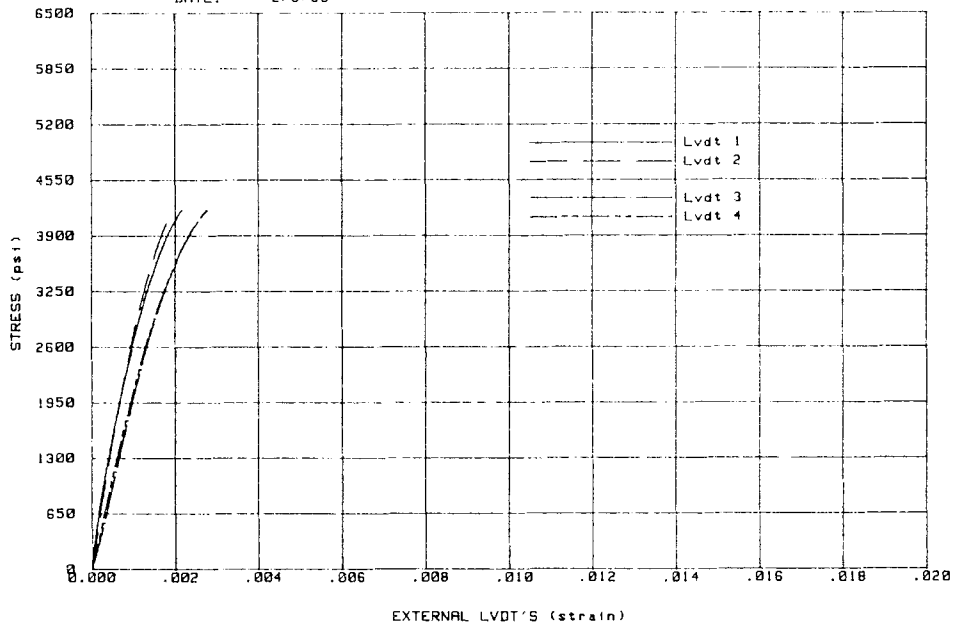
TEST: 6-CLY-G-S
SPECIMEN: 12-11-10



CLAY 5

ATKINSON-NOLAND AND ASSOCIATES
MASONRY PRISM TESTS
DATE: 2/8/85

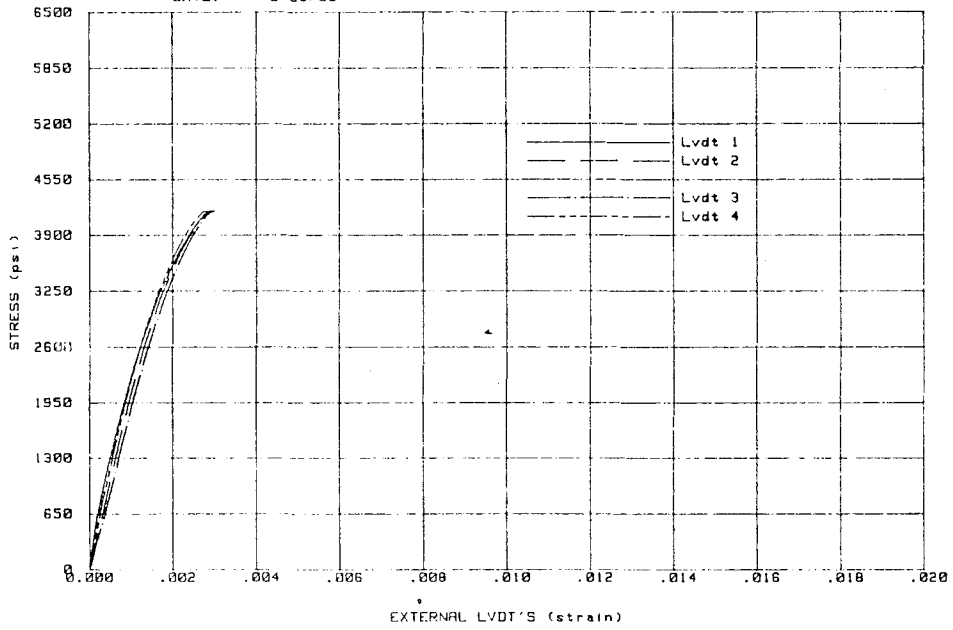
TEST: 6-CNC-G-S
SPECIMEN: 12-11-1



CONCRETE 1

ATKINSON-NOLAND AND ASSOCIATES
MASONRY PRISM TESTS
DATE: 2/25/85

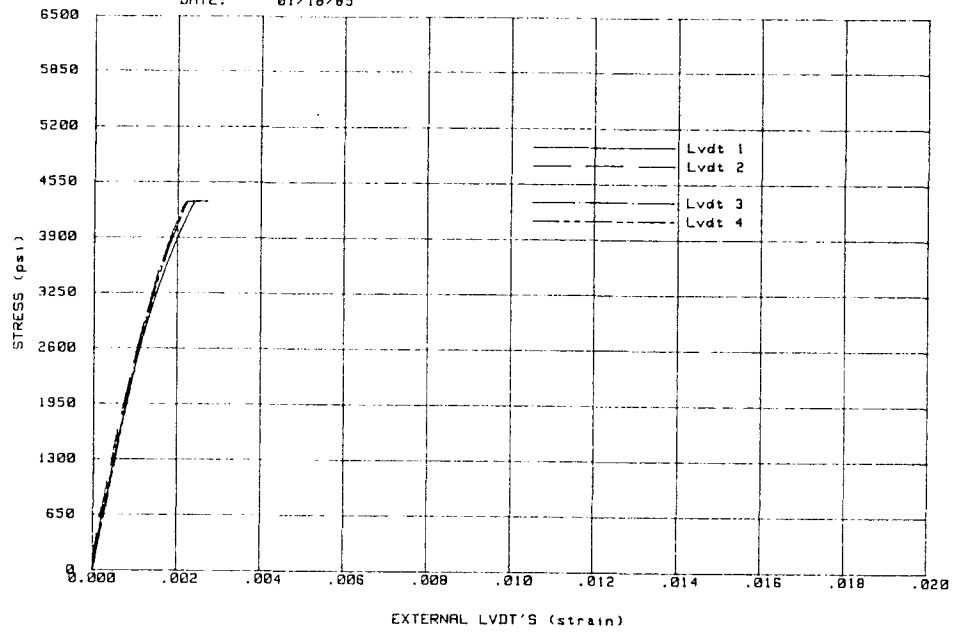
TEST: 6-CNC-G-S
SPECIMEN: 12-11-2



CONCRETE 2

ATKINSON-NOLAND AND ASSOCIATES
MASONRY PRISM TESTS
DATE: 01/18/85

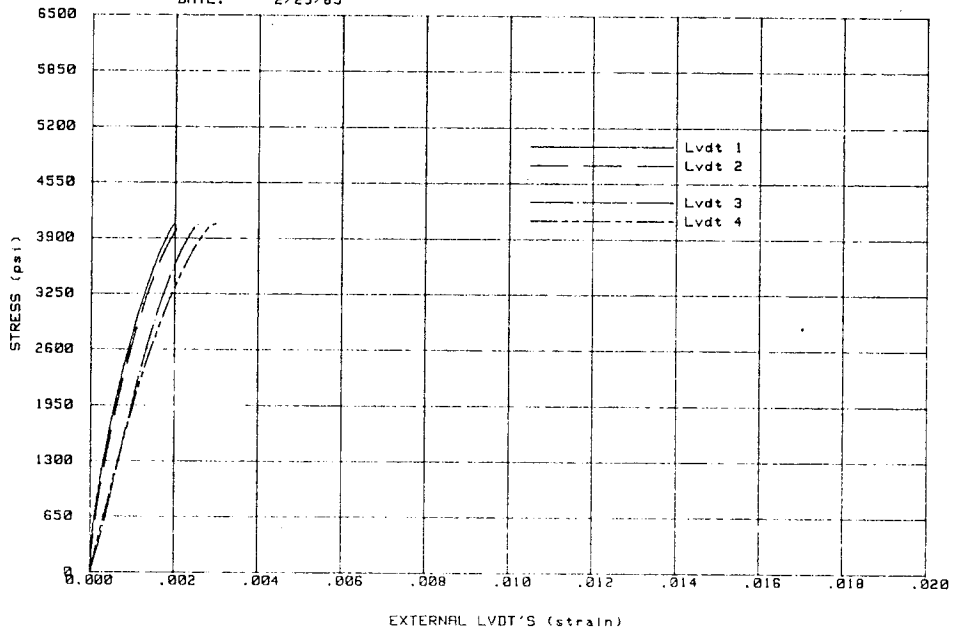
TEST: 6-CNC-G-S
SPECIMEN: 12-11-3



CONCRETE 3

ATKINSON-NOLAND AND ASSOCIATES
MASONRY PRISM TESTS
DATE: 2/25/85

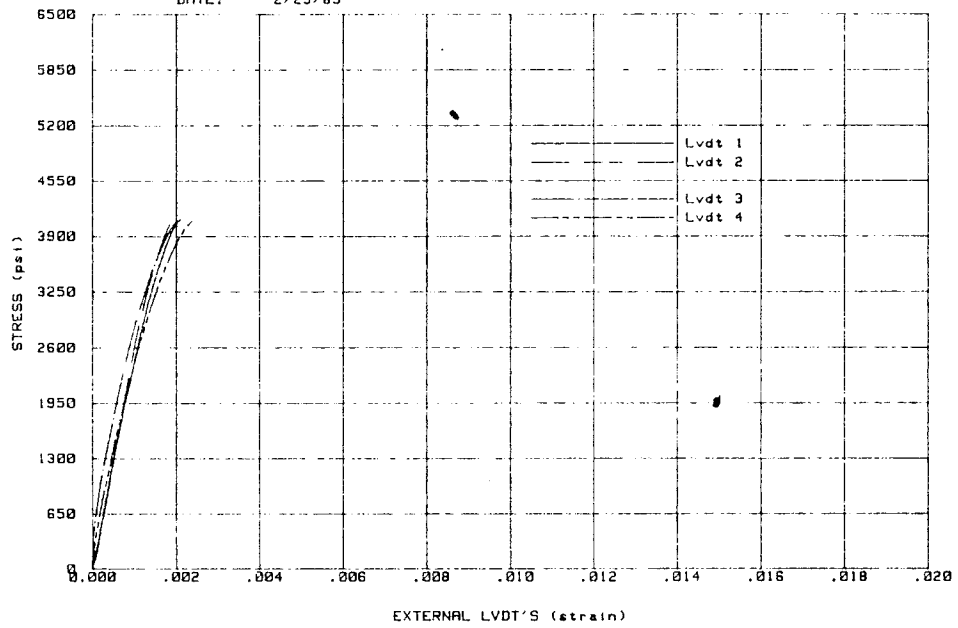
TEST: 6-CNC-G-5
SPECIMEN: 12-11-4



CONCRETE 4

ATKINSON-NOLAND AND ASSOCIATES
MASONRY PRISM TESTS
DATE: 2/25/85

TEST: 6-CNC-G-5
SPECIMEN: 12-11-5



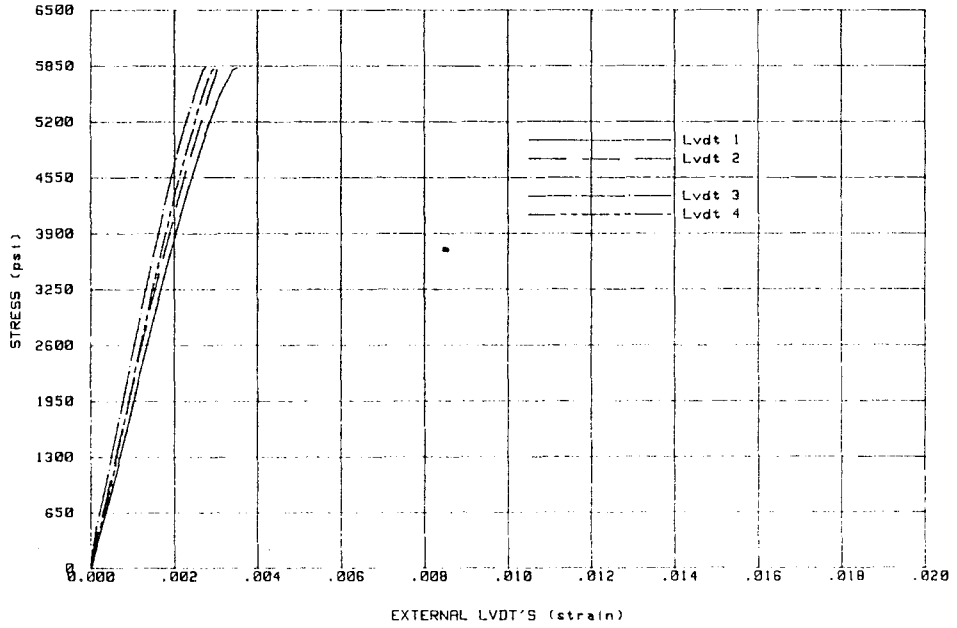
CONCRETE 5

A.8 SERIES 8

UNIT WIDTH	6"
GROUT	HIGH STRENGTH
MORTAR	TYPE N
BOND PATTERN	STACK BOND
LOAD DIRECTION	NORMAL TO BEDJOINT

ATKINSON-NOLAND AND ASSOCIATES
MASONRY PRISM TESTS
DATE: 12/7/84

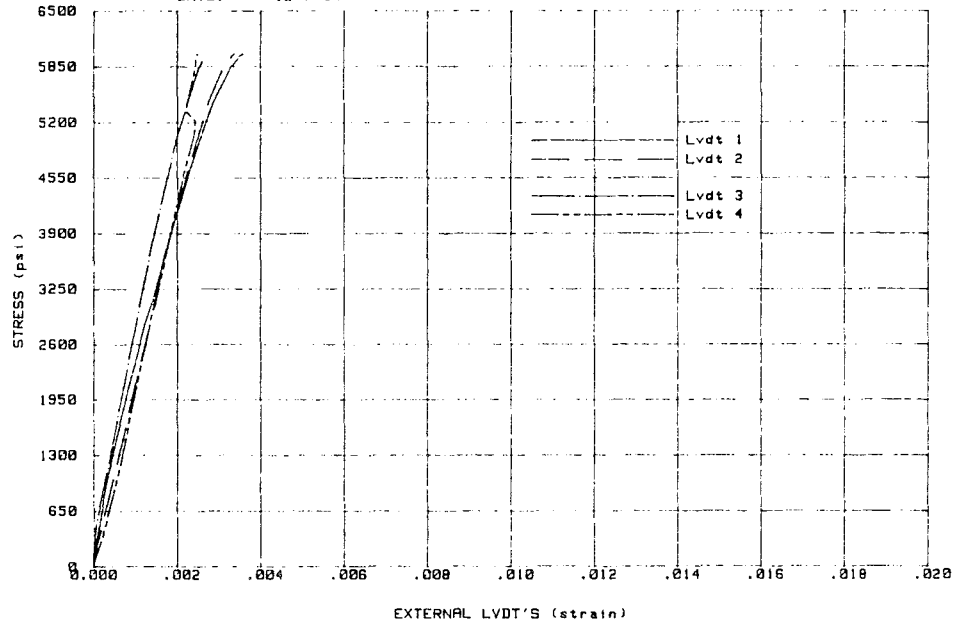
TEST: 6-CLY-SG-0
SPECIMEN: 10-4-6



CLAY 1

ATKINSON-NOLAND AND ASSOCIATES
MASONRY PRISM TESTS
DATE: 12/7/84

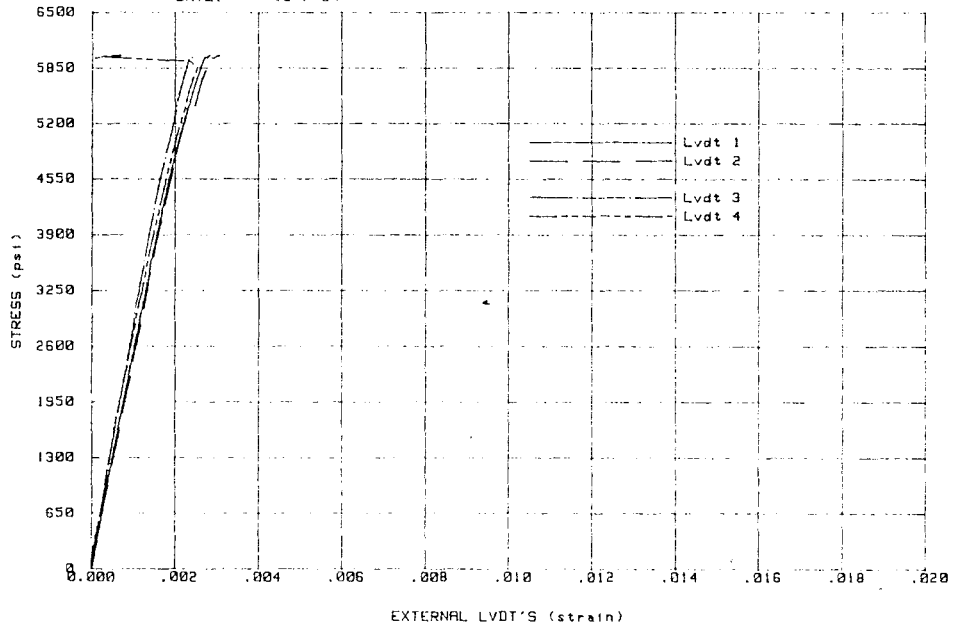
TEST: 6-CLY-SG-0
SPECIMEN: 10-4-7



CLAY 2

ATKINSON-NOLAND AND ASSOCIATES
MASONRY PRISM TESTS
DATE: 12/7/84

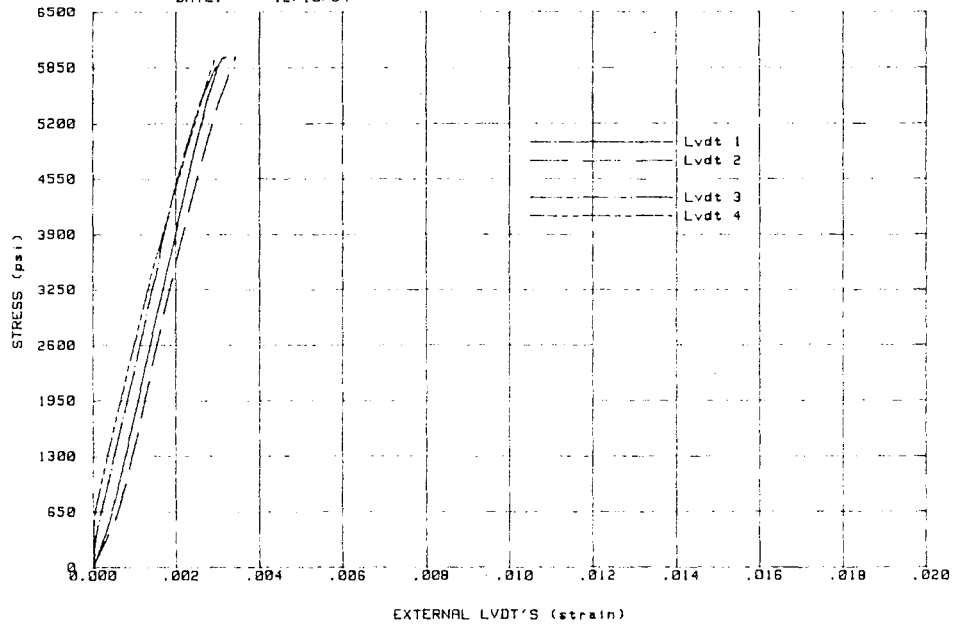
TEST: 6-CLY-SG-0
SPECIMEN: 10-4-0



CLAY 3

ATKINSON-NOLAND AND ASSOCIATES
MASONRY PRISM TESTS
DATE: 12/10/84

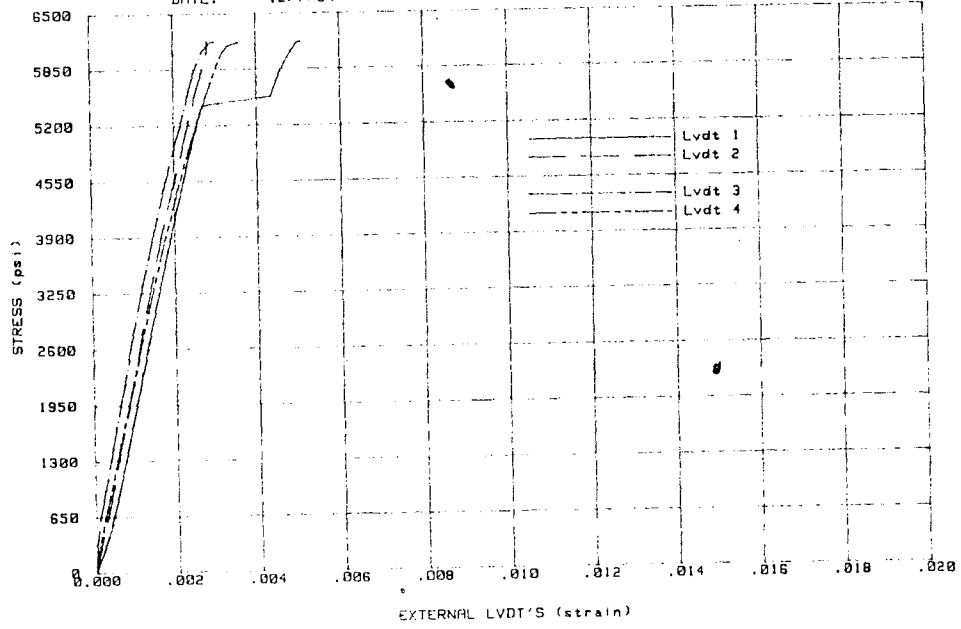
TEST: 6-CLY-SG-0
SPECIMEN: 10-4-9



CLAY 4

ATKINSON-NOLAND AND ASSOCIATES
MASONRY PRISM TESTS
DATE: 12/7/84

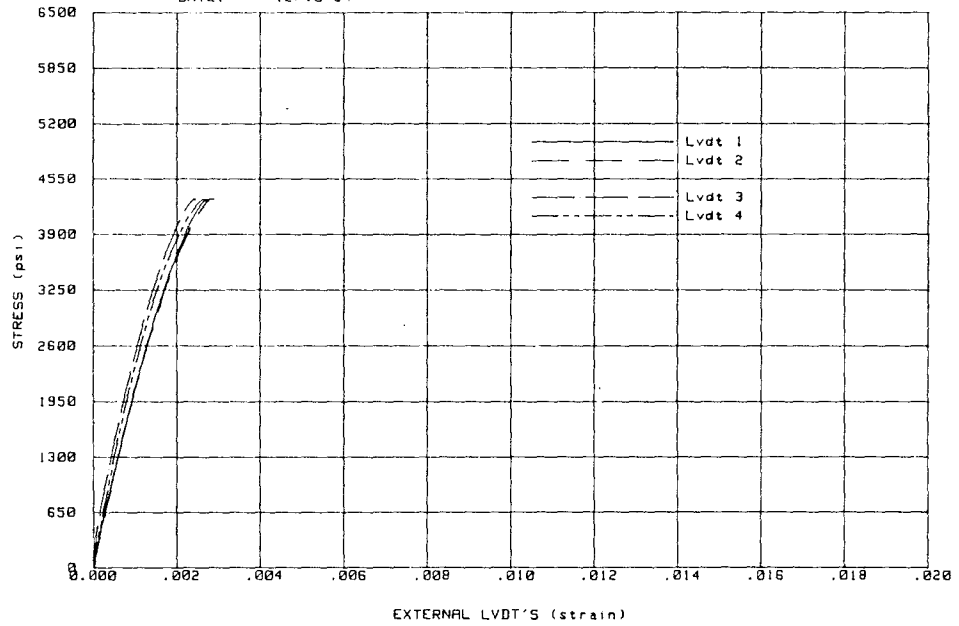
TEST: 6-CLY-SG-0
SPECIMEN: 10-4-10



CLAY 5

ATKINSON-NOLAND AND ASSOCIATES
MASONRY PRISM TESTS
DATE: 12/10/84

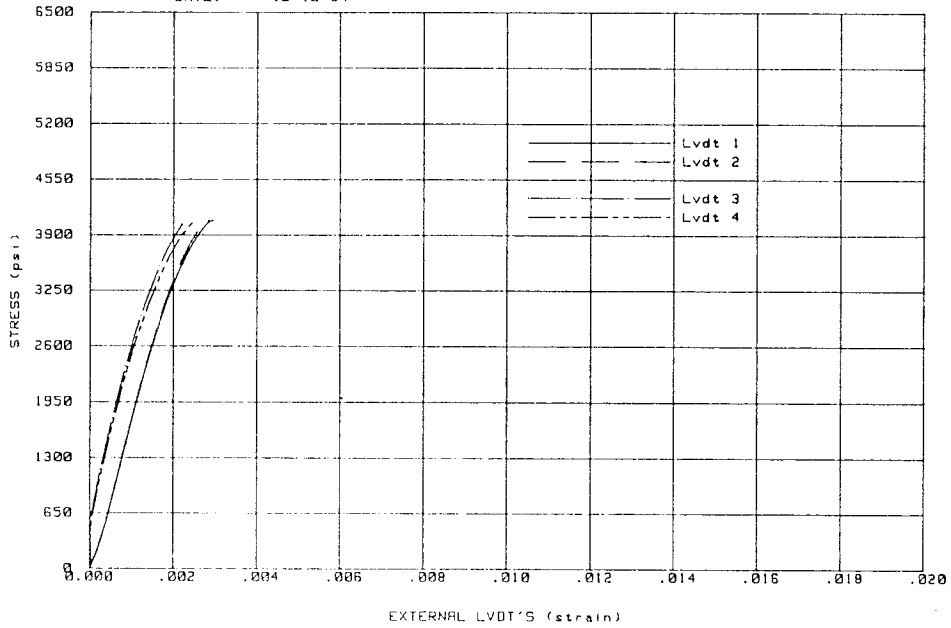
TEST: 6-CNC-SG-0
SPECIMEN: 10-4-1



CONCRETE 1

ATKINSON-NOLAND AND ASSOCIATES
MASONRY PRISM TESTS
DATE: 12/10/84

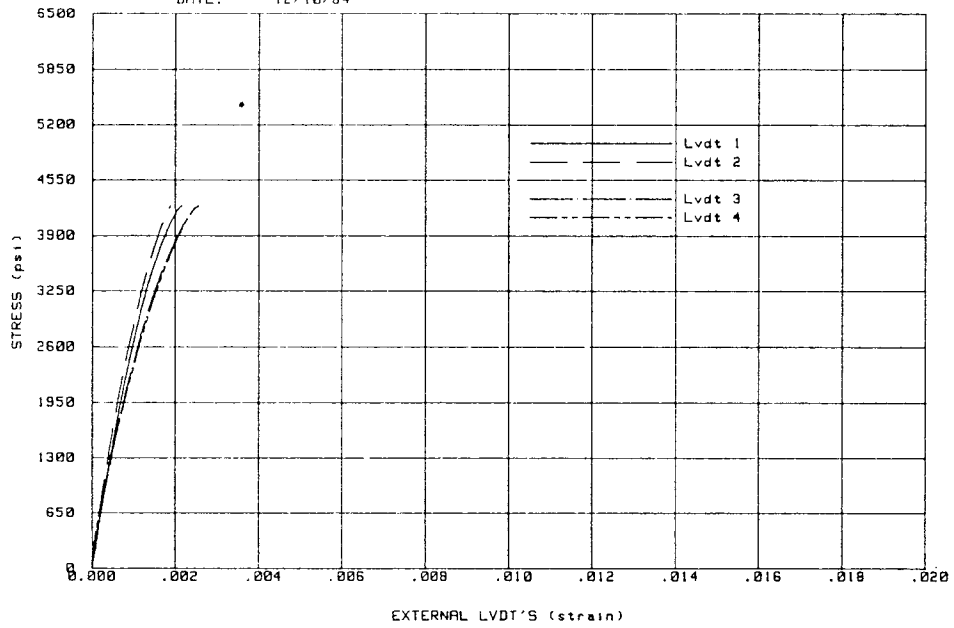
TEST: 6-CNC-SG-0
SPECIMEN: 10-4-2



CONCRETE 2

ATKINSON-NOLAND AND ASSOCIATES
MASONRY PRISM TESTS
DATE: 12/10/84

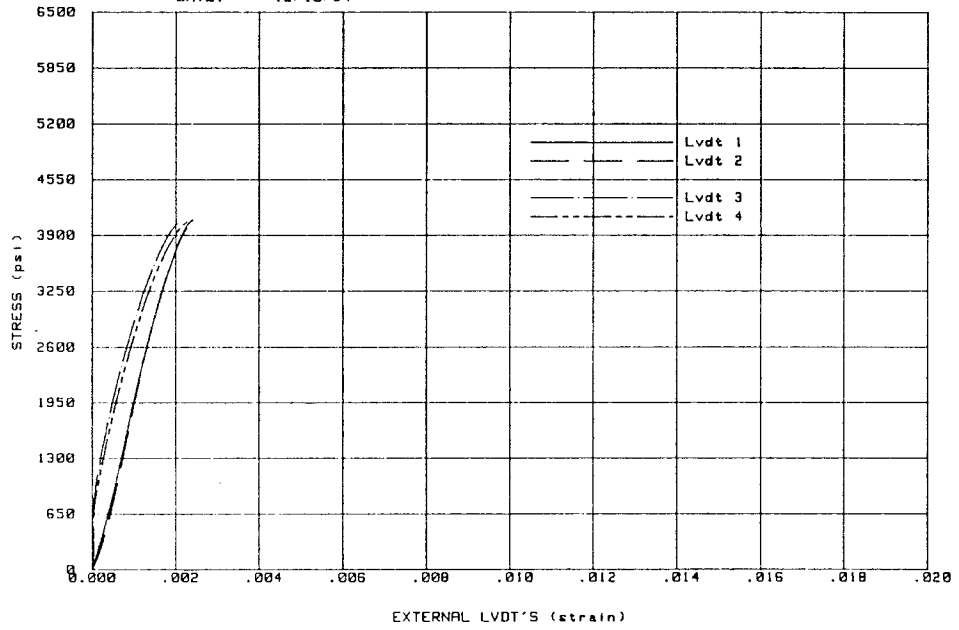
TEST: 6-CNC-SG-0
SPECIMEN: 10-4-3



CONCRETE 3

ATKINSON-NOLAND AND ASSOCIATES
MASONRY PRISM TESTS
DATE: 12/10/84

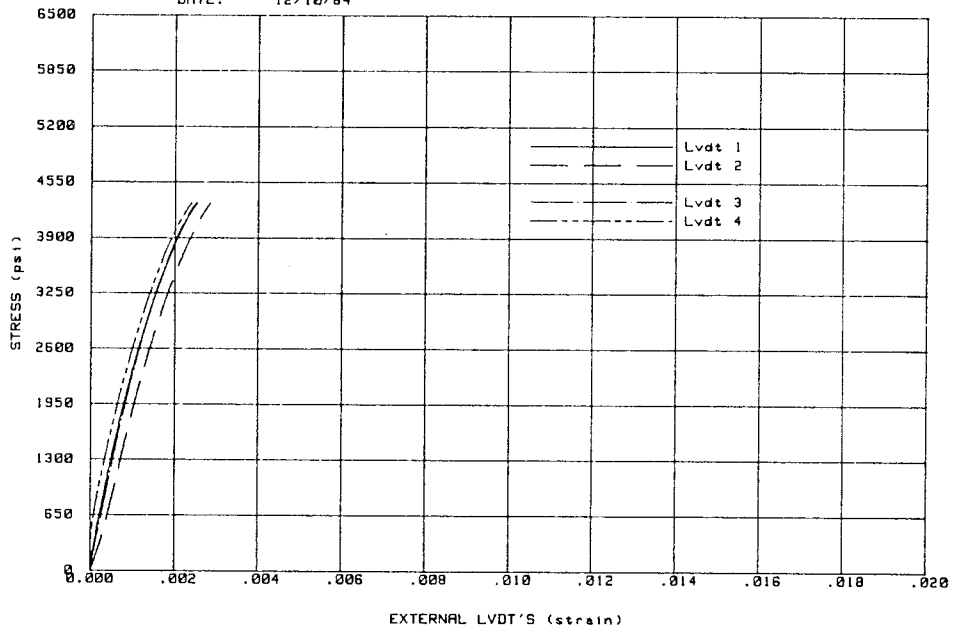
TEST: 6-CNC-SG-0
SPECIMEN: 10-4-4



CONCRETE 4

ATKINSON-NOLAND AND ASSOCIATES
MASONRY PRISM TESTS
DATE: 12/10/84

TEST: 6-CNC-SG-0
SPECIMEN: 10-4-5



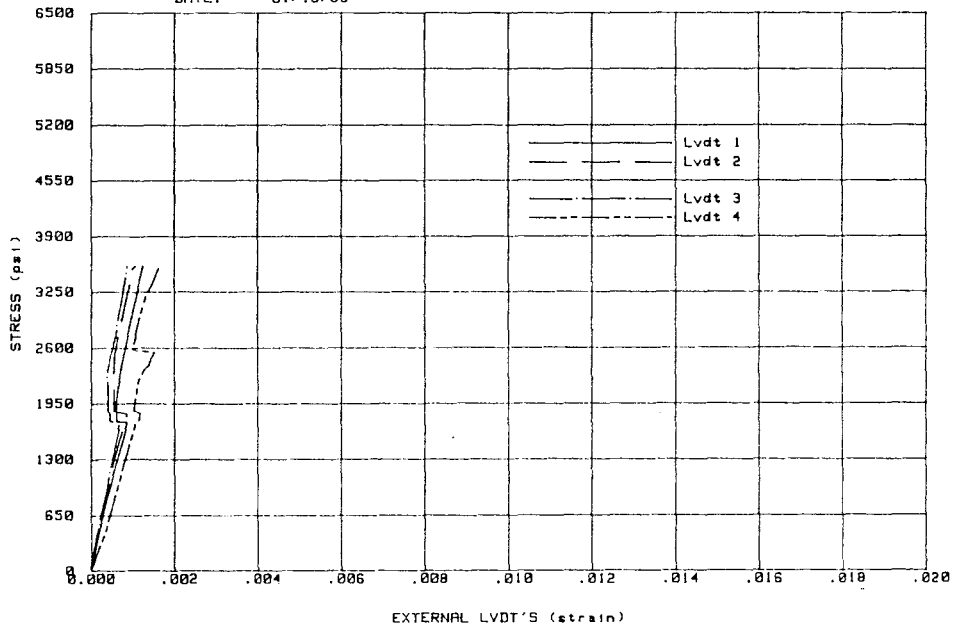
CONCRETE 5

A.9 SERIES 9

UNIT WIDTH	6"
GROUT	STANDARD
MORTAR	TYPE N
BOND PATTERN	STACK BOND
LOAD DIRECTION	PARALLEL TO BEDJOINT

ATKINSON-NOLAND AND ASSOCIATES
MASONRY PRISM TESTS
DATE: 01/18/85

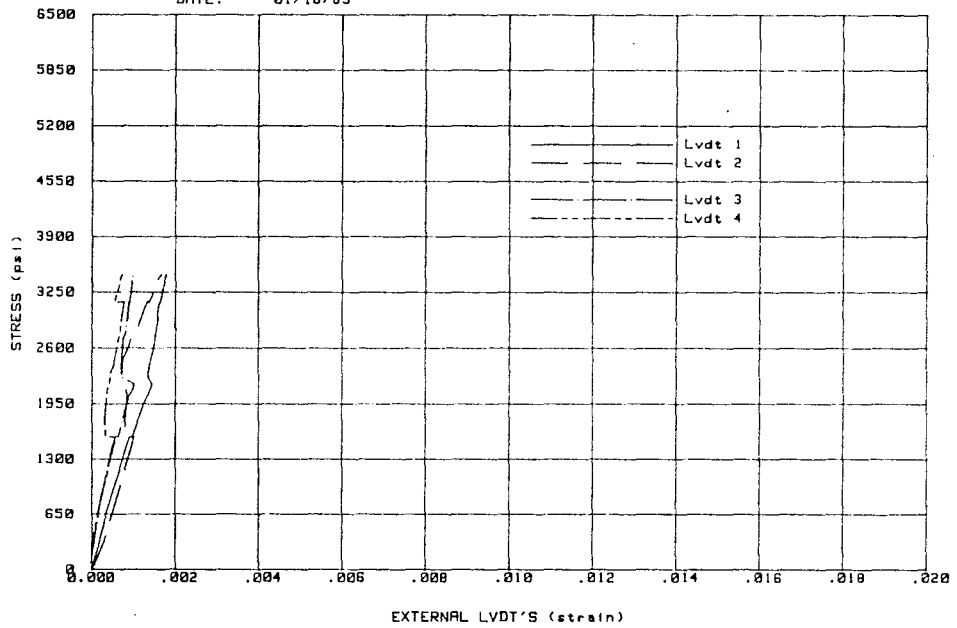
TEST: 6-CLY-G-90
SPECIMEN: 11-8-2



CLAY 1

ATKINSON-NOLAND AND ASSOCIATES
MASONRY PRISM TESTS
DATE: 01/18/85

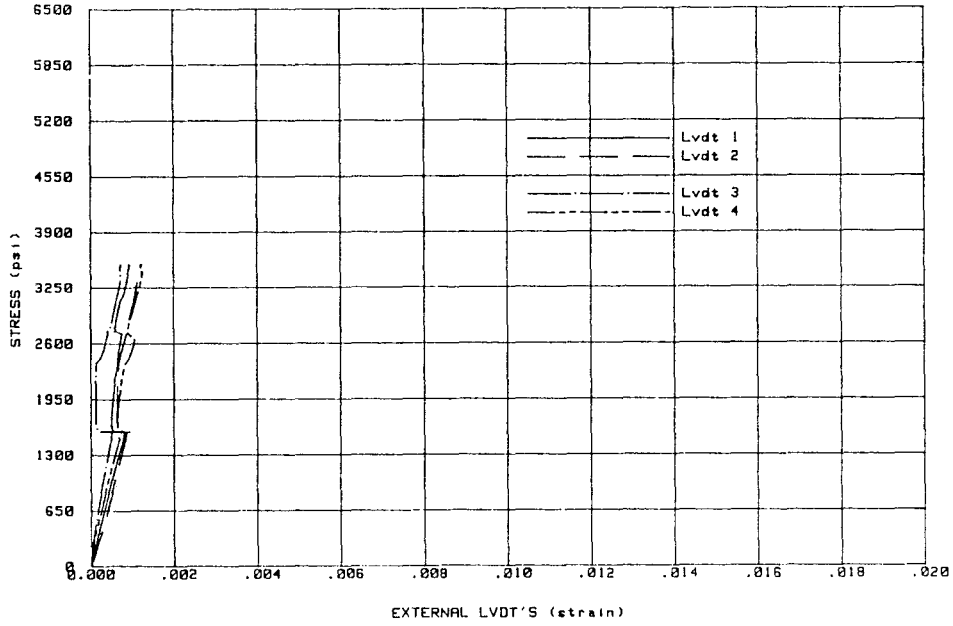
TEST: 6-CLY-G-90
SPECIMEN: 11-8-1 or 2 1st



CLAY 2

ATKINSON-NOLAND AND ASSOCIATES
MASONRY PRISM TESTS
DATE: 01/18/85

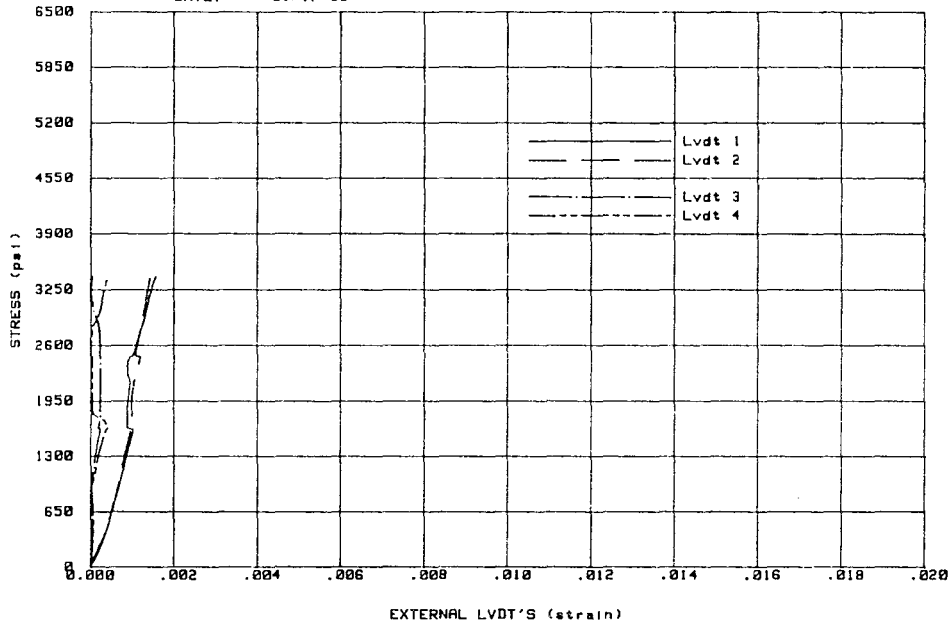
TEST: 6-CLY-G-98
SPECIMEN: 11-8-3



CLAY 3

ATKINSON-NOLAND AND ASSOCIATES
MASONRY PRISM TESTS
DATE: 01/17/85

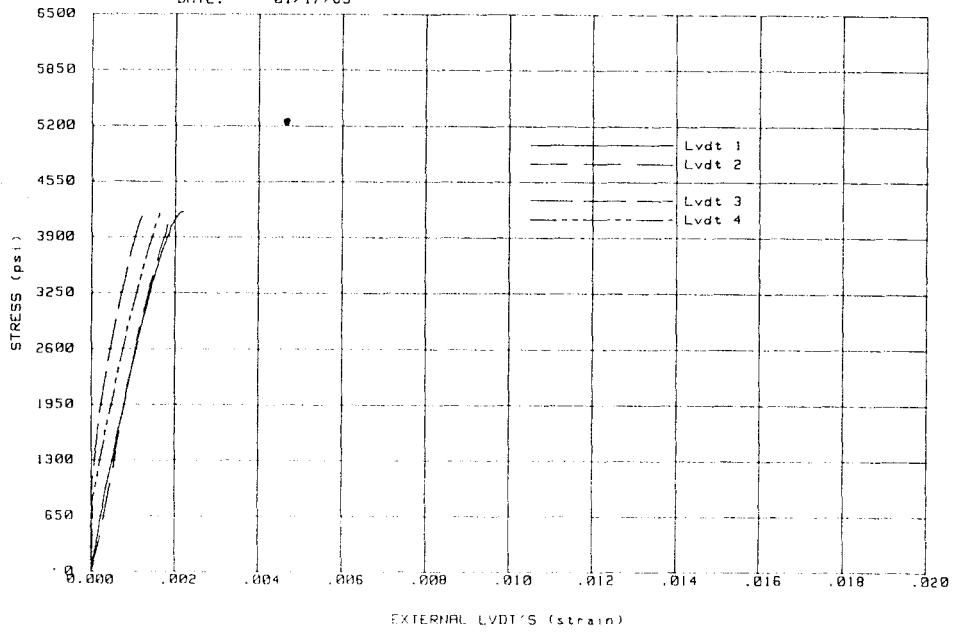
TEST: 6-CLY-G-98
SPECIMEN: 11-8-4



CLAY 4

ATKINSON-NOLAND AND ASSOCIATES
MASONRY PRISM TESTS
DATE: 01/17/85

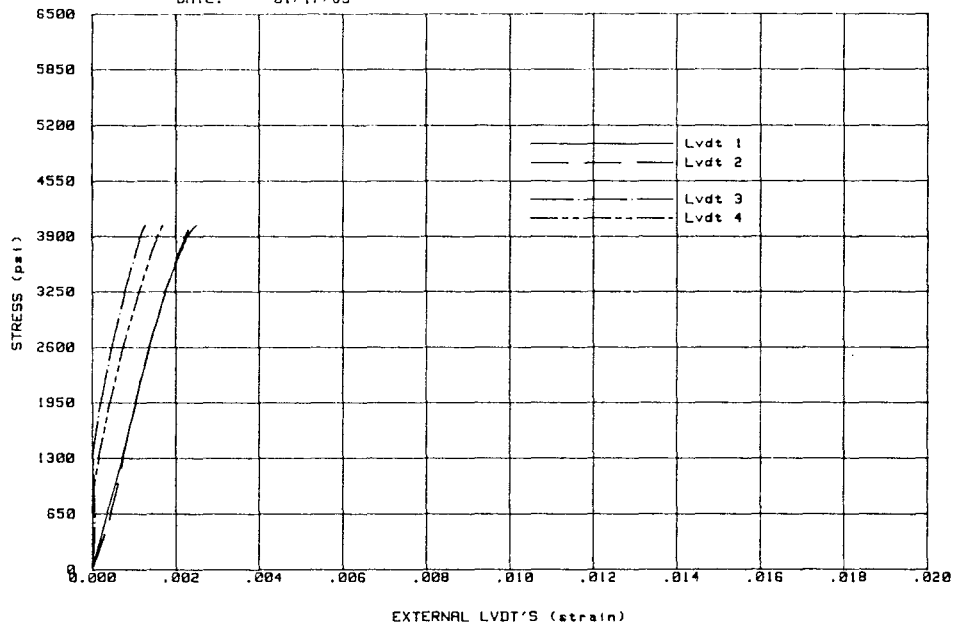
TEST: 6-CNC-G-90
SPECIMEN: 11-7-2



CONCRETE 1

ATKINSON-NOLAND AND ASSOCIATES
MASONRY PRISM TESTS
DATE: 01/17/85

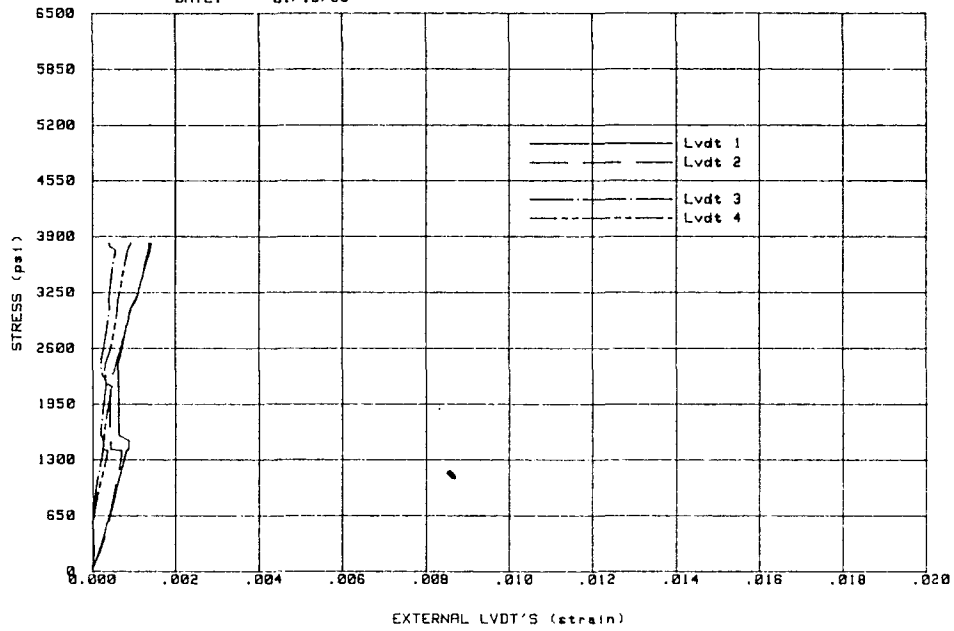
TEST: 6-CNC-G-90
SPECIMEN: 11-7-3



CONCRETE 2

ATKINSON-NOLAND AND ASSOCIATES
MASONRY PRISM TESTS
DATE: 01/10/85

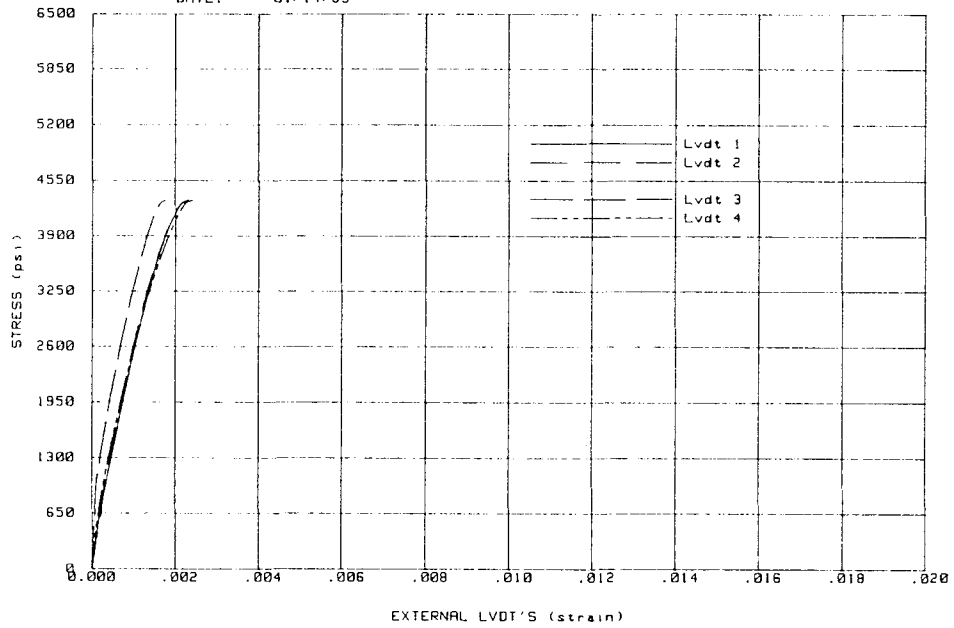
TEST: 6-CLY-G-90
SPECIMEN: 11-8-5



CLAY 1

ATKINSON-NOLAND AND ASSOCIATES
MASONRY PRISM TESTS
DATE: 01/14/85

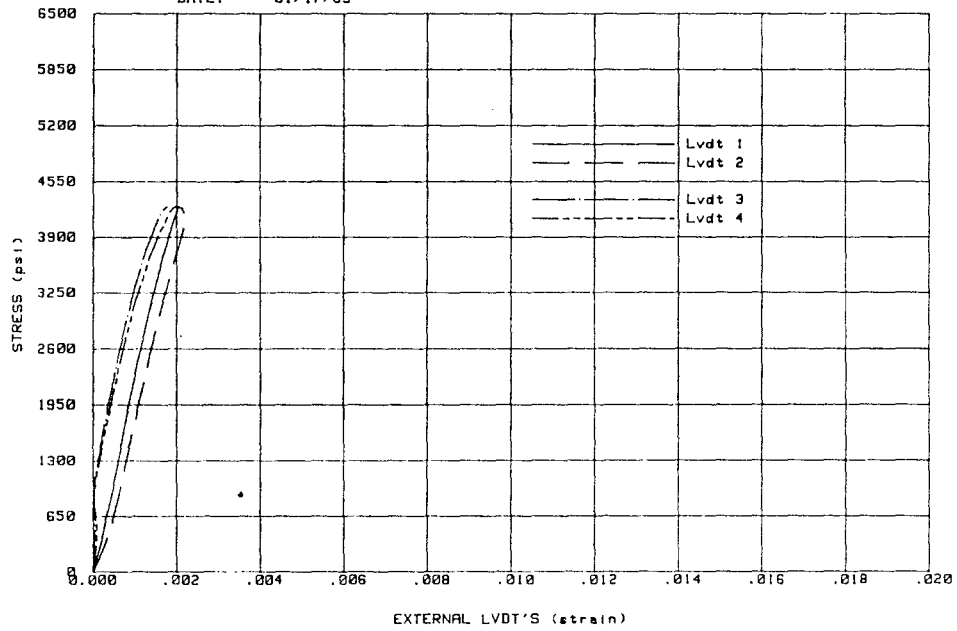
TEST: 6-CNC-G-90
SPECIMEN: 11-7-1



CONCRETE 1

ATKINSON-NOLAND AND ASSOCIATES
MASONRY PRISM TESTS
DATE: 01/17/85

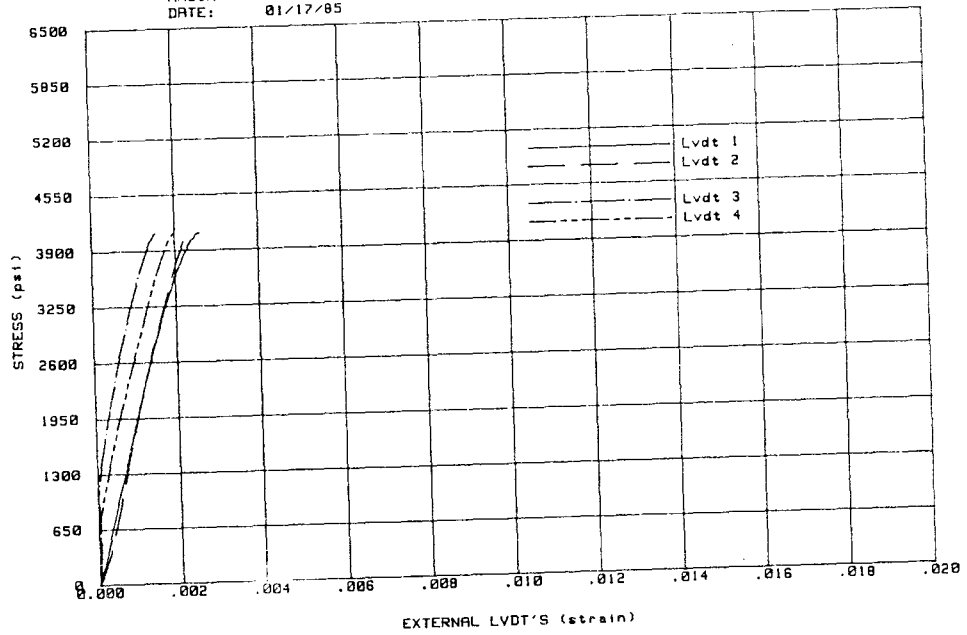
TEST: 6-CNC-G-90
SPECIMEN: 11-7-4



CONCRETE 2

ATKINSON-NOLAND AND ASSOCIATES
MASONRY PRISM TESTS
DATE: 01/17/85

TEST: 6-CNC-G-90
SPECIMEN: 11-7-5



CONCRETE 3

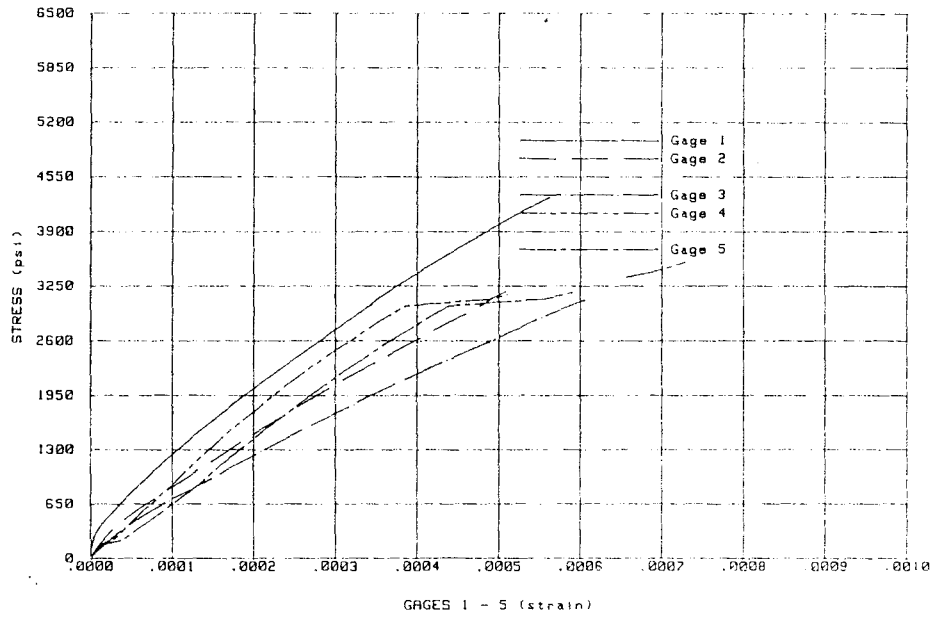
A.10 SERIES 10

UNIT WIDTH	6"
GROUT	STANDARD
MORTAR	TYPE N
BOND PATTERN	STACK BOND
LOAD DIRECTION	NORMAL TO BEDJOINT

TESTED WITH REDUCED PLATEN RESTRAINT

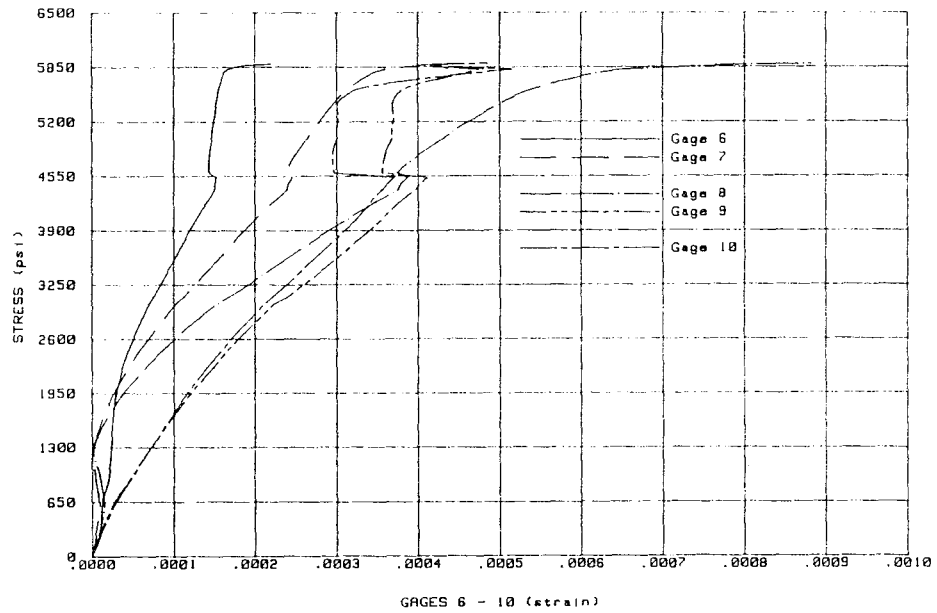
ATKINSON-NOLAND AND ASSOCIATES
MASONRY PRISM TESTS

TEST: 6-CLY-IFR
SPECIMEN: 12-10-10 (NO IFR)



ATKINSON-NOLAND AND ASSOCIATES
MASONRY PRISM TESTS

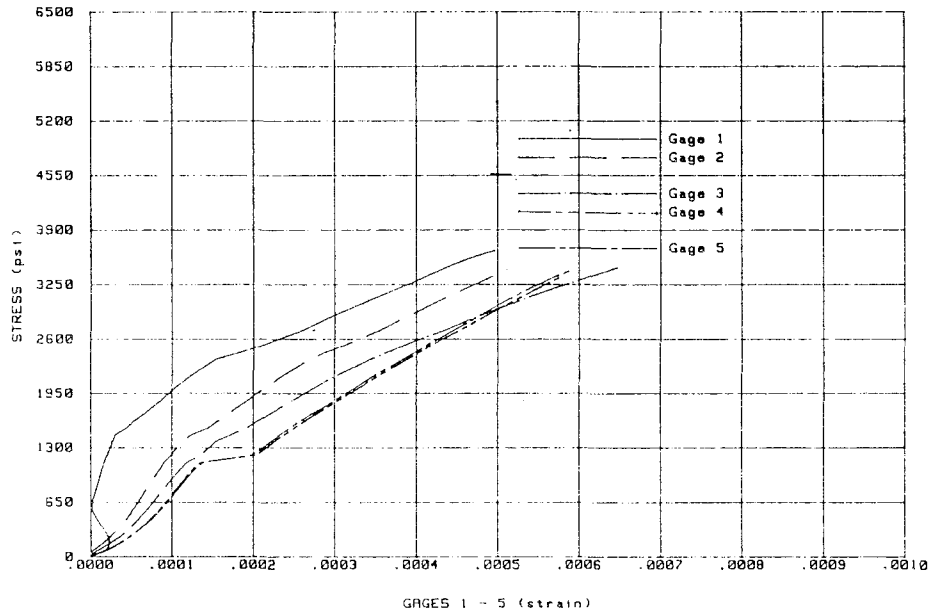
TEST: 6-CLY-IFR
SPECIMEN: 12-10-10 (NO IFR)



CLAY 1

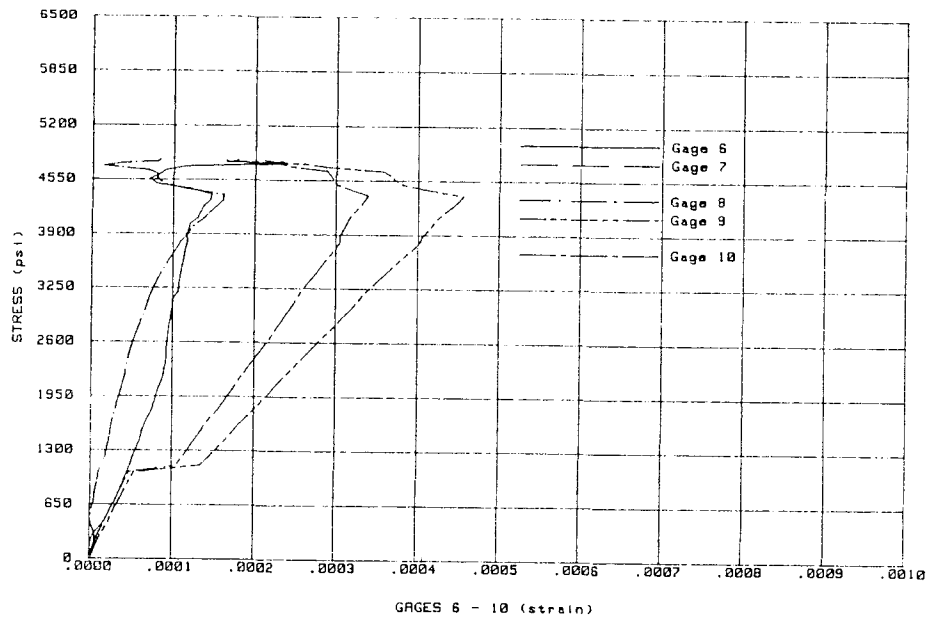
ATKINSON-NOLAND AND ASSOCIATES
MASONRY PRISM TESTS

TEST: 6-CLY-IFR
SPECIMEN: 12-18-6



ATKINSON-NOLAND AND ASSOCIATES
MASONRY PRISM TESTS

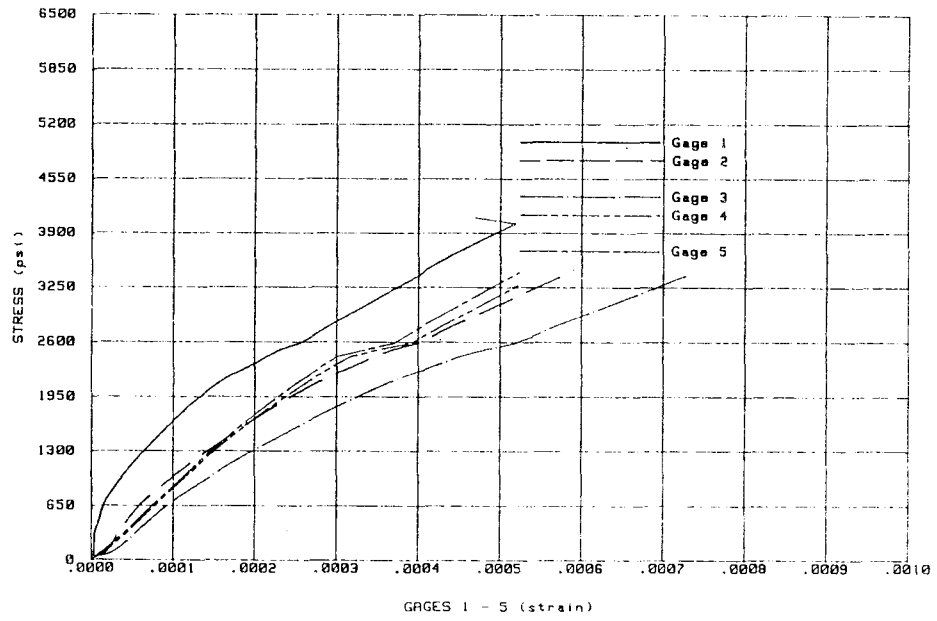
TEST: 6-CLY-IFR
SPECIMEN: 12-18-6



CLAY 2

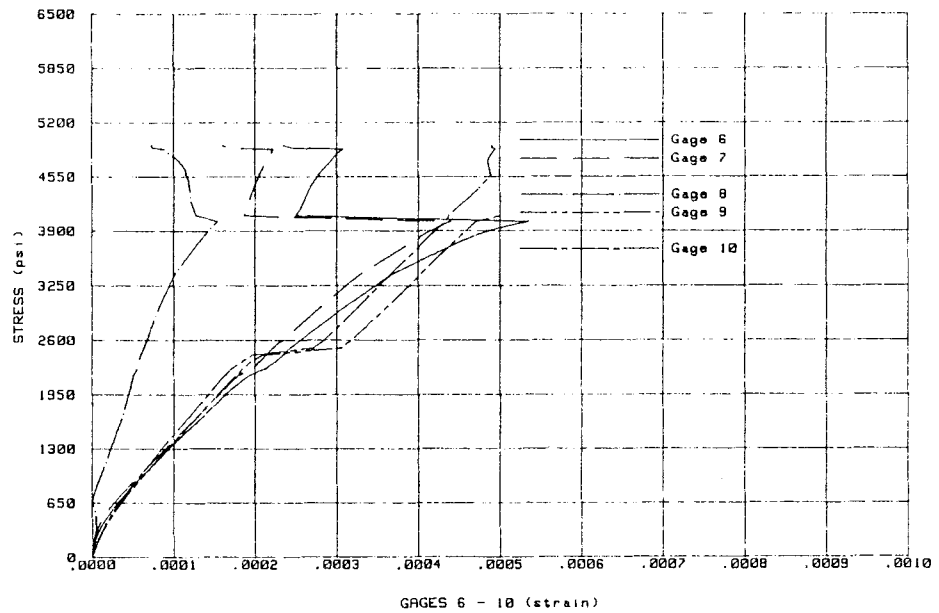
ATKINSON-NOLAND AND ASSOCIATES
MASONRY PRISM TESTS

TEST: 6-CLY-IFR
SPECIMEN: 12-18-7



ATKINSON-NOLAND AND ASSOCIATES
MASONRY PRISM TESTS

TEST: 6-CLY-IFR
SPECIMEN: 12-18-7

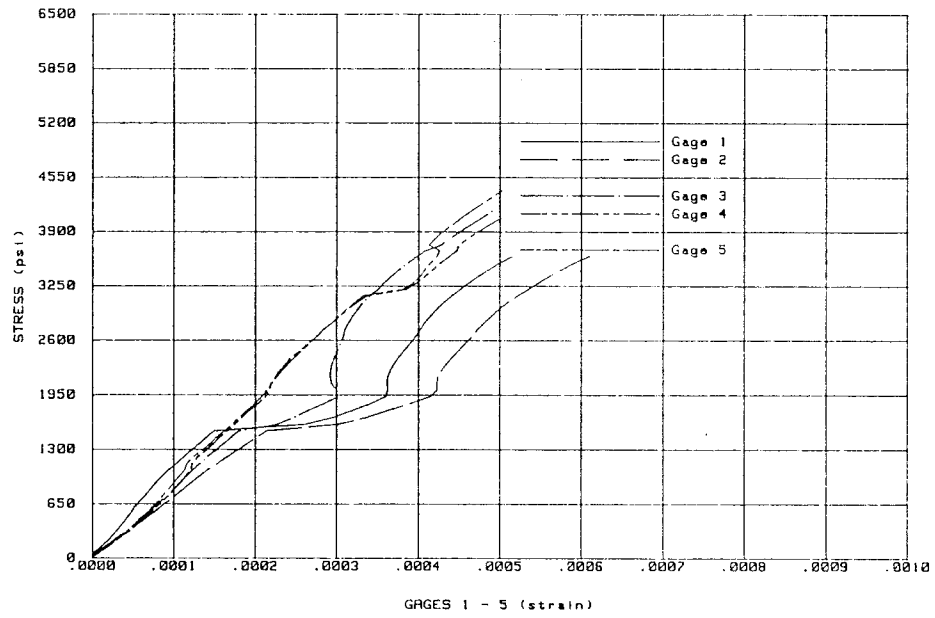


CLAY 3

Reproduced from
best available copy.

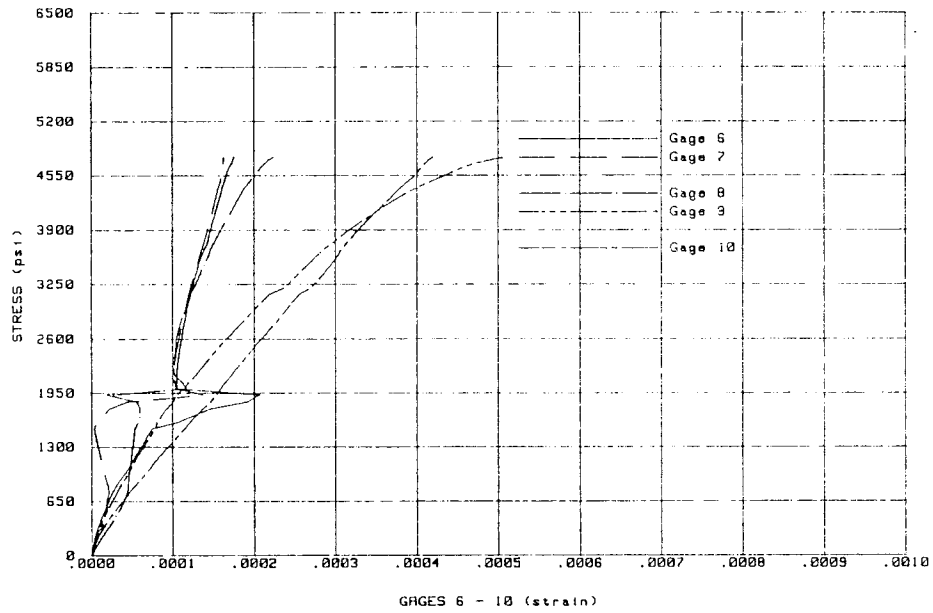
ATKINSON-NOLAND AND ASSOCIATES
MASONRY PRISM TESTS

TEST: 6-CLY-IFR
SPECIMEN: 12-18-8



ATKINSON-NOLAND AND ASSOCIATES
MASONRY PRISM TESTS

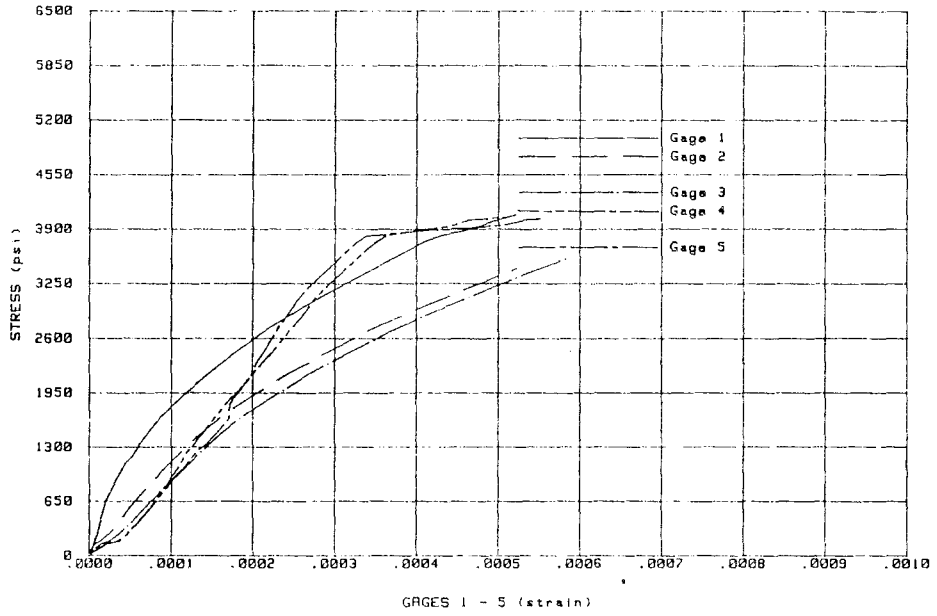
TEST: 6-CLY-IFR
SPECIMEN: 12-18-8



CLAY 4

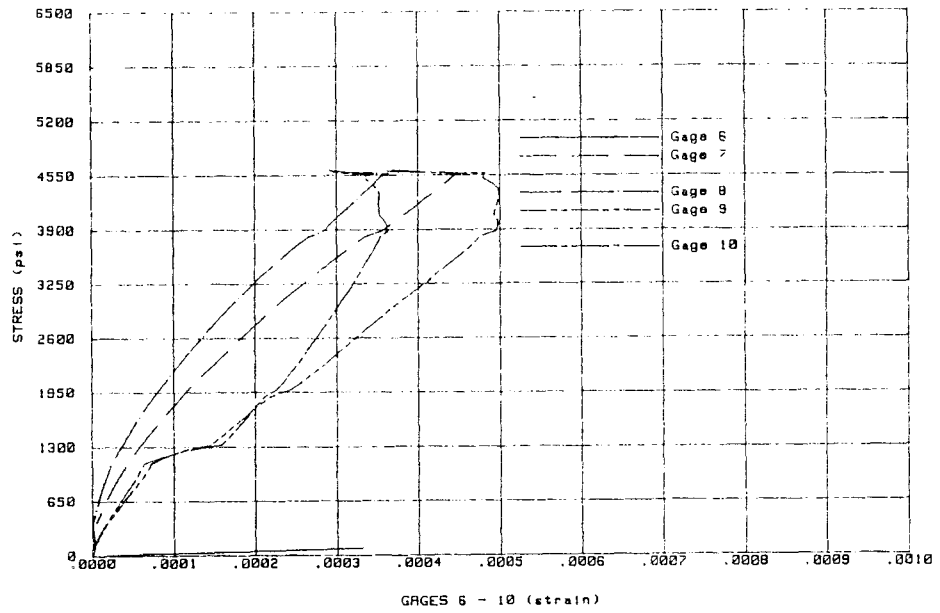
ATKINSON-NOLAND AND ASSOCIATES
MASONRY PRISM TESTS

TEST: 6-CLY-IFR
SPECIMEN: 12-18-9



ATKINSON-NOLAND AND ASSOCIATES
MASONRY PRISM TESTS

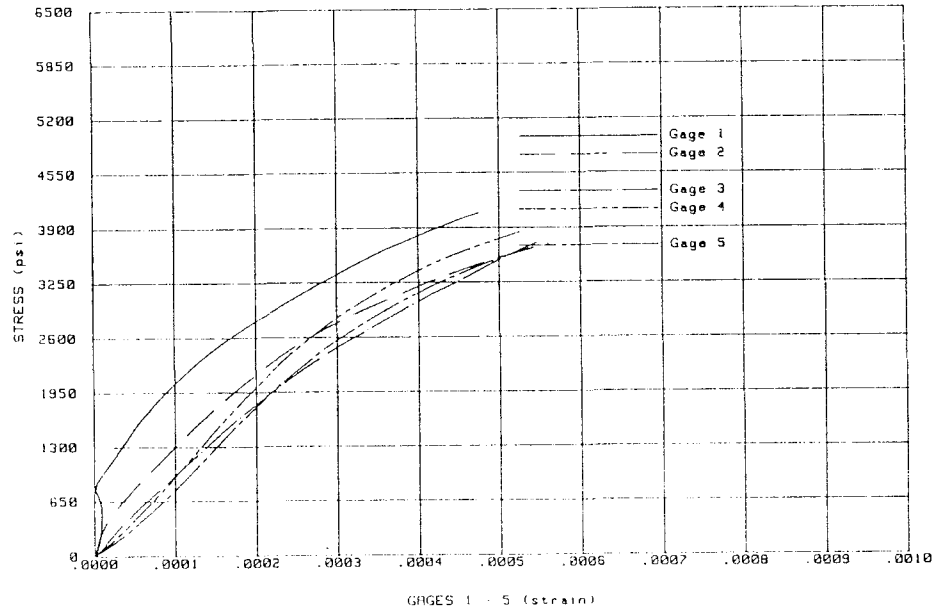
TEST: 6-CLY-IFR
SPECIMEN: 12-18-9



CLAY 5

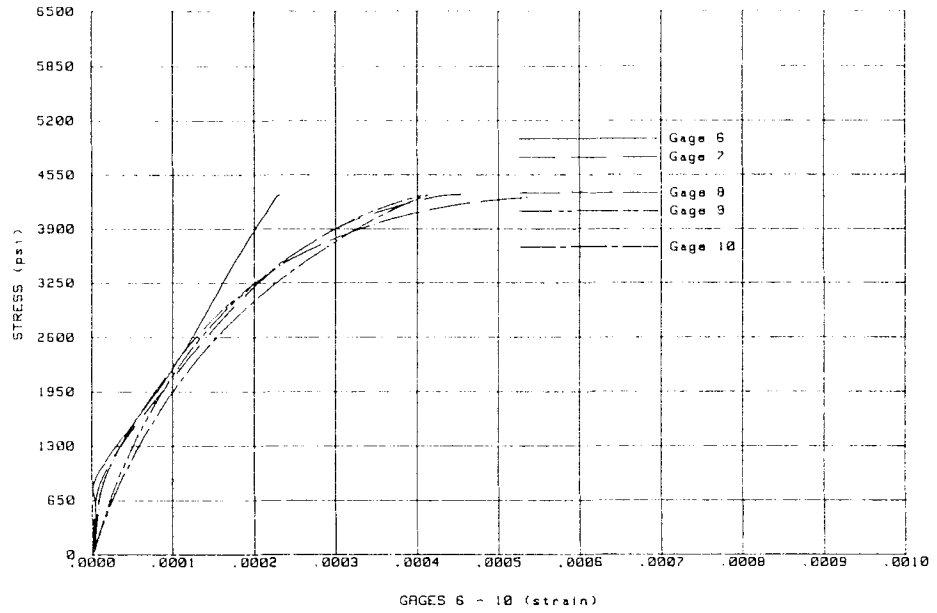
ATKINSON-NOLAND AND ASSOCIATES
MASONRY PRISM TESTS

TEST: 5-CNC-IFR
SPECIMEN: 12-18-1 (NO IFR)



ATKINSON-NOLAND AND ASSOCIATES
MASONRY PRISM TESTS

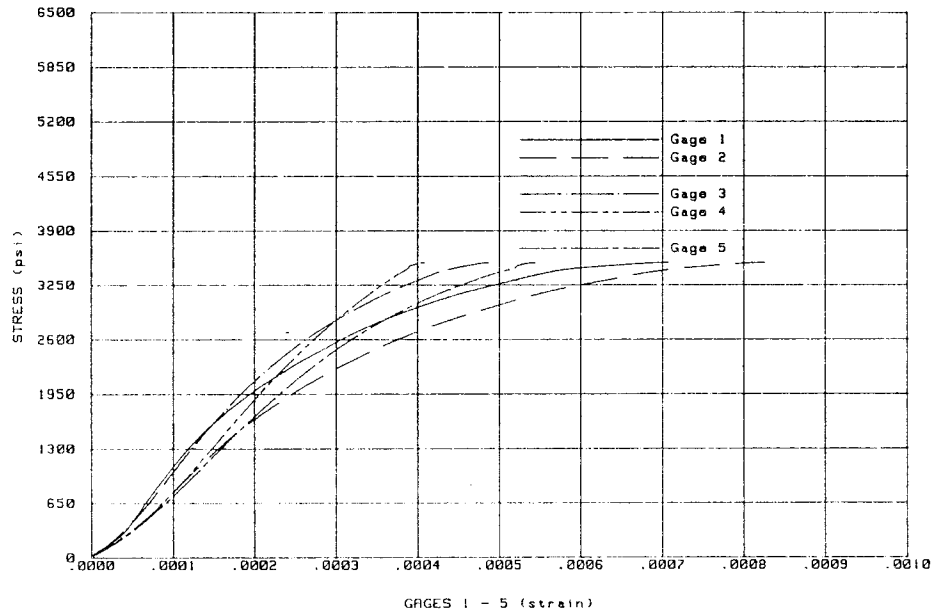
TEST: 5-CNC-IFR
SPECIMEN: 12-18-1 (NO IFR)



CONCRETE 1

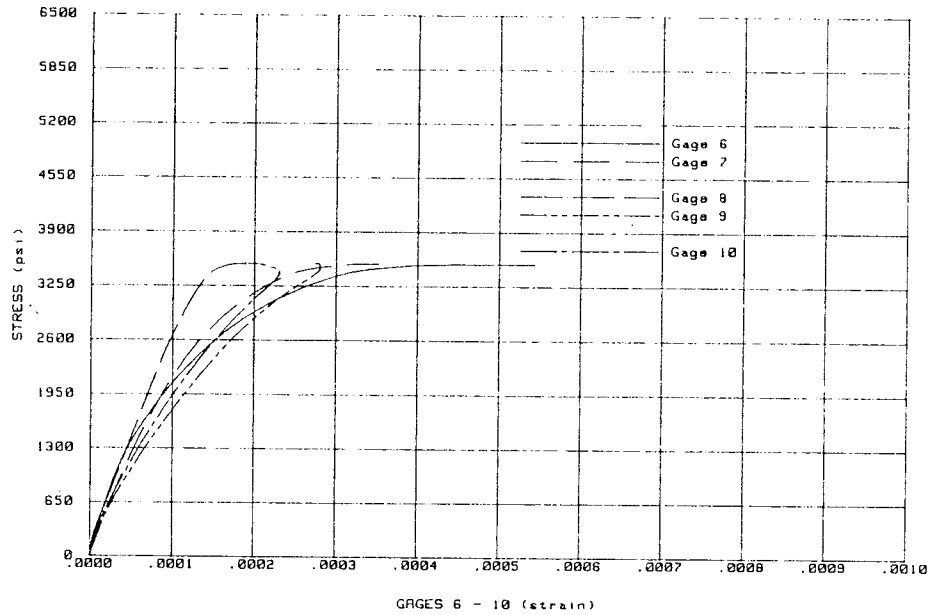
ATKINSON-NOLAND AND ASSOCIATES
MASONRY PRISM TESTS

TEST: 6-CNC-IFR
SPECIMEN: 12-18-2



ATKINSON-NOLAND AND ASSOCIATES
MASONRY PRISM TESTS

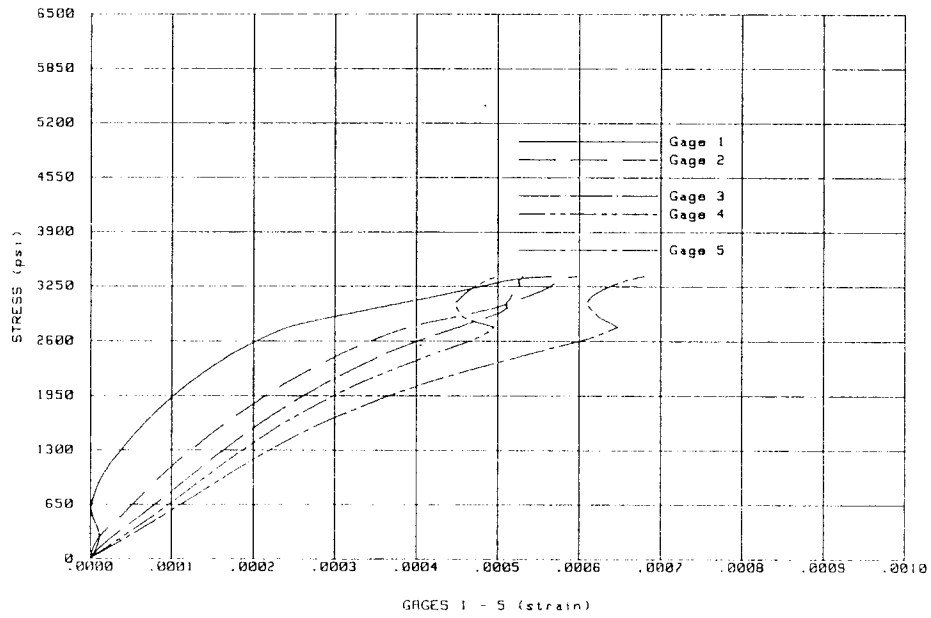
TEST: 6-CNC-IFR
SPECIMEN: 12-18-2



CONCRETE 2

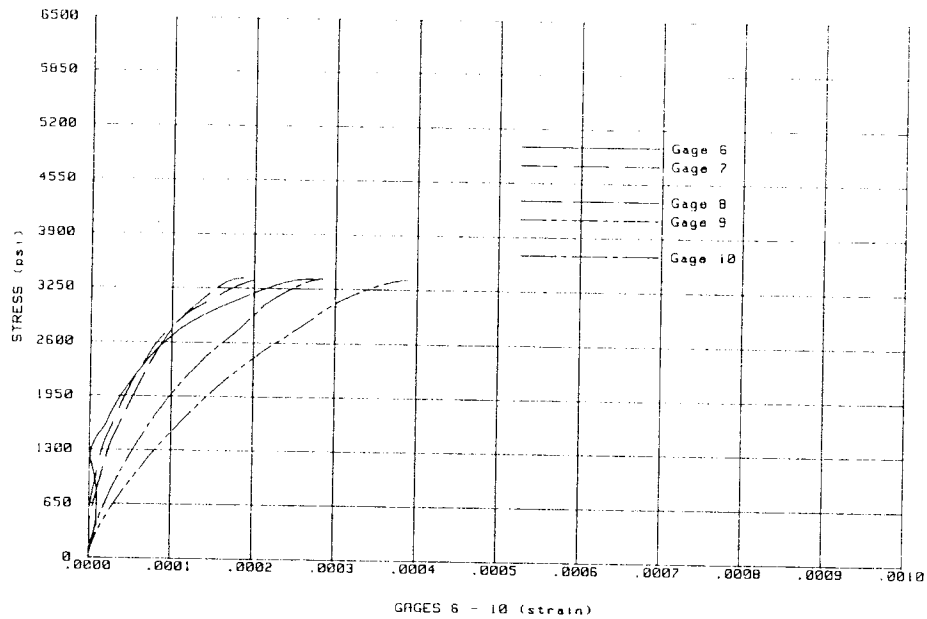
ATKINSON-NOLAND AND ASSOCIATES
MASONRY PRISM TESTS

TEST: 6-CNC-IFR
SPECIMEN: 12-18-3



ATKINSON-NOLAND AND ASSOCIATES
MASONRY PRISM TESTS

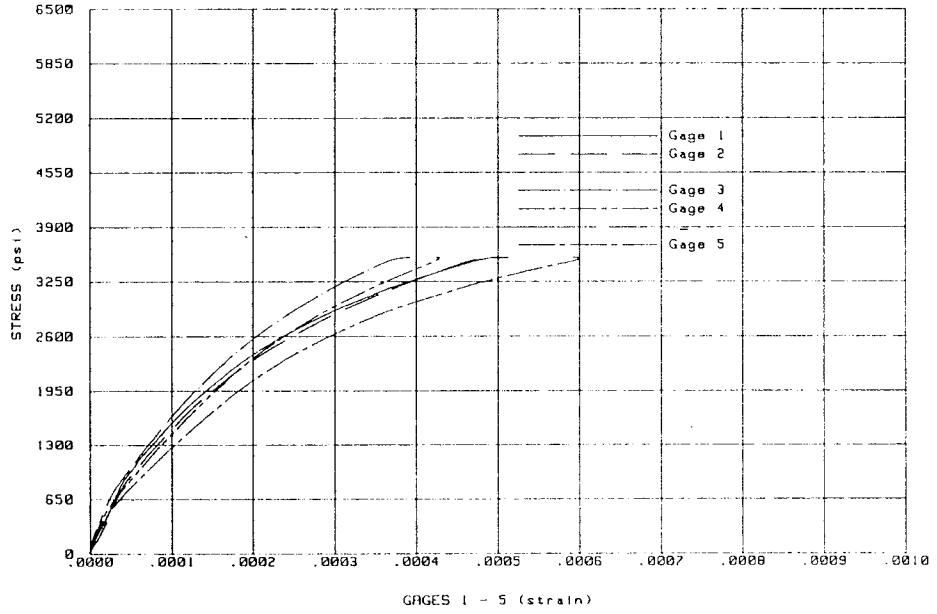
TEST: 6-CNC-IFR
SPECIMEN: 12-18-3



CONCRETE 3

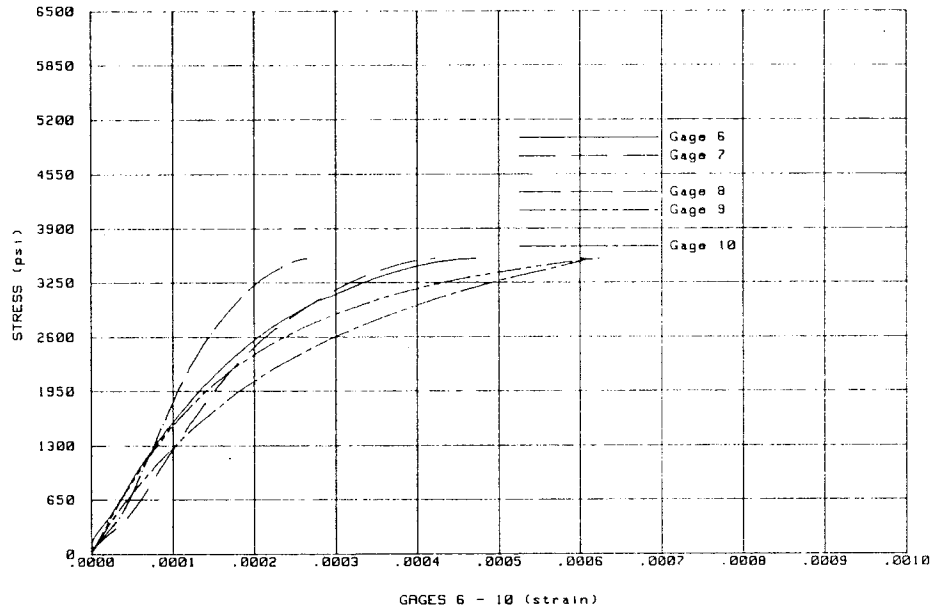
ATKINSON-NOLAND AND ASSOCIATES
MASONRY PRISM TESTS

TEST: 5-CNC-IFR
SPECIMEN: 12-18-4



ATKINSON-NOLAND AND ASSOCIATES
MASONRY PRISM TESTS

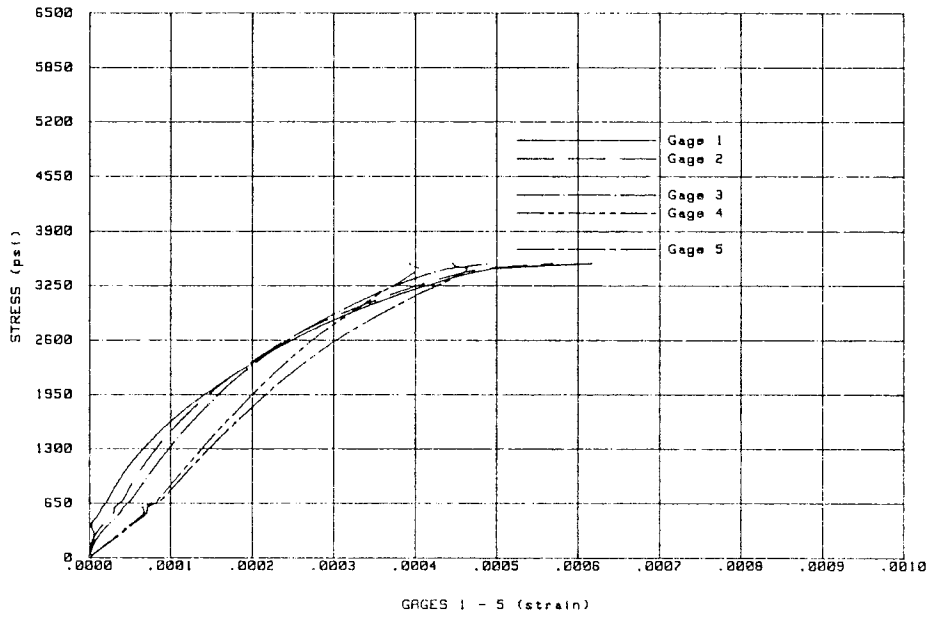
TEST: 6-CNC-IFR
SPECIMEN: 12-18-4



CONCRETE 4

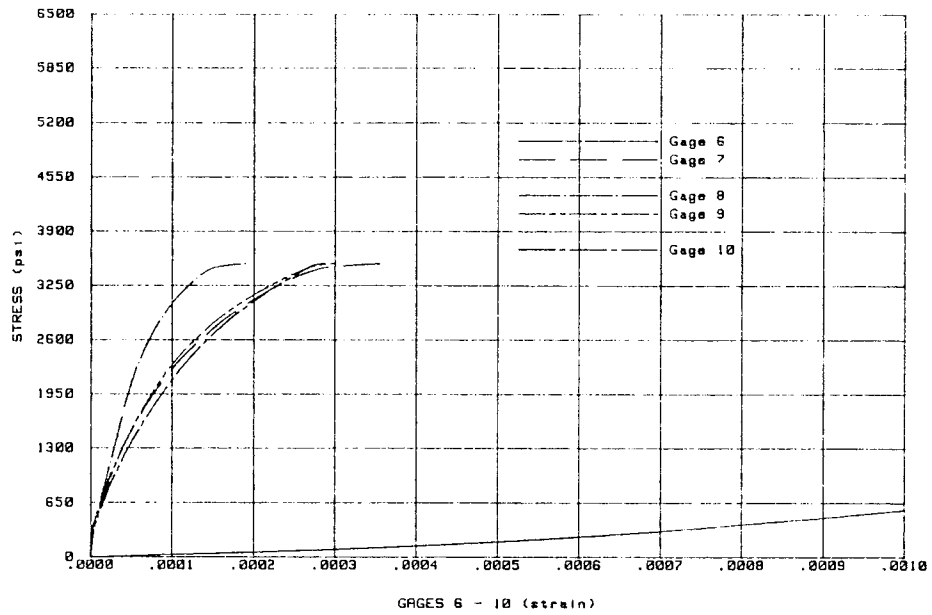
ATKINSON-NOLAND AND ASSOCIATES
MASONRY PRISM TESTS

TEST: 6-CNC-IFR
SPECIMEN: 12-18-5



ATKINSON-NOLAND AND ASSOCIATES
MASONRY PRISM TESTS

TEST: 6-CNC-IFR
SPECIMEN: 12-18-5



CONCRETE 5

Reproduced from
best available copy.

